On-Road Measurement of Light-Duty Gasoline and Heavy-Duty Diesel Vehicle Emissions

Final Report
Contract No. 05-309

Prepared for:

California Air Resources Board
and the California Environmental Protection Agency

Prepared by:

Robert A. Harley
Principal Investigator

Department of Civil and Environmental Engineering
University of California
Berkeley, CA 94720-1710

March 2009

Disclaimer

The statements and conclusions in this Report are those of the authors and not necessarily those of the California Air Resources Board. The mention of commercial products, their source, or their use in connection with material reported herein is not to be construed as actual or implied endorsement of such products.

Acknowledgments

The main researchers involved in this project include Andrew Kean of California Polytechnic State University San Luis Obispo (lead author of chapter on ammonia emissions), George Ban-Weiss, John McLaughlin, and Robert Harley (PI) of the University of California at Berkeley, and Thomas Kirchstetter and Melissa Lunden of Lawrence Berkeley National Laboratory. We also acknowledge co-authors Gary Kendall, Jim Hesson, and Eric Stevenson of the Bay Area Air Quality Management District, Eric Grosjean and Daniel Grosjean of DGA Inc., and Tony Strawa of NASA Ames Research Center.

We wish to thank the staff of the Bay Area Air Quality Management District for assistance with field sampling, calibration issues, laboratory analyses, and data analysis. We thank Chevron for financial support of the carbonyl measurements by DGA Inc., and for liquid fuel analyses. Ted Hehn of UC Berkeley provided assistance with CO_2 measurements. Susanne Hering of Aerosol Dynamics Inc. provided assistance with particle number counters. We also thank Caltrans staff at the Caldecott tunnel for site access and logistical support. Finally we are grateful to ARB staff for their time spent reviewing and commenting on draft versions of chapters of this report as they were written, to Seungju Yoon and Todd Sax for providing vehicle registration data, and to Jim Pederson who served as ARB project manager.

This report was submitted in fulfillment of ARB contract 05-309, On-Road Measurement of Light-Duty Gasoline and Heavy-Duty Diesel Vehicle Emissions, by the University of California at Berkeley under the sponsorship of the California Air Resources Board. Work was completed as of March 16, 2009.

Table of Contents

List of Figures v

List of Tables vii

Abstract viii

Executive Summary ix

1 Introduction 1

2 Nitrogen Oxides and Fine Particle Emission Trends 5

3 Particle Number Emissions and Size Distributions 31

4 Emission Factor Distributions for Individual Heavy-Duty Trucks 44

5 Speciated Hydrocarbon Emission Trends 59

6 Carbonyl and Nitrogen Dioxide Emissions 69

7 Ammonia Emissions 86

8 Conclusions 101

9 References 104

Appendix A: Size-Resolved Particle Emission Factor Data 118

Appendix B: Emission Factors for Individual HD Trucks 124

List of Figures

2.1	Comparison of EC and OC measured by TOA	11
2.2	Light-duty vehicle speed distribution inside the Caldecott tunnel	20
2.3	Light-duty vehicle registrations by zip code	21
2.4	Comparison of BC measured by aethalometer and TOA	22
2.5	NO_x and PM emission factor trends, 1997-2006	26
2.6	Diurnal variations in BC, CO, CO_2 concentrations and ratios	30
3.1	Particle size distributions at tunnel entrance and exit	35
3.2	Size-resolved particulate emission factors	36
4.1	Measured BC, PN, and CO_2 in diesel truck exhaust plume	48
4.2	Histograms of BC and PN emission factors	53
4.3	Probability plots and cumulative distributions for BC and PN	54
4.4	Heavy-duty truck speed distribution inside the Caldecott tunnel	55
4.5	Correlation of BC and PN emission factors for individual trucks	56
4.6	Probability density function of mean BC emission factor	58
5.1	Tunnel exit:entrance concentration ratios for individual VOC	62
5.2	Trends in light-duty vehicle NMOC and benzene emission factors	62
5.3	Comparison of light HC and MTBE in tunnel emissions, 1999-2006	67
5.4	Comparison of C_6-C_8 alkanes in tunnel emissions, 1999-2006	67
5.5	Comparison of aromatics in tunnel emissions, 1999-2006	68
6.1	Formaldehyde and acetaldehyde emission trends	78

6.2 Comparison of carbonyl emission factors for diesel trucks 84

7.1 Tubular wet effluent denuder schematic 90

7.2 Variations in vehicle speed and ammonia emissions 94

7.3 Variations in NH_3, CO, and NO_x emission factors 95

7.4 Ammonia emission factors as a function of NO and CO emissions 98

7.5 Ammonia emission contributions by vehicle as a function of NO and CO 99

List of Tables

2.1	U.S. heavy-duty diesel engine emission standards	6
2.2	Measured NO_x, CO, CO_2, and particulate matter concentrations	12-14
2.3	Parameters used for CO_2 apportionment	17
2.4	Observed traffic volumes by vehicle type	19
2.5	Trends in measured NO_x and PM-related emission factors, 1997-2006	25
3.1	Measured PN concentrations	38-39
3.2	Comparison of CPC and SMPS-derived emission factors	41
3.3	Particle number and volume fractions below 30, 50, and 100 nm	42
5.1	VOC weight fractions in tunnel emissions	63-64
6.1	Carbonyl and CO emission factors	75-76
6.2	Ethanol and carbonyl concentrations in Bay area gasoline	77
6.3	List of heavy carbonyls detected in vehicle emissions	85
7.1	Comparison of LD vehicle ammonia emission factors	93

Abstract

Emissions from light-duty (LD) gasoline and heavy-duty (HD) diesel vehicles were measured at the Caldecott tunnel in the San Francisco Bay area in summer 2006, with comparisons to results from previous years at the same site made to quantify emission trends over time. LD vehicle emissions of nitrogen oxides, volatile organic compounds, carbon monoxide, and particulate matter (PM) continue to decline over time due to fleet turnover effects and improved emission control technologies on new vehicles. Some effects of the switch from methyl-tert butyl ether (MTBE) to ethanol in California gasoline were observed. Substantial reductions in HD diesel truck emissions of PM were also observed between 1997 and 2006. The distributions of black carbon (soot) and ultrafine particle number emissions from individual diesel trucks were measured as part of this study, and sub-populations of high-emitting trucks were identified. NO_x from HD trucks has been decreasing more slowly than for LD vehicles over the last decade, with the result that the relative importance of diesel engines as a source of NO_x emissions in California has increased dramatically. Diesel engines are also an important source of direct emissions of aldehydes, which are malodorous, toxic, and reactive in the atmosphere. Exhaust emissions of ammonia from LD vehicles used to be negligible, then increased with the adoption of three-way catalytic converters, and appear to have declined since 1999 as carbon monoxide emissions and air/fuel ratio for LD vehicles have been brought under better control.

Executive Summary

Gasoline and diesel engines used in on-road vehicles are a significant source of air pollution. Emissions from these engines give rise to a range of air quality problems and human health concerns. In addition to contributing to local and regional air pollution problems, vehicle emissions contribute to climate change. Over the last 20 years, there has been major progress in controlling light-duty vehicle emissions due to the combined effects of improved emission control technologies installed on new vehicles, fleet turnover, and the introduction of reformulated gasoline. Further gasoline changes have occurred since 2000, most notably the phase-out of methyl tert-butyl ether (MTBE) in California, and the switch to ethanol. Also ultra-low sulfur diesel fuel was introduced in 2006 to enable post-combustion exhaust treatment technologies for diesel engines. More stringent emission standards for new vehicles and engines, fleet turnover, and fuel changes discussed above, have certainly led to changes in on-road vehicle emissions since the 1990s. The overall objective of this research is to characterize current emissions of gas- and particle-phase pollutants from on-road motor vehicles, and to compare with previous field study data to quantify emission trends.

Overview of Field Measurements

On-road vehicle emissions were measured in this study during summer 2006 at the Caldecott tunnel in the San Francisco Bay area, as part of a continuing campaign to track changes in vehicle emissions over time. Both gas and particle-phase pollutants were measured at the tunnel entrance and exit, during afternoon hours when traffic through the tunnel was driving uphill (eastbound) on a 4% grade. Measurements were made in two separate sets of traffic lanes: in the center bore of the tunnel where heavy-duty trucks are not allowed, and in a mixed traffic bore where both light-duty (LD) and heavy-duty (HD) vehicles are present. Fleet-average emission factors were calculated from measured data by normalizing background-subtracted pollutant concentrations to total carbon (mainly CO_2) emitted by vehicles driving through the tunnel. Results from the LD-only traffic lanes were used together with traffic counts and other data to apportion pollutant

concentrations in the mixed traffic bore to calculate separate emission factors for HD diesel trucks. Results from summer 2006 were compared to previous observations of vehicle emissions made at the same site to quantify emission trends over time. Measurements reported here do not include the excess emissions associated with cold engine starting, as vehicles observed driving through the tunnel were operating in a fully warmed up mode. Also emission effects of fuel composition changes that are implemented during winter months (e.g., increased gasoline vapor pressure) are not captured in this study. Thus the VOC speciation profiles reported in Chapter 5 may under-represent the relative abundance of n-butane in vehicle emissions for example.

Nitrogen Oxides (NO_x) and Exhaust Particulate Matter (PM) Emissions

When normalized to fuel consumption, NO_x emission factors were found to be 3.0 ± 0.2 and 40 ± 3 g kg^{-1} for LD vehicles and diesel trucks, respectively. Corresponding $PM_{2.5}$ emission factors were 0.07 ± 0.02 and 1.4 ± 0.3 g kg^{-1}. Results from 2006 were compared to similar measurements from 1997 at the same site. For LD vehicles, NO_x and $PM_{2.5}$ emission factors decreased by 67±3 and 36±17%, respectively. Corresponding decreases for diesel trucks were 30±9% for NO_x and 48±12% for $PM_{2.5}$. The ratio of HD to LD emission factor for NO_x increased from 6 ± 1 to 13 ± 1 between 1997 and 2006, which indicates an increase in the *relative* importance of diesel trucks as a source of NO_x emissions. The absorption, scattering, and extinction cross-section emission indices, parameters relevant to climate change and atmospheric visibility, were an order of magnitude higher for diesel trucks than LD vehicles.

Emissions of Ultrafine Particles: Number and Size Distribution

Particle number emission factors (diameter D_p > 3 nm) were found to be $(3.9 \pm 1.4) \times 10^{14}$ and $(3.3 \pm 1.3) \times 10^{15}$ # kg^{-1} for LD vehicles and diesel trucks, respectively. Comparison of these results to previous measurements at the same site indicates that particle number emission factors have decreased for both LD vehicles and diesel trucks since 1997. Measured particle size distribution data indicated that diesel trucks emit at least an order of magnitude more particles than LD vehicles for all

measured particle sizes ($10 < D_p < 280$ nm), per unit mass of fuel burned. The relative importance of LD vehicles as a source of particles increases as D_p decreases.

Black Carbon and Particle Number Emission Rates from Individual Diesel Trucks

Emission factors for black carbon (BC) and particle number (PN) were measured using fast time-response instruments to capture exhaust plumes from 226 individual heavy-duty (HD) diesel trucks driving through the Caldecott tunnel. Emission factors were based on concurrent increases in BC, PN, and CO_2 concentrations (measured at 1 Hz) that corresponded to the passage of individual trucks. The distributions of BC and PN emission factors from individual trucks are skewed, meaning that a large fraction of pollution comes from a small fraction of the in-use vehicle fleet. The highest-emitting 10% of trucks were responsible for ~40% of total BC and PN emissions from all HD trucks. BC emissions were log-normally distributed with a mean emission factor of 1.7 g kg^{-1} and maximum values of ~10 g kg^{-1}. Corresponding values for PN emission factors were 4.7×10^{15} and 4×10^{16} # kg^{-1}. There was minimal overlap among high-emitters of these two pollutants: only 1 of the 226 HD trucks measured was found to be among the highest 10% for both BC and PN. Based on the distribution of BC emission factors observed in this study, uncertainties (1σ) in extrapolating from a random sample of n HD trucks to a population mean emission factor range from ±43% for n=10 to ±8% for n=300.

Volatile Organic Compound Emissions

The emission factor for total non-methane organic compounds from LD vehicles continues to decline over time. The same is true for most individual hydrocarbons, in particular benzene, which is a toxic air contaminant. Changes in the chemical composition of on-road vehicle emissions in recent years include the elimination of MTBE, an increase in 2,2,4-trimethylpentane which is a high-octane gasoline additive, and a decrease in n-butane which may have been required to accommodate the increased use of ethanol as a gasoline blending component.

Aldehydes are toxic, malodorous, and reactive in the atmosphere. Emissions of aldehydes and other carbonyls were measured from LD vehicles in the center bore of the Caldecott tunnel in 1999, 2001, and 2006. The LD vehicle emission factor for formaldehyde, the most abundant carbonyl, did not change between 1999 and 2001, then decreased by 61 ± 7% between 2001 and 2006. This reduction was due to fleet turnover and the removal of MTBE from gasoline. Acetaldehyde emissions decreased by 19 ± 2% between 1999 and 2001, and by the same amount between 2001 and 2006. Absent the increased use of ethanol in gasoline after 2003, acetaldehyde emissions would have further decreased by 2006. Emissions of carbonyls from diesel trucks were measured at the Caldecott tunnel in 2006 for the first time. Emission factors for diesel trucks were higher than those for LD vehicles for all reported carbonyls. Diesel engine exhaust dominates over gasoline engines as a direct source of carbonyl emissions in California. Carbonyl concentrations were also measured in liquid gasoline samples and were found to be low (< 20 ppm). The gasoline brands that contained ethanol showed higher concentrations of acetaldehyde in unburned fuel vs. gasoline that was formulated without ethanol. Measurements of NO_2 showed a yearly rate of decrease for LD vehicle emissions similar to that of total NO_x in this study. The observed NO_2/NO_x ratio was 1.2 ± 0.3% and 3.7 ± 0.3% for LD vehicles and diesel trucks, respectively.

Ammonia Emissions

Prior to the introduction of catalytic converters, ammonia emissions from LD vehicles were negligible. Under fuel-rich conditions, NO_x present in engine exhaust can be over-reduced to ammonia instead of being reduced to the intended target of nitrogen (N_2) gas. Previous studies have documented an increase in ammonia emissions from LD vehicles between about 1980 and 2000, coinciding with the introduction and increasing prevalence of three-way catalytic converters. Between 1999 and 2006, measured LD vehicle ammonia emissions at the Caldecott tunnel decreased by 38 ± 6%, from 640 ± 40 to 400 ± 20 mg kg^{-1}. High time resolution measurements of ammonia made in summer 2001 at the same location indicate a minimum in ammonia emissions correlated with lower speed driving conditions. Variations in ammonia emission rates track changes in carbon

monoxide more closely than changes in nitrogen oxides, especially during later evening hours when traffic speeds are highest. Analysis of remote sensing data of Burgard et al (*Environ. Sci. Technol.* **2006**, *40*, 7018-7022) indicates relationships between ammonia and vehicle model year, nitrogen oxides, and carbon monoxide. Ammonia emission rates from diesel trucks were difficult to measure at the Caldecott tunnel due to the large contribution to ammonia concentrations in the mixed-traffic bore that came from LD vehicles. Nevertheless, it is clear that diesel trucks are currently a minor source of ammonia emissions compared to LD gasoline vehicles.

Implications for Air Pollution Control

1. The importance of diesel engines as a source of air pollution, especially NO_x and aldehydes, has increased in relative terms as other emissions sources of these pollutants have been controlled.

2. There are high-emitting diesel trucks on the road that convert on the order of 1% of the fuel mass entering the engine into black carbon (soot) particles in the exhaust. The high-soot emitting-trucks contribute disproportionately to total emissions, and the share of total emissions coming from high-emitting trucks will increase in future as the truck fleet becomes cleaner on average. There is little overlap between high-emitters of soot and trucks that emit large numbers of ultrafine particles.

3. The light-duty motor vehicle source of ammonia emissions appears to have peaked and is now declining. Ammonia emissions are relevant to the formation of ammonium nitrate, which is a significant contributor to airborne fine particle ($PM_{2.5}$) mass in California.

Recommendations for Future Research

1. Continue tracking mobile source emission trends, with emphasis on NO_x and PM emissions from heavy-duty diesel engines. Large decreases in diesel emissions are expected over the next 20 years due to adopted emission standards and new rules.

2. Develop and apply methods that can measure gas and particle-phase pollutants at high time resolution in the exhaust plumes of individual diesel trucks as they drive by. Deploy on freeway overpasses, along truck routes, at ports, freight terminals, etc.

3. Use electrometer-based and/or other single particle spectrometers to measure exhaust emissions/particle size distributions in real time.

4. Assess the sources and concentrations of ethanol and acetaldehyde in the atmosphere, and their contributions to ozone production.

5. Critically evaluate diesel engine aldehyde emissions, and assess the role that these emissions play in air pollution problems.

1. Introduction

1.1 Background

Gasoline and diesel engines remain as a significant source of air pollution in California, the U.S., and worldwide (Sawyer et al., 2000). Emissions from these engines give rise to a range of air quality problems and human health concerns (Lloyd and Cackette, 2001). In addition to contributing to local and regional air pollution problems, vehicle exhaust emissions contribute to climate change. Motor vehicles are responsible for 35% of California CO_2 emissions (CEC, 2006), the greenhouse gas responsible for the greatest amount of global warming. NO_x is a precursor to tropospheric ozone, which also contributes to global warming. PM has direct and indirect effects on radiative forcing, leading to both global warming and cooling; the direct effect of BC emissions is positive forcing (IPCC, 2007).

Over the last 20 years, there has been major progress in controlling light-duty vehicle emissions due to the combined effects of improved emission control technologies installed on new vehicles, fleet turnover, and the introduction of reformulated gasoline in the 1990s (Kirchstetter et al., 1999b; Harley et al., 2006; Stedman and Bishop, 2008). Further gasoline changes have occurred since 2000, most notably the phase-out of methyl tert-butyl ether (MTBE) in California, and the switch to ethanol. Exhaust and evaporative reactivity also declined, mainly due to lowering the light olefin and heavy aromatic contents in gasoline (Kirchstetter et al., 1999c).

An unintended consequence of catalytic converter use on light-duty motor vehicles has been increased emissions of ammonia due to over-reduction of nitrogen oxides (Fraser and Cass, 1998; Kean et al., 2000; Durbin et al., 2004; Emmenegger et al., 2004). Ammonia is the primary alkaline gas in the atmosphere, and an important precursor to secondary particle formation. For some vehicles, emissions of ammonia exceed the emissions of other regulated compounds, though Durbin et al. found that ammonia emission rates are lower for newer technology vehicles. While probably decreasing, the rate of change in fleet-average ammonia emissions remains unclear.

Heavy-duty diesel engine emission control efforts have lagged behind those for light-duty vehicles. Nitrogen oxide emissions from diesel engines have benefited from only small reductions since 1990, and have not kept pace with rapid growth in diesel fuel use over the same time period (Yanowitz et al., 2000; Harley et al., 2005). Exhaust PM mass emission rates have been reduced through use of higher-pressure fuel injection systems that atomize diesel fuel more finely as it is injected into engine cylinders. This promotes better mixing of air and fuel inside the engine cylinder. There is concern however, that the higher-pressure fuel injection systems may lead to higher numbers of ultrafine mode particles in diesel exhaust (Baumgard and Johnson, 1996; Abdul-Khalek et al., 1999), despite lower overall $PM_{2.5}$ mass emission rates.

More stringent emission standards apply to new heavy-duty diesel engines sold starting in 2007; ultra-low sulfur diesel fuel was introduced in 2006 to facilitate use of post-combustion exhaust treatment devices. Past diesel engine emission control efforts have relied on modifications to fuel injection system pressure and fuel injection timing. In contrast, new engines will be equipped with continuously regenerating traps (CRT), also known as diesel particulate filters (DPF). NO_x present in diesel exhaust is deliberately converted to NO_2 using an oxidation catalyst, then the NO_2 is used to oxidize collected soot particles, so the accumulated carbon particles on the filter can be removed to permit long-term continued use of the exhaust filter. NO_2 emissions may increase using this approach, which is an issue of regulatory and public health concern. Emission control options for NO_x include increased exhaust gas recirculation (EGR), selective catalytic reduction (SCR) systems, and absorbers that store NO_x while the system is operating with excess oxygen, with intermittent operation in NO_x reduction mode to eliminate stored NO_x.

Interest in exhaust particulate matter emissions from vehicles has increased due to epidemiological evidence associating PM exposure with increases in mortality and morbidity (Dockery et al., 1993). Emission inventories suggest that the majority of fine and ultrafine particles in the urban atmosphere result from engine combustion (Schauer et al., 1996). The concerns have lead to a number of near highway and tunnel investigations of time- and size-resolved particle emissions to improve vehicle PM emission inventories (Abu-Allaban et al., 2002; Sturm et al., 2003; Zhu et al., 2004). These studies have shown elevated concentrations of ultrafine particles with number mean diameters between 10 and 20 nm.

On-road measurements are useful as a source of data to document changes in emissions that have occurred and will occur in the future. On-road measurements provide data that are complementary to what can be measured using chassis dynamometers in the laboratory. While fuel and test conditions in the laboratory can be carefully controlled, it is expensive and time-consuming to test large numbers of vehicles. As both LD and HD vehicle emissions become increasingly skewed and dominated by emissions from a small number of gross-polluting vehicles, a large random vehicle sample becomes increasingly important to arrive at a robust estimate of population mean emission rates. Tunnel sampling provides fleet-average emission rates from large samples of vehicles as they are driven on the road.

1.2 Research Objectives

The overall goal of this study is to quantify trends in motor vehicle emissions using on-road measurements at a California highway tunnel made in summer 2006. Specific objectives are to

1. Characterize light- and heavy-duty vehicle nitrogen oxide (NO_x) and exhaust PM emissions, including $PM_{2.5}$ mass, elemental and organic carbon, particle number, and ultrafine (D_P < 100 nm) particle size distribution. Results are compared to previous field study results to describe emission trends.

2. Use fast-time response instruments to characterize distributions of exhaust emissions from individual heavy-duty diesel trucks.

3. Characterize emissions of volatile organic compounds, including total mass emission rates as well as detailed chemical composition. These results are compared to results from previous years.

4. Characterize emissions of species that may increase due to byproduct formation from emission control devices: ammonia (NH_3) and nitrogen dioxide (NO_2).

1.3 Report Organization

This report is organized into chapters that focus on different pollutants and vehicle categories of interest in this study. Chapter 2 addresses trends in NO_x and PM mass emissions, including the black and organic carbon (BC/OC) fractions, for both light-duty and heavy-duty vehicles. Chapter 3 provides results on the total number and size distribution of ultrafine particle emission rates for both vehicle categories. In Chapter 4, the distribution of black carbon and particle number emission factors for an on-road sample of over 200 individual heavy-duty trucks is reported. Chapters 5 and 6 address volatile organic compound emissions, with the first chapter focused on hydrocarbon emissions from light-duty vehicles, and the following chapter providing results for carbonyl (i.e., aldehyde, ketone, and dicarbonyl) as well as nitrogen dioxide emissions from both gasoline and diesel engines. Chapter 7 provides reporting on ammonia emission rates, focusing on emissions of this pollutant from light-duty vehicles. Chapter 8 provides conclusions and recommendations for further research.

2. Nitrogen Oxides and Fine Particle Emission Trends

2.1 Introduction

Motor vehicles span a wide range of sizes from light-duty (LD) vehicles, which in the U.S. are mostly fueled by gasoline, to heavy-duty (HD) trucks, mostly diesel-powered. The *relative* importance of HD diesel truck exhaust as a source of NO_x emissions has increased in the last 15 years because control of LD gasoline vehicle emissions has progressed more than HD diesel truck emissions, and on-road use of diesel fuel has grown faster than gasoline since 1990 (Harley et al., 2005). As shown in Table 2.1, NO_x emission standards for HD diesel engines were gradually reduced during the 1990s. However, most 1990s engines met these standards only during emission certification tests but not while being used on-road (Yanowitz et al., 2000). As a result of increased regulatory pressure, most new engines met the 2004 NO_x standard two years early using exhaust gas recirculation (e.g. Volvo, 2007). To meet increasingly stringent HD diesel NO_x standards in the future, urea-based selective catalytic reduction systems will likely be used in new engines starting in 2010 (Johnson, 2004). Such systems are already being used in HD diesel trucks to meet European emission standards (e.g. Mack, 2006). Trends in on-road LD and HD vehicle emissions in Europe have been reported by Schmid et al. (2001) and Colberg et al. (2005).

PM emission standards for HD diesel engines underwent larger reductions during the 1990s than NO_x (Table 2.1). Yanowitz et al. (2000) have shown that unlike NO_x, exhaust PM mass emissions from HD trucks decreased during this time. New HD diesel trucks started using diesel particle filters in 2007 to meet new emission standards, which required PM emissions to be reduced by an order of magnitude. To enable catalytic diesel exhaust emission controls the sulfur content of diesel fuel was reduced in the U.S. to < 15 ppm by weight starting in 2006. Less is known about PM emission trends for LD vehicles relative to HD trucks; there is continuing controversy about the relative importance of gasoline vs. diesel vehicles as sources of exhaust PM emissions (Gertler, 2005), indicating the need for additional measurements.

Table 2.1 U.S. heavy-duty diesel truck emission standards. [a]

Model Year	NO_x	PM
1979−1984	13.4 [b]	
1985−1987	14.4	
1988−1989	14.4	0.80
1990	8.1	0.80
1991−1993	6.7	0.34
1994−1997	6.7	0.13
1998−2003	5.4	0.13
2004−2006	3.2	0.13
2007−2009	1.7 [c]	0.013
>2010	0.27	0.013

[a] Units of grams per kilowatt-hour (g/kW-h): mass emitted per unit of engine brake work output.

[b] Total hydrocarbon (THC) + NO_x

[c] The NO_x standard for 2007 is 0.27 g/kW-h, but is being phased in over 3 years. 50% of total sales for each engine manufacturer must meet the 0.27 g/kW-h standard from 2007-2010, thus the effective standard is 1.7 g/kW-h.

This chapter reports measured NO_x and exhaust PM emissions from large numbers of on-road vehicles during 2006 in a San Francisco Bay area highway tunnel and compares with data from the same site from previous years to quantify trends over time. Measurements were made immediately after the switch to ultra-low sulfur diesel (ULSD) fuel in California, and immediately prior to the deployment of PM and NO_x control technologies on new HD diesel trucks, so this study can also serve as a baseline to quantify on-road emission trends after the 2007 - 2010 emission standards take effect. Light-absorbing and scattering properties of exhaust PM emissions that are relevant to understanding visibility and climate-forcing effects of vehicle emissions are also quantified here.

2.2 Experimental Methods

2.2.1 Field Site.

Motor vehicle emissions were measured in the Caldecott tunnel during July and August of 2006. The 1.0 km long tunnel is located on highway 24 in the San Francisco Bay area, and has three separate two-lane traffic bores, with a grade of 4% uphill in the eastbound direction. Each bore consists of a traffic tube, through which the vehicles travel, and ventilation air ducts located above the traffic tubes through which fresh outside air and polluted tunnel air flow into and out of the tunnel, respectively. Air flow through the ventilation ducts is facilitated by large fans; these fans were turned off during intensive observation periods to simplify mass balance calculations, which are further discussed below in the *Emission Factors* section. Turning off the fans meant that airflow in the tunnel was longitudinal in the direction of traffic flow. A schematic of the tunnel is available in Kirchstetter et al. (1996). Pollutant concentrations were measured in bores 1 and 2. Bore 1 carries a mix of light-duty passenger vehicles and medium- and heavy-duty trucks; heavy-duty trucks are restricted from traveling through bore 2. This special feature of the Caldecott tunnel allows direct determination of LD vehicle emission factors without having to apportion pollutant concentrations, as must be done in situations with mixed LD and HD traffic (Fraser et al., 2003; Grieshop et al., 2006; Imhof et al., 2006). Bore 1 traffic flows eastbound (uphill) at all times, whereas bore 2 traffic switches from westbound to eastbound at approximately noon on weekdays to accommodate commuter traffic. All results reported here are for uphill traffic conditions in both bores.

Measurements at the tunnel were conducted on 8 weekdays in each traffic bore, for a total of 16 days. Exact dates are listed in Table 2.2. Although most pollutant analyzers ran 24 hours a day, intensive observations were made 1200 – 1400h in bore 1 and 1600 – 1800h in bore 2. These times were chosen to maximize the diesel truck fraction of traffic in bore 1, and LD vehicle traffic volume in bore 2.

2.2.2 Traffic Characterization.

Manual traffic counts of LD vehicles, MD trucks, and HD trucks were performed each day. Vehicles were categorized by number of axles and tires: LD = 2-axle/4-tire, MD = 2-axle/6-tire, and HD = 3 or more axles. Vehicles passing through the tunnel were also recorded using video cameras at the tunnel entrance and exit. Camera clocks were synchronized and used to calculate vehicle transit times, which were combined with known tunnel length to compute average vehicle speeds inside the tunnel. This was done for every individual HD truck entering bore 1 between 1200 and 1400h on seven out of eight sampling days. In bore 2, speeds were calculated every five minutes using vehicles observed in both lanes. This was done between 1600 and 1800h on six out of eight sampling days. On the remaining sampling days, one of the video cameras was repositioned outdoors and used for license plate surveys. License plates were transcribed and matched with registration data to determine vehicle age distributions.

2.2.3 Gas-Phase Measurements.

CO_2, NO_x, and CO concentrations were measured using analyzers set up at the traffic entrance and exit of the tunnel. At the exit (east end), air was drawn from the traffic tube using a pump through a ~40 m Teflon sample line (ID=1.2 cm) to the pollutant analyzers. The residence time of air in the sample line was approximately 20 seconds. At the entrance (west end), tunnel air was drawn through a ~5 m Teflon sample line (ID = 0.48 cm) from the traffic tube to the pollutant analyzers using only the internal instrument pumps.

CO_2 concentrations were measured using LI-COR (Lincoln, NE) model 820 non-dispersive infrared gas analyzers at both ends of the tunnel. NO_x concentrations were measured using chemiluminescent analyzers (Thermo Environmental Instruments (TEI), Franklin, MA, models 42A and 42C at the entrance and exit, respectively). CO was measured using gas filter correlation spectrometers at both ends of the tunnel (TEI model 48). Calibration of all gas-phase analyzers was checked daily prior to sampling. The Bay Area Air Quality Management District's Quality Assurance group audited the gas analyzers in the tunnel to ensure measurement accuracy.

2.2.4 Particle Measurements.

Two-hour average measurements of $PM_{2.5}$, BC, and OC were made at both the entrance and exit of the tunnel using matching experimental systems. The aerosol samples were drawn from approximately 15 cm below the ceiling of the traffic bore. Filter samples were collected downstream of sharp cut cyclones (BGI, Waltham, MA, model VSCCA) at 16.7 L min^{-1} to achieve a particle size cut of 2.5 μm. This flow rate was maintained during sample collection using calibrated mass flow controllers (Alicat Scientific, Tucson, AZ, model MC-50SLPM-D) with the following exceptions. On the first three days of the study (July 18-20, in bore 1) at the exit end of the tunnel, valves and rotameters that were calibrated with a primary air flow standard (Sensidyne/Gilian, Clearwater, FL, model Gilibrator-2) were used to maintain a steady flow rate through the filters. On the ninth day of the study (i.e., July 31, the first sampling day in bore 2) at the exit end of the tunnel, a mass flow controller power supply malfunctioned and the tandem quartz filters sampled tunnel air at 13 L min^{-1} instead of 16.7 L min^{-1}. For this sample, the cyclone established a particle size cut of 3.2 μm instead of 2.5 μm. Particulate carbon concentrations of BC and OC for this sample were calculated using the reduced flow rate. The $PM_{2.5}$ sample was not affected. The total carbon concentration (i.e., BC plus OC) determined for this sample was equal to the average concentration in bore 2, indicating there were no large changes in carbon particle mass collected.

Quartz (Pallflex, East Hills, NY, model 2500QAT-UP) and Teflon (Gelman Sciences, Teflon membrane, 2.0 μm pore size) filters were used to collect particulate matter samples. To determine $PM_{2.5}$ mass, Teflon filters were weighed before and after sampling; the mass difference was divided by the volume of air sampled. Prior to use, quartz filters were baked at 800ºC for six hours to remove carbonaceous impurities. In the tandem filter sampling method (Turpin et al., 2000) employed here, two quartz filters in series are collected in parallel with a Teflon filter and a quartz filter in series. The first filter in the tandem quartz pair collects particulate matter that is subsequently analyzed for carbon content, and the quartz filter behind the Teflon filter is used to correct particulate carbon concentrations for the positive organic carbon sampling artifact, as described by Kirchstetter et al. (2001) and Subramanian (2004).

The carbon content of quartz filter samples was measured using thermal optical analysis (TOA). Filter samples were heated at a constant rate of 40ºC min^{-1} from 50 to 700ºC in a pure oxygen atmosphere. The evolved carbon was fully oxidized over a platinum coated ceramic catalyst maintained at 800ºC, and the resultant CO_2 was measured with a non-dispersive infrared analyzer (LI-COR, Lincoln, NE, model 7000). The intensity of light transmitted through the sample was continuously monitored during analysis and was used to differentiate between organic and light-absorbing black carbon. Transmission was measured using a white light source and a spectrometer (Ocean Optics, Dunedin, FL, model S2000). The recovery of total carbon concentrations measured with this approach was determined to be 100 ± 5% by analysis of prepared samples of potassium hydrogen phthalate and glucose. This TOA protocol will be referred to as the LBNL TOA method henceforth. The LBNL TOA method differs from the more common IMPROVE thermal-optical reflectance (TOR) (Chow et al., 2001) and NIOSH thermal-optical transmission (TOT) (Birch and Cary, 1996) protocols, which expose the sample to helium followed by a helium/oxygen mixture (as opposed to pure oxygen), raise the sample temperature stepwise (as opposed to at a constant rate), and measure optical reflectance or transmission at a single wavelength (as opposed to over a broad spectral region). In a previous sampling campaign at the same tunnel (Kirchstetter et al., 1999a), particulate carbon was determined using the NIOSH TOT protocol. Therefore, in the current study, selected samples were analyzed according to both the NIOSH TOT and LBNL TOA protocol to ensure the two protocols yielded similar results, as shown in Figure 2.1.

In addition to 2-hr average particle measurements, the physical and optical aerosol properties were measured in real-time at both ends of the tunnel. BC concentrations were measured using aethalometers (Magee Scientific, Berkeley, CA, models AE-2 and AE-1 at the entrance and exit, respectively), and scattering coefficients (b_{scat}) were measured at λ = 530 nm using nephelometers (Radiance Research, Seattle, WA, model M902). Aerosol was sampled at both ends of the tunnel through an AIHL cyclone (John and Reischl, 1980) to a common sample manifold to achieve a size-cut of 2.5 µm at a flow rate of 25 L min^{-1}. The aethalometers and nephelometers drew isokinetic samples from the common manifolds.

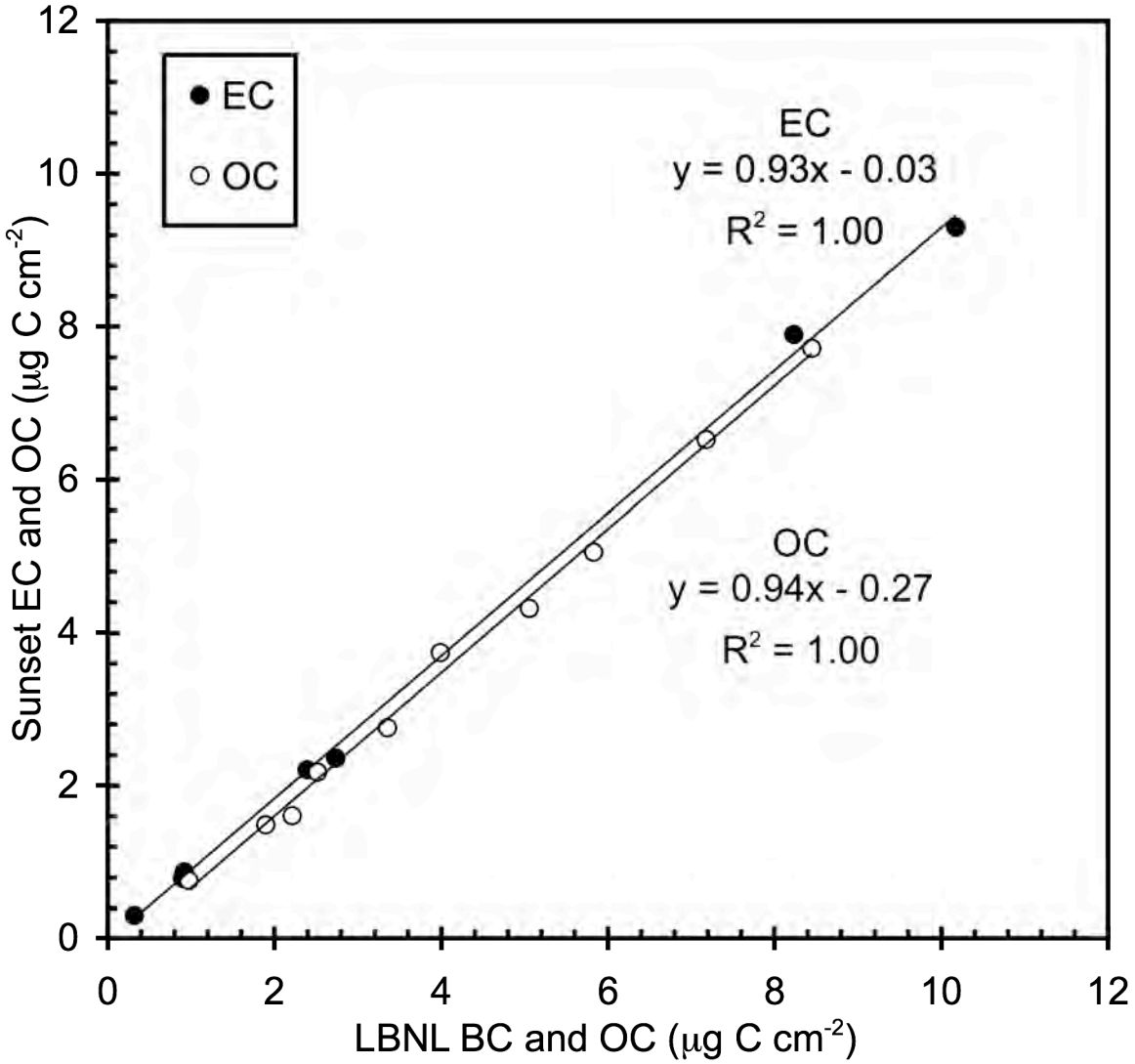

Figure 2.1 Comparison of EC and OC measured by Sunset Labs (NIOSH TOA method), versus BC and OC measured by LBNL (LBNL TOA method). Slopes near unity and y-intercepts near zero indicate good agreement between the two TOA methods.

Table 2.2 2-hour average pollutant concentrations measured at the Caldecott tunnel, summer 2006.

Bore 1

Date	Location	CO_2	CO	NO_x	$PM_{2.5}$	OM [a]	TOA BC [b]	Aeth BC [c]	b_{scat} [d]	b_{scat} [e]	b_{abs} [e]	b_{ext} [e]
		ppm	ppm	ppm	$\mu g\ m^{-3}$	$\mu g\ m^{-3}$	$\mu g\ C\ m^{-3}$	$\mu g\ C\ m^{-3}$	Mm^{-1}	Mm^{-1}	Mm^{-1}	Mm^{-1}
Tue, Jul 18	East	821	8.5	1.18	84.8	22.8	41.9	48.3	117.5	90.6	262.3	356.4
	West	468	2.3	0.15	38.9	4.4	4.6	4.7	41.7			
Wed, Jul 19	East	793	8.7	1.33	101.3	25.5	36.2	44.5	112.2	79.4	252.4	341.0
	West	443	2.2	0.15	24.5	3.5	3.0	3.5	29.0			
Thu, Jul 20	East	830	9.4	1.28	82.3	23.1	39.1	49.3	121.7	77.7	267.4	344.8
	West	451	2.4	0.14	21.0	5.1	3.2	5.2	24.9			
Fri, Jul 21	East	790	9.1	1.30	87.1	25.8	41.1	43.1	125.8	50.6	162.4	214.1
	West	454	2.6	0.17	24.0	5.0	4.5	5.0	26.8			
Mon, Jul 24	East	831	9.9	1.28	110.3	31.2	50.8	50.7	135.6	80.5	267.4	359.7
	West	467	3.0	0.17	23.5	3.8	4.6	6.3	27.4			
Tue, Jul 25 [f]	East	824	9.9	1.28	97.3	28.5	44.7	47.8	136.6	91.0	263.3	354.3
	West	477	3.6	0.22	37.4	5.0	7.0	7.6	22.0			
Wed, Jul 26	East	787	8.6	1.13	61.9	22.0	32.6	34.0	92.6	58.7	162.8	221.6
	West	441	2.4	0.13	8.5	5.1	3.3	3.9	21.6 [g]			
Thu, Jul 27	East	868	7.9	1.30	78.8	23.6	41.3	41.4	127.8	75.7	214.5	290.2
	West	456	2.4	0.15	6.0	1.2	3.5	4.1	30.2			

Table 2.2 (continued)

Bore 2

Date	Location	CO_2	CO	NO_x	$PM_{2.5}$	OM [a]	TOA BC [b]	Aeth BC [c]	b_{scat} [d]	b_{scat} [e]	b_{abs} [e]	b_{ext} [e]
		ppm	ppm	ppm	µg m^{-3}	µg m^{-3}	µg C m^{-3}	µg C m^{-3}	Mm^{-1}	Mm^{-1}	Mm^{-1}	Mm^{-1}
Mon, Jul 31	East	1147	9.7	0.71	32.4	18.1	9.7	11.2	39.6			
	West	474	1.7	0.12	16.5	3.7	2.4	2.1	11.3			
Tue, Aug 01	East	1163	9.0	0.72	33.9	13.4	8.8	9.8	47.7			
	West	471	1.5	0.12	9.0	4.0	2.0	2.4	17.0			
Wed, Aug 02	East	1137	11.0	0.80	53.9	18.7	11.9	13.3	70.5			
	West	466	1.7	0.12	35.9	3.9	1.6	2.2	28.7			
Thu, Aug 03	East	1152	8.9	0.74	43.4	17.1	9.0	13.9	81.7	49.9	97.7	147.7
	West	449	1.3	0.10	19.0	2.9	1.4	3.3	26.9			
Mon, Aug 07	East	1008	8.8	0.62	36.9	11.0	7.9	8.8	40.1	35.2	68.2	103.4
	West	425	1.4	0.07	8.5	1.2	1.1	1.8	7.1			
Tue, Aug 08 [f]	East	1191	11.2	0.76	39.4	18.2	14.2	15.4	63.1	53.6	100.5	155.3
	West	456	1.6	0.10	11.5	4.0	2.0	3.1	13.5			
Wed, Aug 09	East	1270	12.3	0.96	59.4	20.6	13.6	17.2	73.1	63.8	138.9	202.2
	West	470	1.4	0.13	16.5	7.8	2.8	3.6	23.8			
Thu, Aug 10	East	1123	9.6	0.71	51.9	13.6	11.7	15.1	57.8	60.4	110.8	168.7
	West	452	1.1	0.10	16.0	3.8	2.1	1.7	22.5			

Please see next page for footnotes

Table 2.2 (continued)

[a] OM is obtained by multiplying measured OC by 1.4 to account for mass of hydrogen and oxygen (Gray et al., 1986). OC is corrected for the positive sampling artifact by subtracting the quartz behind Teflon filter mass (see text).

[b] BC from thermal optical analysis of filters. Reported as g carbon m^{-3}.

[c] BC reported as 2-hour average of continuous aethalometer data. Reported as g carbon m^{-3}.

[d] Scattering coefficient from nephelometer, measured at λ = 530 nm.

[e] Absorption, scattering, and extinction coefficient from cavity ring-down instrument (Cadenza), measured at λ = 675 nm. b_{abs} is calculated from measured b_{scat} and b_{ext} by $b_{abs} = b_{ext} - b_{scat}$

[f] TOA analysis was performed twice on two separate punches of the filter on July 25 and Aug 08 for quality assurance. Values in the table represent averages of these two points.

[g] West end nephelometer data not available on July 26. This data point is estimated as b_{scat} from the east end multiplied by the average bore 1 west/east ratio of b_{scat} from the nephelometer.

Aerosol optical properties of b_{scat} and extinction coefficient (b_{ext}) were measured with 1-second temporal resolution at λ = 675 nm using the cavity ring-down instrument of Strawa et al. (2003; 2006) known as Cadenza. Particulate matter concentrations and emission factors are generally reported on a mass basis. However, for purposes of visibility or climate effects the relevant parameter is b_{ext}, which is a measure of the amount of light attenuated over a linear distance, typically reported as 10^{-6} m^{-1} or Mm^{-1} for atmospheric conditions. Measurement of b_{ext} is generally difficult because long pathlengths are required. The cavity ring-down technique in this study employs a long effective pathlength (~1 km) in a 20x20 cm optical cell. Cadenza simultaneously measures b_{scat} in the same measurement cell as b_{ext} using a reciprocal nephelometer technique (Mulholland and Bryner, 1994). Absorption coefficient (b_{abs}) can be subsequently calculated as b_{ext} minus b_{scat}. Based on laboratory calibrations and airplane flight experience, the measurement uncertainty for b_{ext} is 2%. Strawa et al. (2006) compared Cadenza measurements of b_{ext} with the sum of b_{scat} measured with a nephelometer and b_{abs} measured with a Particle Soot Absorption Photometer (PSAP), and found agreement within 2%.

2.2.5 Emission Factors.

Emission factors were computed using the carbon balance method shown by eq 2.1, and expressed per unit mass of fuel burned separately for LD vehicles and MD/HD diesel trucks. Most of the carbon in gasoline and diesel fuel is emitted as CO_2, with smaller amounts emitted as CO. Even smaller amounts of fuel carbon emitted as particulate matter (Kirchstetter et al., 1999a) and unburned hydrocarbons (Kirchstetter et al., 1999b) are neglected in the denominator of eq 2.1. The emission factor E_p (grams of pollutant P per kg fuel burned) can be calculated as

$$E_p = \left(\frac{\Delta[P]}{\Delta[\mathrm{CO_2}] + \Delta[\mathrm{CO}]} \right) w_c \qquad (2.1)$$

where $\Delta[P]$ is the background-subtracted (exit minus entrance) mass concentration of pollutant P ($\mu g\ m^{-3}$), and $\Delta[CO_2]$ and $\Delta[CO]$ are background-subtracted concentrations in mg C m^{-3}. The fuel carbon mass fraction is w_c = 0.87 for diesel, and 0.85 for oxygenated gasoline (Kirchstetter et al., 1999a). To calculate emission factors from b_{abs}, b_{scat}, and b_{ext}, P in eq 2.1 is replaced by b (Mm^{-1}). The resulting emission factors are total optical cross-section of particles emitted per unit

mass of fuel burned (m^2 kg^{-1}). Background (tunnel entrance) values of light absorption, scattering, and extinction were not measured by Cadenza. To estimate background values for use in eq 2.1, we used the ratio of tunnel entrance to exit values of BC and b_{scat} from the aethalometer and nephelometer, respectively. For bores 1 and 2, the entrance to exit ratio for BC was 0.11 and 0.19, and b_{scat} was 0.23 and 0.32, respectively. Entrance values of b_{ext} were estimated by summing entrance values of b_{abs} and b_{scat}.

Emission factors for LD vehicles were calculated with eq 2.1 using measured concentrations from bore 2. To calculate emission factors for MD/HD diesel trucks, contributions to bore 1 concentrations first need to be apportioned between LD vehicles and MD/HD diesel trucks. Pollutants other than CO_2 in bore 1 were apportioned using estimates of CO_2 emissions from gasoline engines, and LD vehicle pollutant to CO_2 emission ratios measured in bore 2, as shown in eq 2.2

$$\Delta[P]_{1,D} = \Delta[P]_1 - \Delta[\mathrm{CO}_2]_{1,G}\left(\frac{\Delta[P]_2}{\Delta[\mathrm{CO}_2]_2}\right) \qquad (2.2)$$

where subscripts D and G indicate diesel and gasoline, subscripts 1 and 2 outside the brackets indicate tunnel bore number, and $\Delta[CO_2]_{1,G}$ is the concentration of CO_2 in bore 1 attributed to LD vehicles, calculated using eq 2.3. Previously (Kirchstetter et al., 1999a), CO was used as a tracer for LD vehicle emissions assuming that diesel trucks and LD vehicles emit similar amounts of CO per vehicle-km traveled. This assumption is questionable especially in 2006 since CO emissions have been reduced more for LD vehicles than for MD/HD diesel trucks (e.g. Bishop and Stedman, 2006; Burgard et al., 2006). Fuel economy, and thus CO_2 emissions per vehicle-km traveled have changed little in the last 10 years (Heavenrich, 2006).

Diesel contributions to CO_2 concentrations in the mixed traffic bore were calculated from observed traffic counts, estimated fuel economies, and known fuel properties using eq 2.3a. This is similar to the method used previously by Kirchstetter et al. (1999a), but is revised to include MD trucks explicitly rather than counting half of them as HD trucks.

$$\frac{\Delta[\mathrm{CO}_2]_{1,D}}{\Delta[\mathrm{CO}_2]_1} = \frac{\rho_D w_D (f_{hd}U_{hd} + f_{md}FU_{mdD})}{\rho_D w_D (f_{hd}U_{hd} + f_{md}FU_{mdD}) + \rho_G w_G (f_{ld}U_{ld} + f_{md}(1-F)U_{mdG})} \qquad (2.3a)$$

LD vehicle contributions to CO_2 concentrations in bore 1 were subsequently calculated as

$$\Delta[CO_2]_{1,G} = \Delta[CO_2]_1 - \Delta[CO_2]_{1,D} \qquad (2.3b)$$

In eq 2.3a, f_x are the observed fractions of total vehicles that are LD, MD, and HD vehicles. F is the fraction of MD vehicles equipped with diesel engines, as determined from truck census data for the U.S. (TIUS, 1992; VIUS, 1997; VIUS, 2002). For 1997, F = 0.42, and by extrapolating to 2006, F was projected to have increased to 0.53. Gasoline and diesel (subscripts G and D, respectively) fuel densities ρ and carbon weight fractions w are from Kirchstetter et al. (1999a). Estimates of fuel consumption rates by vehicle category are presented in Table 2.3; these are derived from uphill traffic results in the Ft. McHenry tunnel reported previously by Pierson et al. (1996), and an extrapolation of in-use truck census data to 2006. Only the *relative* magnitudes of fuel consumption for different vehicle categories matter for the CO_2 apportionment in eq 2.3a; absolute amounts of CO_2 emitted inside the tunnel are measured directly to calculate emission factors via eq 2.1.

Table 2.3 Parameters used for bore 1 CO_2 apportionment in eq 2.3.

Parameter	**Symbol**	**Value (L/100 km)**
LD vehicle fuel consumption	U_{ld}	10.3
MD diesel fuel consumption	U_{mdD}	27.0
MD gasoline fuel consumption	U_{mdG}	28.4
HD diesel fuel consumption	U_{hd}	49.5

2.3 Results

2.3.1 Traffic Characterization.

Table 2.4 shows traffic volumes by vehicle category observed on each day for 1200-1400h in bore 1 (mixed traffic) and 1600-1800h in bore 2 (LD only). Midday traffic volumes in bore 1 are approximately half those observed in bore 2 during the afternoon peak period. The MD and HD truck fraction in bore 2 is low (<1%) in contrast to midday traffic in bore 1, which includes 7.3 ± 0.6% MD plus HD trucks. Since bore 2 opens to eastbound (uphill) traffic around noon on weekdays, many eastbound LD vehicles use bore 2 instead of bore 1 in the afternoon, increasing the MD/HD truck fraction in bore 1 compared to morning hours.

Figure 2.2 shows a histogram of light-duty vehicle speeds from bore 2 including data from 2006 and 1997 for comparison. Average LD vehicle speeds were similar in both years (57 and 59 km h^{-1}). The mean speed of all HD trucks observed driving through bore 1 (N = 702) was 64 km h^{-1}, which is similar to the mean truck speed from the 1997 study of 65 km h^{-1}. The average LD vehicle model year was 2000.3 ± 0.2 (N = 1711 vehicles). The average model year of diesel trucks was 2000 ± 1.6 for MD trucks (N = 22) and 1997 ± 2.2 for HD trucks (N = 24). This matches results of an earlier study from 1997 (Kirchstetter et al., 1999a), which found average LD vehicle and HD truck ages of 6 and 9 years, respectively, corresponding to the same vehicle ages as the present study. Figure 2.3 shows a map of the greater San Francisco Bay area with registration locations for a sample of ~1600 LD vehicles that traveled through bore 2 of the Caldecott tunnel between 1600 – 1800h on Aug. 3 and 7. This shows that the highest fraction of vehicles comes from the area surrounding Concord, CA.

2.3.2 Carbon Particle Comparisons.

BC concentrations measured in this study with the aethalometer agree well with those measured using TOA, as shown in Figure 2.4. This is despite reports of large discrepancies between BC measured with these two methods (Kirchstetter and Novakov, 2007). On average, the aethalometer yielded BC concentrations that were 1.09 and 1.21 times those determined by TOA in tunnel bores 1 and 2, respectively. Aethalometer-derived BC emission factors were therefore higher than those calculated from TOA.

Table 2.4 Traffic volumes (vehicles h^{-1}) in Caldecott tunnel, summer 2006.

Date	LD	MD	HD	MD + HD fraction of total
	2-axle/4-tire	2-axle/6-tire	≥ 3-axle	
Bore 1 (1200-1400 h)				
18-Jul	1877	88	58	7.2%
19-Jul	1897	106	49	7.6%
20-Jul	1949	111	50	7.6%
21-Jul	2011	105	64	7.7%
24-Jul	1853	105	57	8.0%
25-Jul	1835	89	54	7.2%
26-Jul	1933	99	48	7.1%
27-Jul	2308	90	52	5.8%
Average [a]	1958 ± 127	99 ± 8	54 ± 4	7.3% ± 0.6%
Bore 2 (1600-1800 h)				
31-Jul	3955	13	0	0.3%
1-Aug	3973	24	0	0.6%
2-Aug	3660	30	0	0.8%
3-Aug	3913	16	0	0.4%
7-Aug	3783	19	0	0.5%
8-Aug	3524	26	0	0.7%
9-Aug	3732	28	1	0.8%
10-Aug	3861	27	0	0.7%
Average [a]	3800 ± 131	23 ± 5	0 ± 0	0.6% ± 0.2%

[a] Reported as mean ± 95% confidence interval.

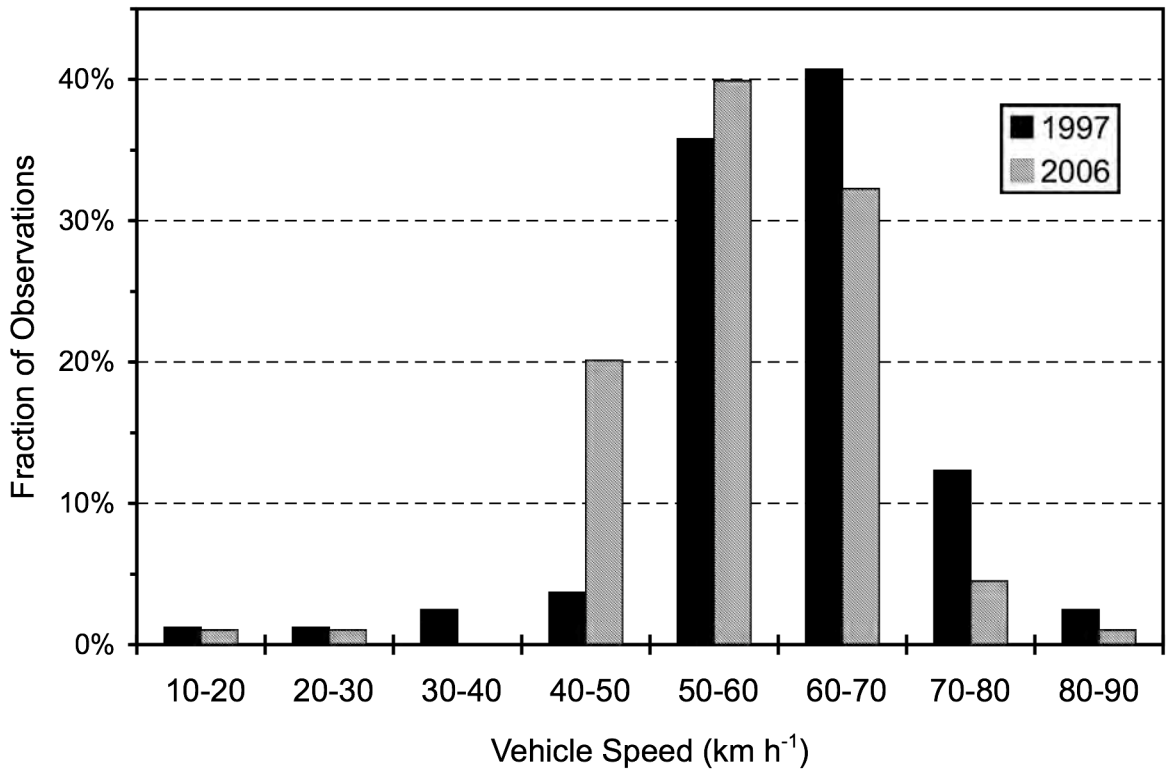

Figure 2.2 Vehicle speed distribution for light-duty vehicles in bore 2 based on average values per vehicle through the tunnel. Mean vehicle speed was 57 km h^{-1} (N=288 vehicles) in 2006, and 59 km h^{-1} (N=27) in 1997.

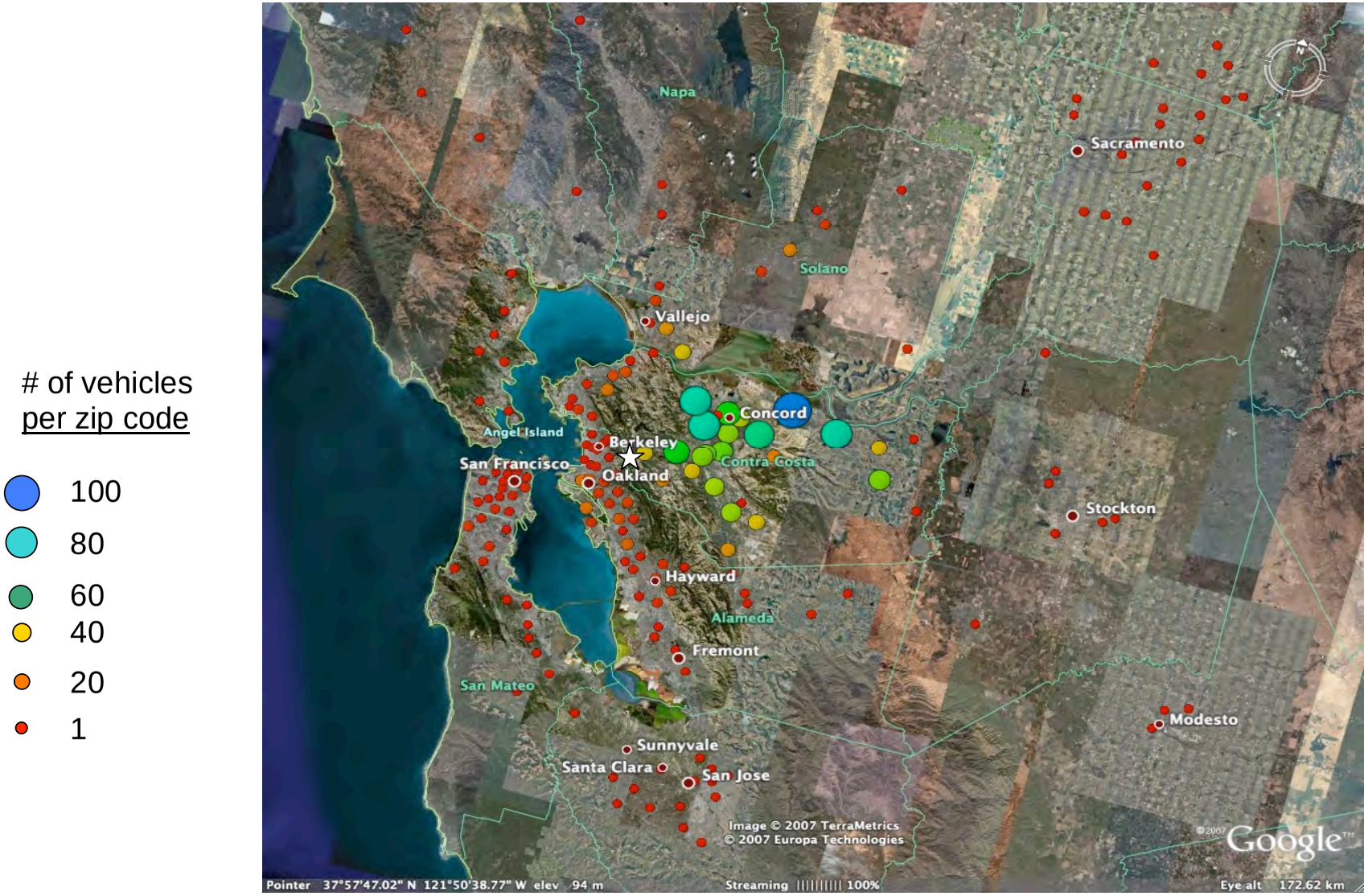

Figure 2.3 This map shows the LD vehicle registration data in terms of number of vehicles per registered zip code. A sample of 1822 license plates were transcribed from camera images of traffic collected on August 3rd and 7th. 90% of the transcribed license plates were succesfully matched with registration data. The white star shows the location of the Caldecott tunnel.

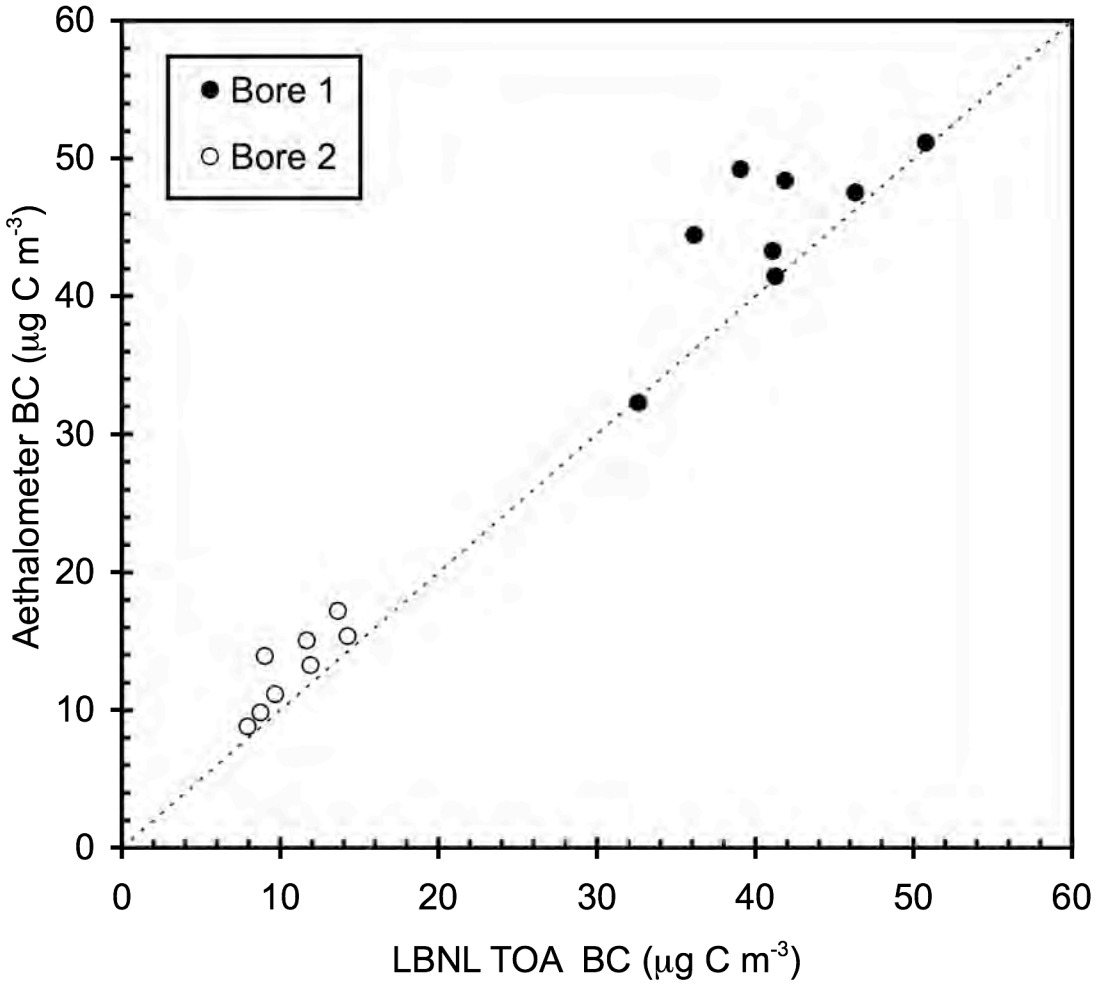

Figure 2.4 Black carbon concentrations measured with two different methods: aethalometer (y-axis) and thermal optical analysis of quartz filters (x-axis). Note the good agreement between the two methods, which can be viewed by proximity of the data points to the dashed line.

Ten filter samples were analyzed by Sunset Laboratory (Tigard, OR) using the NIOSH TOT method to compare with parallel analysis of the same samples by the LBNL TOA method. This comparison was done because previous Caldecott tunnel data from 1997 used the NIOSH TOT method, whereas this study used the LBNL TOA method. A comparison of carbon contents of particulate matter samples analyzed by the two methods is shown in Figure 2.1. While different TOA methods can yield large differences in OC and BC contents, there is generally good agreement when the analyzed samples do not contain organic compounds that pyrolyze to form char during analysis (Watson et al., 2005; Kirchstetter and Novakov, 2007). Charring was not observed during analysis of any of the tunnel samples in this study. As a result, the OC and BC contents measured with the LBNL and NIOSH TOA methods are in good agreement.

2.3.3 Emission Factors.

Table 2.5 shows emission factors for LD vehicles and MD/HD diesel trucks, calculated using eq 2.1 through 2.3. Both NO_x and $PM_{2.5}$ emission factors decreased between 1997 and 2006 for all vehicle categories. The largest decrease was for NO_x from LD vehicles.

Note that reported emission factors for MD/HD diesel trucks in Table 2.5 are less certain than corresponding results for LD vehicles due to the need to apportion pollutant concentrations in the mixed traffic bore (bore 1) between gasoline and diesel contributions. Values reported in Table 2.5 for 1997 differ from those in Kirchstetter et al. (1999a) due to changes in data analysis methods (eqs. 2.2 and 2.3). The diesel NO_x emission factor for 1997 is 36% higher than reported previously, and lies at the high end of the range reported in other studies as reviewed by Jimenez et al. (2000).

Also note that the measured OC concentrations used to calculate emission factors have been corrected for the positive sampling artifact (see the Methods section), and have been multiplied by 1.4 to account for the mass of hydrogen and oxygen (Gray et al., 1986), as was done by Kirchstetter et al. (1999a). Thus, we report organic mass (OM) emission factors, an estimate of total particulate organic mass, not just the mass of organic carbon. Carbon particles (BC plus OM) account for 76 ± 23% and 91 ± 21% of $PM_{2.5}$ mass for LD vehicles and diesel trucks, respectively.

Although absolute PM emission factors have decreased since 1997, ratios of black carbon to organic mass (BC/OM) and black carbon to total carbon (BC/TC) did not change significantly. The BC/OM ratio was 0.71 ± 0.15 and 2 ± 1 for LD vehicles and MD/HD diesel trucks, respectively. Likewise, the BC/TC ratio was 0.42 ± 0.08 and 0.7 ± 0.3 for LD vehicles and diesel trucks, respectively. BC dominates $PM_{2.5}$ emissions for diesel trucks.

Table 2.5 also shows absorption, scattering, and extinction cross-section emission factors. The optical cross-section emission factors for diesel trucks are an order of magnitude larger than for LD vehicles.

2.4 Discussion

2.4.1 Emission Trends.

NO_x. Bishop and Stedman (2006) measured LD vehicle NO emission factors by remote sensing in Los Angeles in 1999, 2001, 2003, and 2005. As shown in Figure 2.5a, this study indicates a 9% per year reduction in the NO emission factor from LD vehicles, similar to the 7% per year reduction observed at the Caldecott tunnel. Absolute NO emission factors in Los Angeles are higher than NO_x emissions at the Caldecott tunnel due to an older vehicle fleet (6.5 versus 5.7 years old). Note that NO emission factors by remote sensing are reported as NO_2 equivalents to allow for comparison with tunnel results.

Burgard et al. (2006) measured HD diesel truck NO and NO_2 emission factors by remote sensing at two Colorado locations in 2005, as shown in Figure 2.5b. Dumont is at an elevation of 2530 m with a +1.8% grade, and Golden is at 1695 m with a grade of +0.2%. Burgard et al. suggest that the difference in NO_x between these two sites is likely due to altitude effects. NO at Golden is 20% below the 2006 Caldecott tunnel result, and NO at Dumont is 17% higher. When compared to remote sensing data at the same locations from 1999 (Bishop et al., 2001), the annual rate of reduction in NO_x emission factor at Golden was similar to the Caldecott tunnel. The lack of change in NO at Dumont is attributed to a different engine calibration that is allowed under high-altitude operating conditions (Stedman, 2007).

Table 2.5 Trends in Measured LD Vehicle and MD/HD Diesel Truck Emission Factors. [a]

		LD Vehicles			MD/HD Diesel Trucks		
pollutant	**units**	**1997**	**2006**	**% change**	**1997** [b]	**2006**	**% change**
NO_x [c]	$g\ kg^{-1}$	9.0 ± 0.4	3.0 ± 0.2	−67 ± 3	57 ± 7	40 ± 3	−30 ± 9
$PM_{2.5}$	$g\ kg^{-1}$	0.11 ± 0.01	0.07 ± 0.02	−36 ± 17	2.7 ± 0.3	1.4 ± 0.3	−48 ± 12
TOA OM [d]	$g\ kg^{-1}$	0.05 ± 0.01	0.031 ± 0.005	−38 ± 16	0.59 ± 0.08	0.41 ± 0.07	−31 ± 14
TOA BC [e]	$g\ kg^{-1}$	0.035 ± 0.004	0.022 ± 0.004	−37 ± 13	1.4 ± 0.6	0.86 ± 0.07	−39 ± 26
Aeth BC [f]	$g\ kg^{-1}$		0.026 ± 0.004			0.92 ± 0.07	
Sct Cross-sec[g,i]	$m^2\ kg^{-1}$		0.10 ± 0.02			2.0 ± 0.3	
Sct Cross-sec[h,i]	$m^2\ kg^{-1}$		0.090 ± 0.009			1.1 ± 0.2	
Abs Cross-sec[h,i]	$m^2\ kg^{-1}$		0.20 ± 0.05			4.4 ± 0.8	
Ext Cross-sec[h,i]	$m^2\ kg^{-1}$		0.29 ± 0.05			5.6 ± 1.0	

[a] Emission factors reported per unit mass of fuel burned. All values are mean ± 95% confidence interval.
[b] Diesel truck emission factors for 1997 differ from those reported previously due to changes in apportionment method (see text).
[c] NO_x is reported as NO_2 equivalents (i.e. a molecular mass of 46 g mol^{-1} was used to convert ppm to μg m^{-3}).
[d] OM is obtained by multiplying measured OC by 1.4 to account for mass of hydrogen and oxygen (Gray et al., 1986). OC is corrected for the positive sampling artifact by subtracting the quartz behind Teflon filter mass (see text).
[e] BC from thermal optical analysis of filters.
[f] BC reported as 2 hour average of continuous aethalometer data.
[g] Measured by nephelometer at λ = 530 nm.
[h] Measured by Cadenza at λ = 675 nm.
[i] As with all emission factors, the denominator is kg of fuel burned. These values should not be confused with mass specific cross sections in units of $m^2\ g^{-1}$ of particle mass.

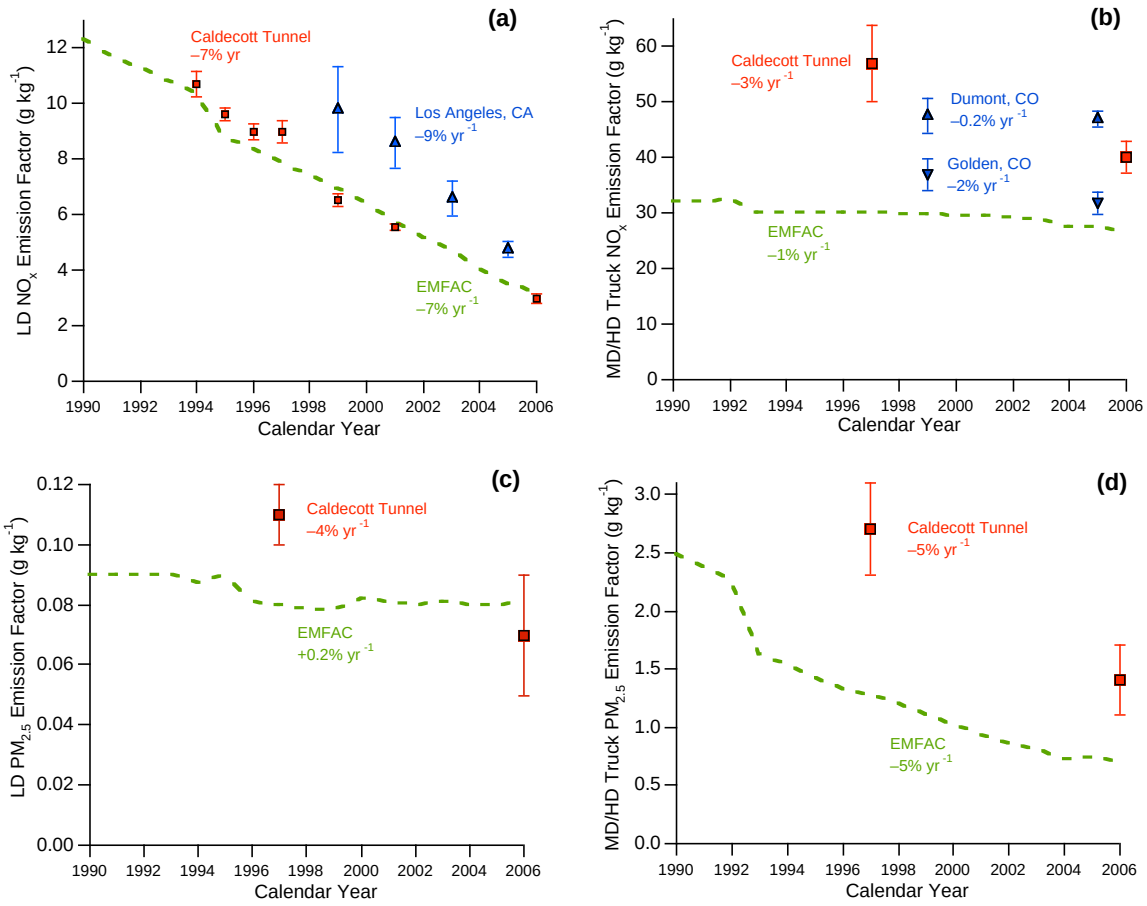

Figure 2.5 NO_x emission indices for (a) LD vehicles and (b) MD/HD trucks. $PM_{2.5}$ emission indices for (c) LD vehicles and (d) MD/HD diesel trucks. Tunnel studies are squares, and remote sensing studies are triangles, both shown as mean ± 95% confidence interval. EMFAC predictions shown as the dashed line. Caldecott tunnel and EMFAC yearly percent reductions are shown for 1997-2006, even when data prior to 1997 are shown. NO emission indices are shown as NO_2 equivalents for remote sensing studies.

2.4.2 Particulate Matter.

Geller et al. (2005) measured particulate matter emissions at the Caldecott tunnel in 2004. Their emission factors for LD vehicles and MD/HD diesel trucks was 0.07 ± 0.03 and 1.02 ± 0.06 g kg^{-1}, respectively, matching 2006 results from the Caldecott tunnel within the stated uncertainties (95% confidence interval). However, note that Geller et al. used a longer sample period in both bores (1200-1800h), whereas we measure bore 1 in the early afternoon (1200-1400h) and bore 2 in the late afternoon (1600-1800h). Thus, our average pollutant concentrations for bore 2 are more heavily weighted toward high-traffic conditions during rush hour, which lead to higher CO_2 concentrations. Note in Figure 2.6 that $\Delta[CO_2]$ is higher from 1600-1800h than 1200-1600h. Geller et al. note that their $\Delta[CO_2]$ in bore 2 is lower than reported by Kirchstetter et al. (1999a) and hypothesize that the change is due to increased fuel efficiency of the on-road vehicle fleet. This CO_2 difference is actually due to comparing 6-hour versus 2-hour average concentration levels.

2.4.3 Comparison to EMFAC.

EMFAC, a statistical model of on-road vehicle emissions (CARB, 2007), was used to predict light-duty vehicle and MD/HD diesel truck emissions. Emission factors for the San Francisco Bay area during the summers 1990 to 2006 are plotted in Figure 2.5. Idle emissions and cold engine-starts were not included in this analysis since vehicles driving through the tunnel were already warmed up. EMFAC brake-wear emissions were not included in $PM_{2.5}$ as eastbound vehicles are generally accelerating or cruising after they enter the tunnel. Emission factors were calculated at vehicle speeds matching averages for LD vehicles and diesel trucks observed in the tunnel. EMFAC labels in Figure 2.5 show yearly percent reductions from 1997-2006 for direct comparison with the Caldecott tunnel results. EMFAC predicts matching rates of emission reduction versus those observed at the tunnel for LD NO_x and diesel truck $PM_{2.5}$. EMFAC predicts lower rates of reduction for LD $PM_{2.5}$ and diesel NO_x relative to the tunnel results.

2.4.4 LD vehicle vs. MD/HD diesel truck.

NO_x and particle emission factors for diesel trucks are higher than LD vehicles by an order of magnitude or more (Table 2.5). NO_x from diesel trucks has decreased at a slower rate than for LD vehicles; the ratio of HD to LD emission factor for NO_x increased from 6 ± 1 to 13 ± 1

between 1997 and 2006, which indicates an increase in the *relative* importance of diesel trucks as a source of NO_x emissions. Comparing absolute values of LD vs. diesel truck PM emission factors may be misleading due to the load-sensitivity of diesel engines for which BC emissions especially are expected to increase for uphill driving. In this case, comparing percent reductions is preferred. At first glance, Table 2.5 suggests that $PM_{2.5}$ emission factors for diesel trucks decreased more since 1997 than for LD vehicles. Given associated uncertainties, however, the rate of decrease for $PM_{2.5}$ emission factors is not statistically different for the two vehicle categories. Since sulfate comprised only 1.8% of $PM_{2.5}$ mass from HD trucks in 1997 (Kirchstetter et al., 1999a), the introduction of ultra-low sulfur diesel fuel in 2006 is likely to have played a small direct role in $PM_{2.5}$ reduction thus far. This fuel change is intended mainly to enable use of catalytic exhaust after-treatment devices starting in 2007. Therefore, $PM_{2.5}$ emission decreases reported here are attributed to vehicle technology improvements that occurred prior to the fuel change.

The scattering cross-section emission factors measured by the nephelometer and Cadenza are nearly the same for LD vehicles, but differ by a factor of two for diesel trucks (Table 2.5). This is likely due to the wavelength dependence of light scattering by diesel engine BC emissions. Single-scattering albedo ω is an important parameter in assessing the climate and visibility impacts of an aerosol, and is calculated by taking the ratio of scattering to extinction coefficient. Using emission factors measured by Cadenza shown in Table 2.5, ω was found to be 0.31 ± 0.06 and 0.20 ± 0.05 for LD vehicles and diesel trucks, respectively. Two caveats should be noted. First, ω is a strong function of wavelength. Values of ω measured by Cadenza at $\lambda = 675$ nm are expected to be lower than atmospheric values typically reported at $\lambda = 550$ nm. Second, the relatively fresh aerosol found in the tunnel has not significantly aged in the atmosphere.

2.4.5 Modal Effects.

In order to apportion pollutant concentrations in bore 1 accurately, the emission ratio, $\Delta[P]/\Delta[CO_2]$, for LD vehicles needs to be well-represented by bore 2 measurements. Since the mean vehicle speed in bore 2 from 1600-1800h is slightly lower than bore 1 from 1200-1400h (Kirchstetter et al., 1999a), driving mode effects (i.e., effects due to changes in vehicle speed and engine load) on $\Delta[P]/\Delta[CO_2]$ may be an issue. Modal effects on LD vehicle CO and NO_x

emission factors have already been discussed for the Caldecott tunnel (Kirchstetter et al., 1999b; Kean et al., 2003). These studies found that both CO, and to a lesser extent, NO_x emission factors increased with vehicle speed through the tunnel. Here we consider modal effects on BC emissions from LD vehicles.

Figure 2.6 plots values of Δ[CO], Δ[BC], Δ[CO_2], Δ[BC]/Δ[CO], and Δ[BC]/Δ[CO_2] measured in bore 2. Generally, as the afternoon progresses vehicle speeds decrease due to increased traffic. It can be seen that CO_2, BC, and CO concentrations increase during the afternoon rush hour due to increased traffic volumes. Figure 2.6 also shows that BC and CO_2 increase by similar relative amounts. Thus, Δ[BC]/Δ[CO_2] does not show any trend over the afternoon, whereas Δ[BC]/Δ[CO] increases over the same period. This illustrates an added advantage of using CO_2, rather than CO, as the basis for tracking LD vehicle emissions: Δ[BC]/Δ[CO_2] is more stable than Δ[BC]/Δ[CO]. The lack of any trend in Δ[BC]/Δ[CO_2] (proportional to BC emission factor) in Figure 2.6 suggests that LD vehicle emissions of BC per unit fuel do not show strong dependence on driving mode over the range of uphill driving conditions observed here.

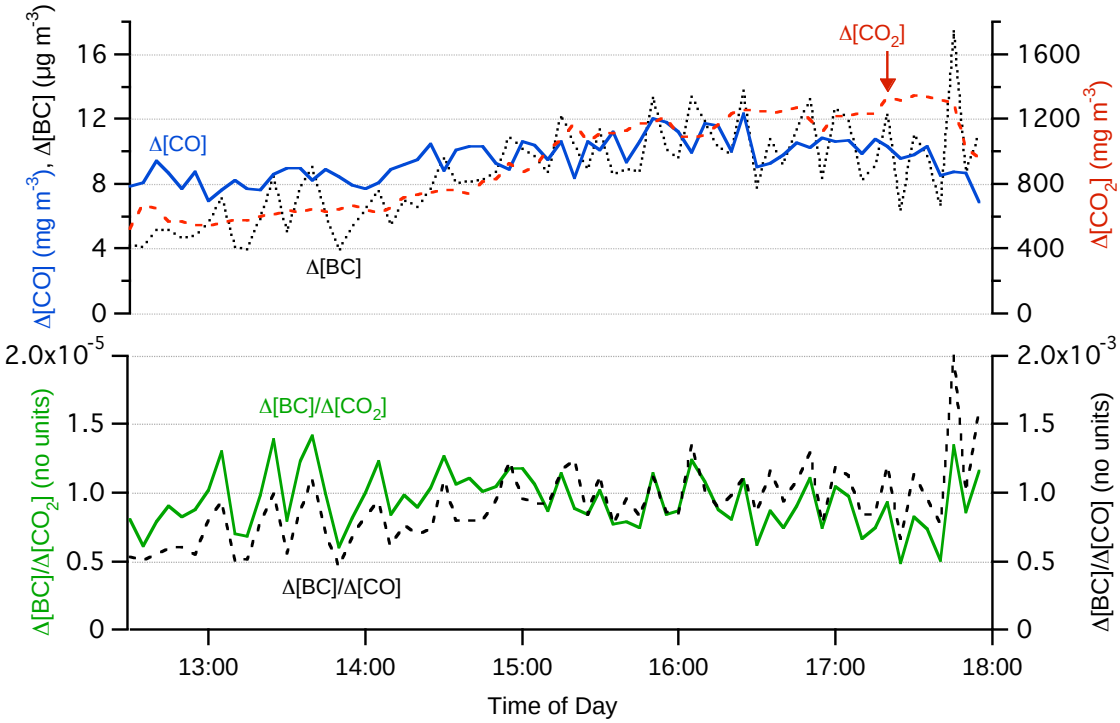

Figure 2.6 Pollutant concentrations and BC ratios to CO and CO_2. Five minute averages from 12:30 to 18:00 h, averaged over the eight sampling days for bore 2. Top: pollutant concentrations (exit-entrance) of CO, black carbon, and CO_2. Bottom: ratios of Δ[BC] to Δ[CO] and Δ[CO_2].

3. Particle Number Emissions and Size Distributions

3.1 Introduction

Particulate matter emissions from motor vehicles are regulated on a mass basis, whereas the number of particles emitted is currently unregulated. Particulate mass and number concentrations show little correlation since most particles are emitted in the nuclei mode (particle diameter D_p < 50 nm); these particles have negligible mass. There are not nearly as many particles emitted in the accumulation mode (100 < D_p < 2000 nm), but these particles are typically responsible for the majority of exhaust particulate mass (Kittelson, 1998).

Particles of various sizes and compositions originate from different phases of the combustion process. Accumulation mode particles in diesel engines are carbonaceous soot agglomerates, formed early in the combustion process within fuel-rich pockets inside the engine cylinder. Nuclei mode particles are formed in diesel and gasoline engines when hydrocarbons and sulfates, stemming from fuel and vaporized lubricating oil, nucleate as exhaust dilutes and cools. The nuclei mode is highly dependent on the degree of supersaturation of the nucleating species. High concentrations of accumulation mode particles in engine exhaust suppress particle formation by scavenging or sorbing precursors needed for nucleation to occur (Kittelson et al., 2006a).

Particle size is important in determining health and environmental impacts of PM. Ultrafine particles (D_p < 100 nm) have been identified as a particular concern for human health (Pope et al., 1995; Pope and Dockery, 2006). Laboratory studies have shown that particles that are non-toxic with D_p ~ 1 μm can be toxic when D_p ~ 10 nm (Seaton et al., 1995; Donaldson et al., 1996). Nuclei mode particles can penetrate deeply into the lung and enter the circulatory system, whereby they may deposit in other vital organs such as the brain or heart (Kennedy, 2007). It has been suggested that adding particle number-based air quality standards and/or engine emissions limits to the current mass-based limits could help in identifying and reducing adverse health impacts (Kennedy, 2007). Since nuclei mode particles in the atmosphere coagulate with accumulation mode particles in minutes to hours, health effects are especially detrimental to those in close proximity of fresh emissions. The residence time of accumulation mode particles in the atmosphere is ~ 1 week, orders of magnitude longer than that of ultrafine particles. Light

absorption is stronger than scattering for soot particles in the accumulation mode with important implications on regional visibility degradation and global warming (Ramanathan and Carmichael, 2008).

There is an ongoing debate about the importance of gasoline vs. diesel engines as sources of fine PM (Johnson et al., 2005). Results from Chapter 2 indicate that on average, diesel engines emit an order of magnitude more PM mass than gasoline engines, per unit of fuel burned. But the *relative* importance of gasoline vehicles as a source of PM is higher when considering number rather than mass emissions; the fraction of particles that are emitted in the nuclei mode is higher in gasoline vs. diesel engines (Graskow et al., 1998; Maricq et al., 1999a; Maricq et al., 1999b; Kayes et al., 2000; Johnson et al., 2005). However, variations in sampling protocols, both in terms of driving cycles and PM measurement methods (Ayala et al., 2003), and a lack of definitive "real-world" studies, have made direct comparison of gasoline vs. diesel particle number emissions difficult. Further complications arise due to dilution and atmospheric aging of aerosols; semi-volatile organic compounds that are emitted in the particle-phase from engines can evaporate upon dilution in the atmosphere. These gas-phase species may undergo subsequent photochemical reactions to form secondary organic aerosol (Robinson et al., 2007).

This paper provides a unique opportunity to directly compare fresh particle number emissions from a large sample of LD vehicles and diesel trucks under similar driving conditions, using identical particle analyzers and sampling protocols. Size-segregated particle number emissions were measured in a highway tunnel, and thus the aerosol was freshly emitted without undergoing atmospheric aging. Results are reported separately for light-duty (LD) vehicles, and for medium- (MD) and heavy-duty (HD) diesel trucks.

3.2 Experimental Methods

3.2.1 Field Measurements.

Pollutant concentrations were measured simultaneously at the traffic entrance (west end) and exit (east end) of the Caldecott tunnel, as described previously in Chapter 2. Particle analyzers were located in the exhaust duct directly above the traffic. Sample air was carried from the sample inlet, located ~15 cm below the ceiling of the traffic bore, through approximately 1 m of

conductive silicone tubing to the particle analyzers. An upper size cutoff of 2.5 μm was achieved using sharp cut cyclones (BGI, Waltham, MA, model VSCCA). Particle size distributions were measured at each end of the tunnel using TSI (Shoreview, MN) model 3080L scanning mobility particle sizers (SMPS) paired with TSI model 3025A ultrafine condensation particle counters (CPC). This system was configured to measure number concentration as a function of particle size for $10 < D_p < 290$ nm. Separate CPCs were used to determine total particle number concentrations. An ultrafine water CPC (TSI model 3786) was used to measure particle number concentrations ($D_p > 3$ nm) at the traffic exit, whereas a butanol-based TSI 3022A CPC ($D_p > 7$ nm) was used at the traffic entrance. Due to the high particle concentrations inside the tunnel, the CPC sample air was diluted prior to being analyzed. The sample line was split into two parallel lines. One line passed through an orifice and the other through a HEPA filter; the lines were recombined prior to passing through the CPC. The pressure drop across the orifice caused a large and stable fraction of the sample flow to pass through the lower pressure drop line where the HEPA filter removed all of the particles. Because 2 different orifices were used throughout the measurement campaign, dilution ratios varied as follows. All measurements in the mixed-traffic bore (bore 1) had a dilution ratio of 15.2. Measurements in the LD-only bore (bore 2) were undiluted except for August 9 and August 10, which had dilution ratios of 7.9 and 15.2, respectively. Particle measurements at the tunnel entrance were not diluted.

3.2.2 Data Analysis.

Two-hour average particle number concentrations and size distributions were calculated for each sample day in both traffic bores. Particle number emission factors, E_N (# of particles emitted per kg fuel burned), were calculated by eq 3.1,

$$E_N = \frac{\Delta[\mathrm{N}]}{\Delta[\mathrm{CO_2}] + \Delta[\mathrm{CO}]} w_c \cdot 10^{12} \qquad (3.1)$$

where $\Delta[\mathrm{N}]$ is the background-subtracted (i.e. tunnel exit – entrance) particle number concentration in units of # cm^{-3}, $\Delta[CO_2]$ and $\Delta[CO]$ are background-subtracted concentrations in units of mg C m^{-3}, and w_c = 0.85 or 0.87 is the mass fraction of carbon in gasoline and diesel fuel, respectively. Size-segregated particle number emission factors, $dE_N/d\log D_p$, were calculated by applying eq. 3.1 separately for each of the 102 particle size bins (10-290 nm size range) from

the SMPS data. Size distributions at the tunnel entrance (background) were measured on 2 days in both bores. The average entrance size distribution for each traffic bore was used for the background subtraction in eq 3.1 on all days.

To calculate LD vehicle emission factors, eq 3.1 was used directly with pollutant concentrations from the LD-only traffic bore. To calculate diesel truck emission factors, pollutant concentrations from the mixed-traffic bore were apportioned between LD vehicles and diesel trucks as described in detail in Chapter 2. Briefly, observed traffic counts and estimated fuel consumption rates by vehicle category were used to apportion contributions to total CO_2 emissions inside the tunnel. Then particle emissions from diesel trucks were estimated by subtracting LD vehicle emissions (measured in bore 2) from totals observed in the mixed-traffic bore (bore 1).

3.3 Results and Discussion

Figure 3.1 shows average size distributions for the tunnel exit (east end) and entrance (west end) in both traffic bores. The error bars represent the day-to-day variation (1σ) in 2-hr average size distributions. It can be seen that tunnel exit concentrations are considerably higher than background (entrance) values for all particle diameters shown.

Figure 3.2 shows number (a) and volume (b) emission factors as a function of particle size separately for LD vehicles and diesel trucks (Table A1 and A2 in Appendix A contains the data used to create Figure 3.2). For all particle sizes measured, diesel trucks emit at least an order of magnitude more particles than LD vehicles, per unit of fuel burned. The *relative* importance of LD vehicles as a source of particle number emissions increases as D_p decreases. Diesel truck emissions have a peak at D_p ~ 16 nm in the particle number distribution. LD vehicles show a peak in the number distribution slightly higher at D_p ~ 22 nm. Figure 3.2b shows a peak in particle volume, and thus PM mass, at D_p ~ 150 nm for LD vehicles. For diesel trucks, the particle volume emissions appear to be at or near a plateau at D_p = 290 nm where SMPS scans ended. Kleeman et al. (2000) found a single peak in particle mass distributions between 100 and 200 nm for both gasoline and diesel vehicles.

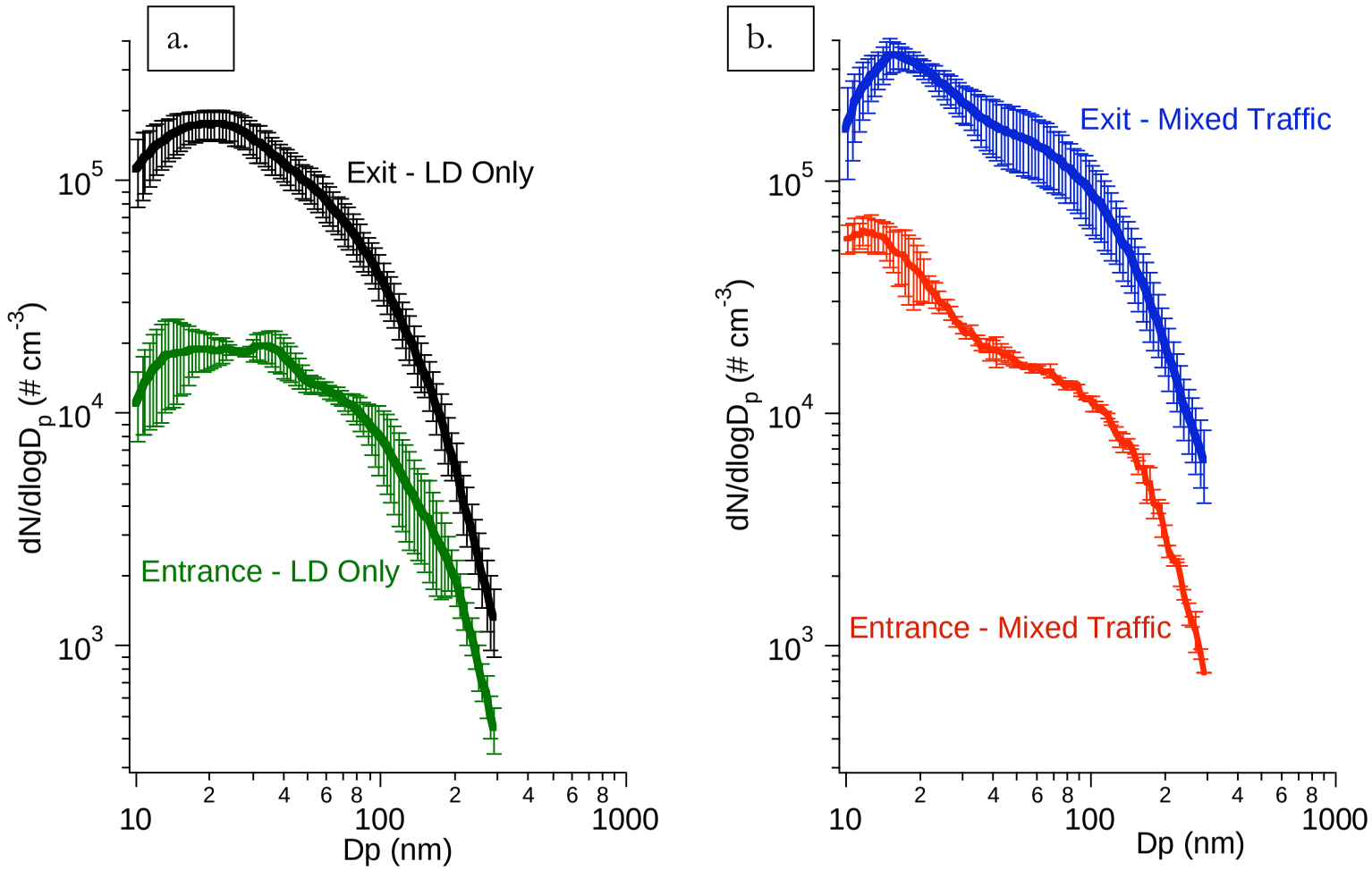

Figure 3.1 Average particle size distributions measured at both ends of the LD-only bore (a) and mixed traffic bore (b). Error bars represent the day-to-day variation (1σ) in 2-hr average size distributions.

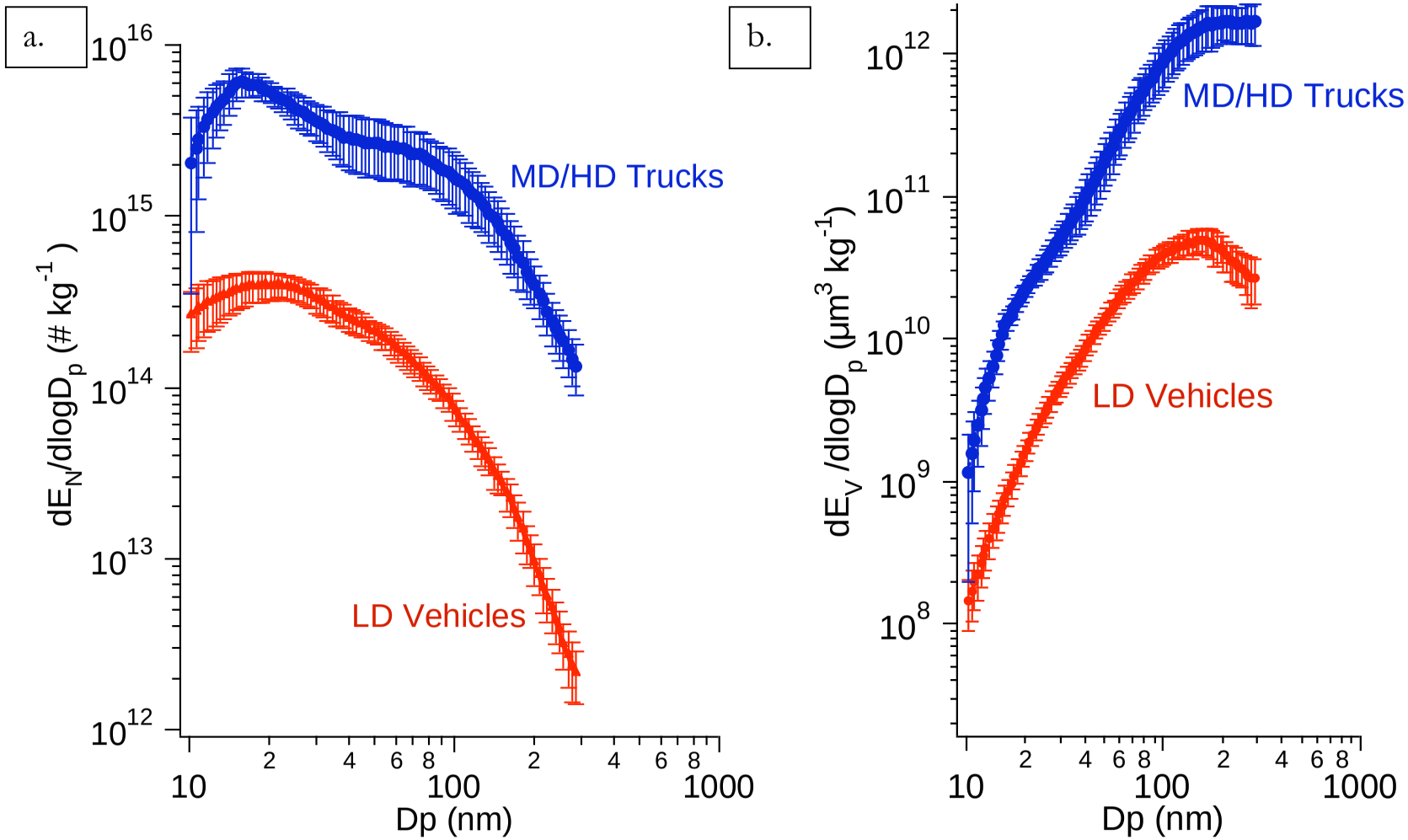

Figure 3.2. Size-resolved emission factors for (a) particle number and (b) volume.

3.3.1 Particle Number Emissions

Daily 2-hr average particle number concentrations at both ends of the tunnel are shown in Table 3.1. Number concentrations are shown both from the CPC measurements, and from integration of the measured size distributions. Because the standalone CPC counted particles below the lower limit of the SMPS, CPC-derived number concentrations are higher than obtained by integrating over the SMPS-derived size distributions.

Table 3.2 shows particle number and volume emission factors. Error bars reflect day-to-day variability (95% confidence interval) in the calculated emission factors. Results calculated using the CPC data agree with size distribution integrations to within the stated uncertainty. Diesel trucks dominate particle number emissions per unit of fuel burned with an emission factor ratio of 8 ± 5.

Particle number emission rates were also measured in the Caldecott tunnel during summer 1997 using a TSI model 3760, which measured particles with $D_p > 10$ nm (Kirchstetter et al., 1999). Note that the diesel truck emission factor for 1997 shown in Table 3.2 is slightly higher than reported in Kirchstetter et al. due to changes in data analysis methods (see Chapter 2). Direct comparison between results from 2006 and 1997 is complicated because of the differences in the lower limit of particle sizes measured (10 nm in 1997 vs. 3 nm in 2006). However, number emissions were lower in 2006 despite the inclusion of particles in the 3-10 nm range; had the measurements in 2006 and 1997 used the same CPC, the reduction in emission rate would have been greater. The conclusion therefore is that particle number emission rates for both LD vehicles and diesel trucks have decreased since 1997, at least for the vehicle fleets and driving conditions observed at the Caldecott tunnel. There is no statistically significant difference in the diesel/gasoline emission factor ratio for 2006 vs. 1997.

Emission factors size distributions were integrated over select ranges of D_p to find number emissions for particles with diameters less than 30, 50, and 100 nm (N_{30}, N_{50}, and N_{100} respectively). As shown in Table 3.3, the ratio of particles with $D_p < 30$ nm to total particle number (N_{30}/N) was found to be approximately 0.6 for both LD vehicles and diesel trucks. This indicates that the majority of particles emitted are in the nuclei mode, as expected. Values

Table 3.1 Measured 2-hour average particle number concentrations

Bore 1

Date	Location	CPC [a, c] # cm^{-3}	SMPS [b, c] # cm^{-3}
Tue, Jul 18	East	2.40×10^5	2.41×10^5
	West	8.11×10^4	
Wed, Jul 19	East	4.17×10^5	1.82×10^5
	West	1.09×10^5	
Thu, Jul 20	East	3.02×10^5	1.75×10^5
	West	7.71×10^4	2.96×10^4
Fri, Jul 21	East	3.35×10^5	1.93×10^5
	West	1.04×10^5	3.51×10^4
Mon, Jul 24	East	2.65×10^5	2.67×10^5
	West	8.27×10^4	
Tue, Jul 25	East	2.11×10^5	2.75×10^5
	West	1.07×10^5	
Wed, Jul 26	East	2.63×10^5	2.31×10^5
	West	8.39×10^4	
Thu, Jul 27	East	2.60×10^5	2.66×10^5
	West	6.86×10^4	
mean ± std dev	East	$(2.9 \pm 0.7) \times 10^5$	$(2.3 \pm 0.4) \times 10^5$
	West	$(8.9 \pm 1.5) \times 10^4$	

Table 3.1 Continued

Bore 2

Date	Location	CPC [a, c] # cm^{-3}	SMPS [b, c] # cm^{-3}
Mon, Jul 31	East	1.77×10^5	1.46×10^5
	West	3.75×10^4	
Tue, Aug 01	East	1.60×10^5	1.04×10^5
	West	3.78×10^4	
Wed, Aug 02	East	1.60×10^5	1.43×10^5
	West	3.36×10^4	
Thu, Aug 03	East	1.48×10^5	1.28×10^5
	West	2.93×10^4	
Mon, Aug 07	East		1.34×10^5
	West		
Tue, Aug 08	East	1.61×10^5	1.30×10^5
	West	3.55×10^4	
Wed, Aug 09	East	2.60×10^5	1.32×10^5
	West	2.73×10^4	1.69×10^4
Thu, Aug 10	East	3.04×10^5	1.20×10^5
	West	3.36×10^4	1.72×10^4
mean ± std dev	East	$(2.0 \pm 0.6) \times 10^5$	$(1.3 \pm 0.1) \times 10^5$
	West	$(3.4 \pm 0.4) \times 10^4$	

[a] Measurements were made with a water-based CPC ($D_p > 3$ nm) at the exit (east end), and a butanol-based CPC ($D_p > 7$ nm) at the entrance (west end) of the tunnel

[b] Size distributions were integrated from $10 < D_p < 290$ nm

[c] Blank entries indicate that no measurement was made or data not available

reported here are slightly lower than reported in Johnson et al. (2005) (see Table 3.3). N_{50}/N and N_{100}/N reported in Imhof et al. (2006) for the Plabutsch tunnel are considerably lower than in the present study because of differences in the range of measured particle size (18 – 700 nm in Imhof et al. vs. 10 – 290 nm in the present study).

3.3.2 Particle Volume Emissions

Particle volume emission factors were calculated by integrating the number size distributions with $\frac{\pi}{6}D_p^3$ weighting. As shown in Table 3.2, the particle volume emission factor was 28 ± 11 times larger for diesel trucks than for LD vehicles. The diesel/gasoline emission factor ratio is larger for particle volume than for number because of the large mass of accumulation mode particles emitted by diesel trucks.

Particle volume emission factors as a function of D_p were integrated to find total volumes of particles emitted with diameters less than 30, 50, and 100 nm (V_{30}, $V_{50,}$ and V_{100} respectively). As shown in Table 3.3, the ratios of V_{30}/V and V_{50}/V were < 0.1, indicating that the majority of particle volume, and thus mass, is found in the accumulation mode. Kittelson et al. (2006ab) compared laboratory vs. on-road measurement methods for determining LD vehicle particle emissions. Laboratory results indicated that V_{30}/V was ~0.98, suggesting that the majority of particulate mass was in the nuclei mode. On-road results from Kittelson et al., however, agree with the conclusion found in the present study that the majority of particulate volume is in the accumulation mode (see Table 3.3). Also shown in Table 3.3 are values reported in Imhof et al. (2006) for the Plabutsch tunnel. Results are not directly comparable to Caldecott tunnel values because of the different particle size ranges measured, leading to the lower values reported in Imhof et al.

Table 3.2 Particle number and volume emission factors measured by the CPC and SMPS.

Emission Measure	Size Range	Year Measured	LD Vehicles	Diesel Trucks	Diesel/Gasoline Ratio [a]
E_N (# kg^{-1})					
	> 10 nm [b]	1997	$(4.6 \pm 1.3) \times 10^{14}$	$(7.1 \pm 3.3) \times 10^{15}$ [c]	15 ± 8
	> 3 nm [d]	2006	$(3.9 \pm 1.4) \times 10^{14}$	$(3.3 \pm 1.3) \times 10^{15}$	8 ± 5
	10 - 290 nm [e]	2006	$(2.8 \pm 0.4) \times 10^{14}$	$(4 \pm 1) \times 10^{15}$	14 ± 4
E_V (μm^3 kg^{-1})					
	10 - 290 nm [e]	2006	$(2.9 \pm 0.5) \times 10^{10}$	$(8 \pm 3) \times 10^{11}$	28 ± 11

[a] Diesel/gasoline ratio is unitless

[b] Kirchstetter et al. (1999) used a butanol CPC (TSI model 3760) to count particles D_p > 10 nm

[c] Result reported here is different than in Kirchstetter et al. (1999) due to a change in the apportionment method (see Chapter 2)

[d] Present study used a water CPC (TSI model 3786) to count particles D_p > 3 nm

[e] Integral of SMPS-derived particle number or volume as a function of particle size

Table 3.3 Comparison of N_x/N and V_x/V to other studies. This represents the fraction of particle number and volume to total measured particles that have $D_p < x$ nm. Note that these ratios are highly dependent on lower and upper size cutoffs (see footnotes).

	LD Vehicle				Diesel truck			
	This study [a] Caldecott	Johnson et al., 2005 [b]	Kittelson et al., 2006b [c]	Imhof et al., 2006 [d, e] Plabutsch	This study [a] Caldecott	Johnson et al., 2005 [b]	Kittelson et al., 2006b [c]	Imhof et al., 2006 [d, e] Plabutsch
N_{30}/N	0.61 ± 0.05	0.77 ± 0.09	0.62 ± 0.17		0.58 ± 0.06	0.76 ± 0.13	0.74 – 0.83 [f]	
N_{50}/N	0.80 ± 0.04			0.2 ± 0.1	0.74 ± 0.04			0.39 ± 0.07
N_{100}/N	0.96 ± 0.01			0.6 ± 0.2	0.91 ± 0.02			0.7 ± 0.1
V_{30}/V	0.027 ± 0.007	0.059 ± 0.017	0.022 ± 0.007		0.012 ± 0.003	0.008 ± 0.002	0.007 – 0.015 [f]	
V_{50}/V	0.09 ± 0.02			0.004 ± 0.002	0.035 ± 0.005			0.0050 ± 0.0008
V_{100}/V	0.36 ± 0.03			0.09 ± 0.02	0.20 ± 0.02			0.044 ± 0.006

[a] $10 < D_p < 290$ nm. Uncertainty estimates are 95% CI
[b] $10 < D_p < 300$ nm. Uncertainty estimates are standard deviations of the mean
[c] $8 < D_p < 283$ nm. Uncertainty estimates are standard deviations of the mean
[d] $18 < D_p < 700$ nm. Uncertainty estimates are 95% CI
[e] Direct comparison of this study to the others is misleading because of the difference in measured size range
[f] This represents the range of values reported for a variety of cruise and acceleration conditions

3.4 Air Sampling Issues

The Caldecott tunnel provides dilution of vehicle exhaust emissions prior to sampling. Given tunnel exit CO_2 concentrations of ~1000 ppm (0.1%) versus ~10% CO_2 in raw exhaust, we estimate that exhaust emissions were diluted inside the tunnel by a factor of about 100 prior to sampling. Particle number is not a conserved quantity, and the extent of exhaust dilution affects processes such as condensation, volatilization, and coagulation. It is also known that particle number concentrations fall off with distance from a roadway. Such effects of further dilution on fresh vehicle emissions moving away from the roadway to ambient/downwind locations were not observed in this study.

Note that the CPCs used to measure particle number concentrations at the tunnel entrance and exit were of different design and had lower size counting thresholds of 7 and 3 nm, respectively. Therefore the background subtraction (tunnel exit–entrance) used here may lead to slightly over-stated PN emission factors, though it is unlikely to be a major source of error since tunnel exit concentrations were high and the background subtraction did not lead to large adjustments for vehicle-related pollutants other than CO_2 (which has a significant global background concentration).

In principle, CPC and SMPS-derived particle counts shown in Table 3.1 should match, though there were differences in lower size cutoffs between the measurements, and there are uncertainties in inversion of raw SMPS counts due to the fraction of uncharged particles, which becomes large as particle size decreases. Given the uncertainties, the two measures of particle number are in reasonable agreement as shown at the bottom of each section of Table 3.1.

Kleeman et al. (2000) reported a single peak in particle mass distributions between 100 and 200 nm for both gasoline and diesel vehicle emissions. SMPS scans in this study were cut off at 290 nm to shorten scan times; prior work suggests we captured the peak in the fine particle volume distribution, but we cannot exclude the possibility that a second peak in fine particle volume emissions is present above 290 nm.

4. Emission Factor Distributions for Individual HD Trucks

4.1 Introduction

Black carbon (BC), which accounts for more than half of $PM_{2.5}$ mass from diesel engines under load (see Chapter 2), is of concern not only because of adverse effects on human health, but also as it relates to climate change. A recent assessment indicates that BC is the second largest contributor to global warming (next to CO_2) and alters regional precipitation and snow and cloud albedos (Ramanathan and Carmichael, 2008). Studies have suggested that reducing BC emissions, of which diesel engines are a major source, should be an element in the effort to counteract global warming (Hansen and Sato, 2001). Bond and Sun (2005) note, however, that BC reduction in developed countries is relatively costly as a means for mitigating climate change unless local air quality and public health benefits are considered simultaneously. Unlike CO_2 which is long-lived in the atmosphere, BC concentrations could be reduced rapidly following widespread implementation of emission reduction measures.

Motor vehicles emit the largest number of particles in the ultrafine mode, defined as particles with diameter $D_P < 100$ nm (Kittelson et al., 2006ab). These particles are small enough to penetrate deeply into the lung, enter the circulatory system, and accumulate in organs such as the brain, heart, and liver (Kennedy, 2007). There is an ongoing debate about whether particle number (PN), mass, or chemical composition is most important in causing adverse human health effects (Kennedy, 2007). Current mass-based emission standards may not be optimal in reducing health effects if particle number turns out to be the more harmful factor.

One of the challenges in characterizing vehicle emissions is extrapolating from a sample of vehicles to the entire in-use population. HD trucks are especially time-consuming and expensive to test in the laboratory, and therefore dynamometer studies of HD vehicle emissions have generally been limited to small sample sizes (1-25 vehicles). On-road remote sensing techniques have been used to measure snapshots of gaseous pollutant emissions from large numbers of vehicles; remote sensing of PM emissions is difficult due to the need to relate integrated measures of particle optical properties back to particle number as a function of size and chemical

composition. While measurements of vehicle emissions in roadway tunnels can capture a large sample of on-road vehicles, such studies usually provide only fleet-average results.

It is known that high-emitting vehicles contribute disproportionately to gaseous pollutant emissions from the on-road LD vehicle fleet. Emission factor data from Bishop and Stedman (2008) for NO_x, CO, and hydrocarbons show that the skewness of on-road emissions distributions (i.e., the relative importance of high-emitters as a source of vehicle-related pollution) has been increasing at the same time that fleet-average emissions have declined significantly. Gas-phase emissions from HD diesel vehicles have been found to be skewed to a lesser extent than light-duty vehicles (Jimenez et al., 2000). Less is known about PM emissions from motor vehicles, due in part to difficulties in making fast time-response measurements. Various studies have reported distributions of PM emissions for LD vehicles (Hansen and Rosen, 1990; Mazzoleni et al., 2004; Kurniawan and Schmidt-Ott, 2006). Other studies have focused on PM emissions from large samples of high-emitting LD vehicles (Cadle et al., 1997; Sagebiel et al., 1997; Cadle et al., 1999). Jiang et al. (2005) reported distributions of BC and $PM_{2.5}$ emissions for a mixed LD/HD fleet in Mexico City. One study measured particle number emission rates from high-emitting HD diesel buses (Jayaratne et al., 2007). In summary, to date there have been relatively few studies that report fine particle emission distributions from large samples of HD vehicles.

The goal of the present study was to measure BC and PN emission factors for a large sample of individual HD trucks as they drove through a San Francisco Bay area highway tunnel. The individual and joint distributions of BC and PN emission factors from HD trucks are presented. We also consider how vehicle sample size affects uncertainty in estimates of the population mean BC emission factor.

4.2 Methods

4.2.1 Field Measurements

For this component of the field study, HD truck emissions were measured in the southernmost lanes (bore 1) of the Caldecott tunnel, where a mixture of LD vehicles and MD/HD trucks travel uphill on a 4% grade. Truck emissions were measured on 4 days (19-21 and 24 July 2006) from

12-2 PM, which is the time of day when trucks comprise the largest fraction of total traffic in bore 1 of the tunnel.

Pollutant concentrations were measured near the exit (east end) of the tunnel with 1-second time resolution. The sample inlets for the analyzers were located approximately 15 cm below the ceiling of the traffic bore, which was near the exhaust stacks of passing HD trucks. To measure BC and particle number concentrations, sample air was drawn through approximately 1 m of conductive silicone tubing to analyzers located above the traffic in a ventilation duct. A sharp cut cyclone (BGI, Waltham, MA, model VSCCA) was used to achieve a particle size cut of 2.5 μm. BC was measured using a single-wavelength aethalometer (Magee Scientific, Berkeley, CA, model AE-16) capable of high-time resolution measurements. Particle number was measured using an ultrafine water-based condensation particle counter or CPC (TSI, Shoreview, MN, model 3786), which measures particles with diameter $D_P \geq 3$ nm. Due to high particle number concentrations inside the tunnel, CPC measurements were diluted by splitting the incoming aerosol flow. One line passed through an orifice and the other through a HEPA filter; the lines were recombined before passing into the CPC. The pressure drop across the orifice caused a large and stable fraction of the sample flow to pass through the HEPA filter that removed all of the particles, leading to a dilution ratio of 15.2. A parallel ~40 m Teflon sample line carried tunnel air to a non-dispersive infrared CO_2 analyzer (LI-COR, Lincoln, NE, model 820), located in the east end tunnel fan room. In order to align the plumes, BC and PN data were shifted by 25 seconds to account for the longer residence time in the CO_2 analyzer inlet line.

Laboratory tests have shown that when sampling a constant BC concentration, the aethalometer reports decreasing BC concentrations as the filter tape becomes increasingly loaded (Kirchstetter and Novakov, 2007). In this study, we account for the varying aethalometer response to BC within each operating cycle between filter tape advances. Raw data from the aethalometer were adjusted based on laboratory calibration experiments of Kirchstetter and Novakov (2007), as shown in eq. 4.1,

$$BC = \frac{BC_0}{(0.88Tr + 0.12)} \qquad (4.1)$$

where BC_0 and BC are the raw and adjusted concentrations respectively (μg m^{-3}), and *Tr* is the filter transmission, calculated using attenuation data measured by the aethalometer (Kirchstetter and Novakov, 2007). Two-hour average BC concentrations from the aethalometer matched BC concentrations measured in parallel via thermal optical analysis of quartz filters as discussed in Chapter 2. Thus, a further scaling factor of 0.6 suggested by Kirchstetter and Novakov to account for potential discrepancies between these two measurement techniques was omitted in eq. 4.1.

Video cameras were used to record the times when vehicles entered and exited the tunnel allowing for calculation of average truck speeds through the tunnel. Camera locations used here were not suitable for recording truck license plates. Based on visual observations of the traffic, it is likely that some of the trucks drove through the tunnel and were measured more than once over the 4 sampling days. Trailer loads were observed to vary from truck to truck.

4.2.2 Plume Analysis

Emission factors for individual trucks were calculated by carbon balance from analysis of exhaust plumes present in the 1 Hz BC, PN, and CO_2 data. An exhaust plume from a passing HD truck is shown in Figure 4.1 as the sudden rise, and subsequent fall of all 3 pollutant concentrations. Truck exit times from the videotape were used as a trigger to search for corresponding CO_2 peaks in the data. Only the plumes of HD trucks (defined here as trucks or tractor/trailer combinations with 3 or more axles) with vertical exhaust stacks were analyzed due to the proximity of exhaust emissions to the air sampling inlets located above the traffic. Plume analyses were not attempted when multiple trucks drove by simultaneously or in rapid succession (e.g., a slow-moving truck sometimes would have one or more additional trucks following immediately behind it). There was no screening of the data based on BC or PN emissions; only recorded truck exit times and presence of a matching CO_2 peak were used to determine success in identifying individual truck exhaust plumes. For a successful exhaust plume capture, CO_2 was required to increase by >30 ppm coincident with the time of a passing truck noted on the video camera. The 12-2 PM average CO_2 concentration inside the tunnel near the exit was ~800 ppm, so the minimum CO_2 increase required for a passing truck was about 4% above baseline. Exhaust plumes were identified for 50% (226) of the 459 HD trucks traveling through the tunnel during the present study using the above criteria. Reasons for not capturing

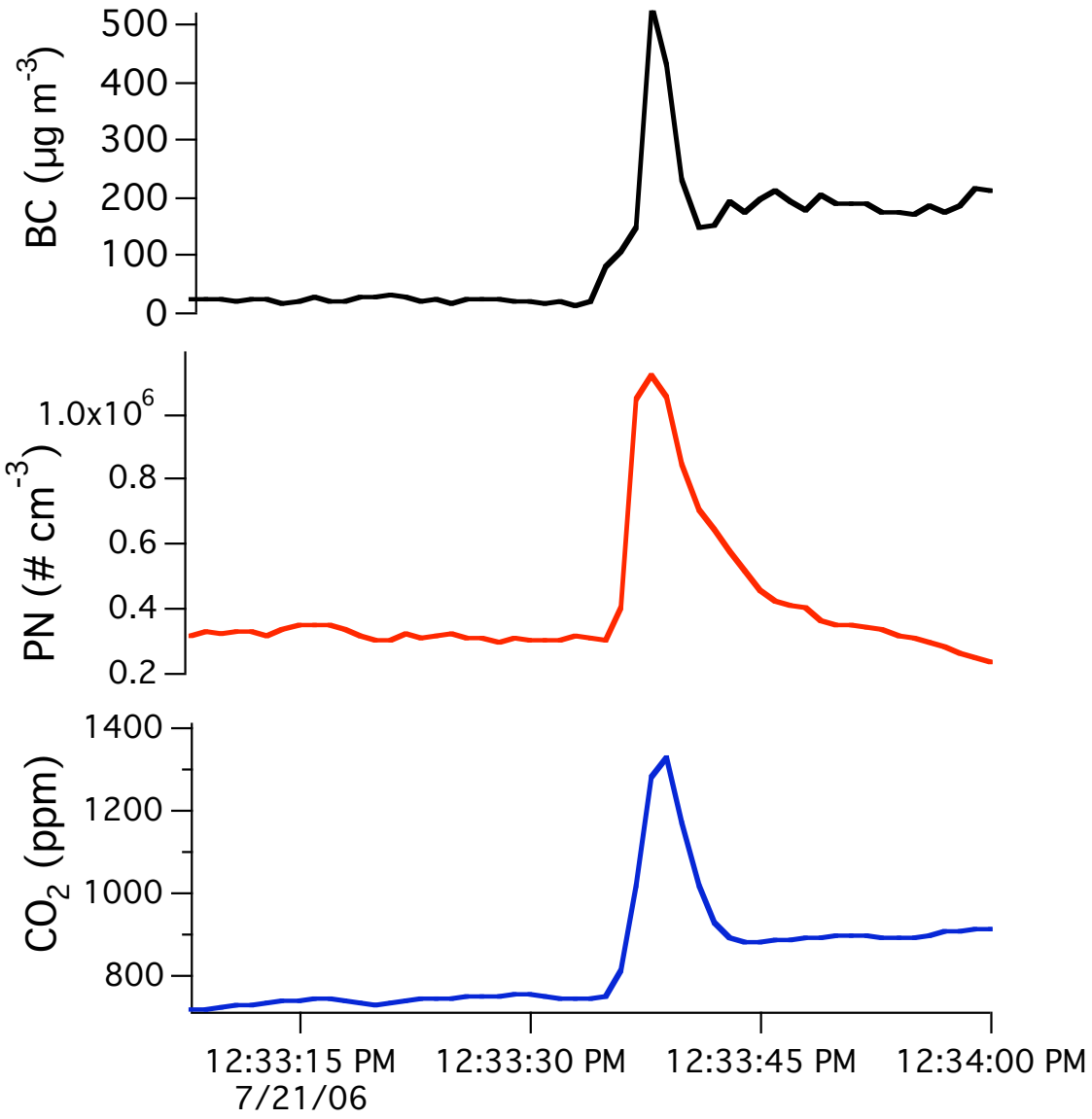

Figure 4.1. Measured black carbon (BC), particle number (PN), and CO_2 concentrations in the exhaust plume of a passing HD truck.

the exhaust plume of some passing trucks include under-body instead of vertical exhaust pipes, multiple trucks passing by at nearly the same time, and lack of sufficient increase in CO_2 above tunnel background levels.

E_{BC}, the BC emission factor (g kg^{-1} fuel burned) for individual HD trucks was calculated using eq. 4.2,

$$E_{\mathrm{BC}} = \frac{\int_{t_1}^{t_2} ([\mathrm{BC}]_t - [\mathrm{BC}]_{t_1})dt}{\int_{t_1}^{t_2} ([\mathrm{CO}_2]_t - [\mathrm{CO}_2]_{t_1})dt} w_c \qquad (4.2)$$

where w_c = 0.87 is the mass fraction of carbon in diesel fuel, $[BC]_t$ is the time-varying mass concentration of BC in units of μg m^{-3}, $[CO_2]_t$ is the time varying concentration of CO_2 in mg C m^{-3}, t_1 is the time at which the plume begins, and t_2 is the time at which the plume ends.

To calculate the number of particles emitted per unit of fuel burned, E_{PN} (# kg^{-1}), a similar equation was used:

$$E_{\mathrm{PN}} = \frac{\int_{t_1}^{t_2} ([\mathrm{PN}]_t - [\mathrm{PN}]_{t_1})dt}{\int_{t_1}^{t_2} ([\mathrm{CO}_2]_t - [\mathrm{CO}_2]_{t_1})dt} w_c \cdot 10^{12} \qquad (4.3)$$

where [PN] is in units of # cm^{-3}.

As indicated in eqs. 4.2 and 4.3, pollutant concentrations were baseline-subtracted using measured values at time t_1. This time was determined manually for each truck by finding an inflection point to the left of the peak, indicating the start of the rapid rise in pollutant concentration associated with a truck's exhaust plume (see Figure 4.1). Likewise, t_2 was determined by finding an inflection point to the right of the peak. However, if the pollutant concentration at t_2 was lower than the concentration at t_1, t_2 was instead chosen to be the time when the CO_2 concentration decreased to match that measured at t_1. This was to avoid subtracting pollutant concentrations using values below the baseline during plume integration.

Plume widths ($t_2 - t_1$) were determined from CO_2 data only. The plume widths for all pollutants were kept the same for each truck. They ranged from 4-12 s depending on the truck, with the majority of plume widths ~10 s. Carbon monoxide and unburned hydrocarbon emissions were neglected in the denominator of eq. 4.2 and 4.3 since high time-resolution measurements of these pollutants were not available.

4.3 Results and Discussion

4.3.1 Black Carbon Emissions

A histogram of BC emission factors is presented in Figure 4.2a. The distribution appears normal when the emission factors are plotted using a logarithmic rather than linear scale. Figure 4.3a shows emission factors for each truck plotted on log-probability axes; log-normal distributions will plot as straight lines on these axes. Only two trucks at the low end deviate from a log-normal distribution for BC. This is likely because plume integrations for BC lose precision at low emission levels due to high baseline BC concentrations inside the tunnel. Emission factors are not shown in Figure 4.3a below the 6th percentile for BC because the lowest-emitting trucks had negative calculated emission factors. Emission factors for each truck are listed in Appendix B.

The arithmetic mean of all BC emission factors was 1.7 g kg^{-1} with a standard deviation of 2.3 g kg^{-1}. The mean value reported here is ~ 2× higher than the fleet-average value of 0.92 ± 0.07 g kg^{-1} reported in Chapter 2. Note that the main goal of this chapter is to evaluate emission distributions, not fleet average emission factors. In Chapter 2, fleet-average emission factors were calculated by apportioning pollutants in the mixed traffic bore between LD vehicles and MD and HD trucks. Potential reasons for the different average BC emission factor in the present plume-based study are as follows: (1) Only trucks with vertical exhaust pipes were included – this excludes some HD trucks and virtually all MD trucks from the plume analysis, so the fleet-average emission factor reported here reflects only a subset of the truck emissions analyzed previously; (2) There are uncertainties in calculated emission factors, such as the apportionment of CO_2 in the mixed traffic bore in the fleet-average results from Chapter 2, and the appropriate start/stop times for plume integration coupled with need to subtract baseline pollutant concentrations from measured peak levels in the current analysis; (3) CO was not measured at high time resolution and therefore was not included in the denominator of eq. 4.2. Data reported

in Chapter 2 indicate the CO effect is small (~4%) on average, though it may be a more significant term in the carbon balance for high-emitting trucks.

The distribution of BC emissions is skewed with the highest-emitting 10% of HD trucks responsible for 42% of total BC emissions, as shown in Figure 4.3b. Emission measurements were made as trucks neared the end of a 1-km uphill section of highway, with an average truck speed inside the tunnel of 64 km h^{-1} (truck passing times and speeds can be found in Appendix B). Emissions from cold or idling engines, or from trucks operating under stop-and-go or high-speed cruise conditions were not observed in this study. Trailer loads varied from truck to truck and thus some of the variance in emission factors could have resulted from differences in engine speed and load, not just differences in basic emission rates among engines. Some heavily loaded trucks traveled more slowly through the tunnel, and vice versa, leading to a distribution of average speeds as shown in Figure 4.4. Further analysis showed no correlation between truck speed and fuel-normalized BC or PN emission factors in the present study. Table 2 of Gajendran and Clark (2003) provides PM and CO_2 emissions for 5 trucks, each tested at different operating weights. These data show no large (or even directionally consistent) effect of truck test weight on fuel-normalized PM emission factors. Thus we believe the variation in BC emission factors observed in the present study is due mainly to differences in basic emission rates among trucks, rather than differences in vehicle speed or engine load. Effects of vehicle speed on emissions may not be readily apparent in this study due to extra engine load from uphill driving, and normalization of emissions to fuel consumed rather than distance traveled. Also offsetting effects of increased cargo weight and decreased vehicle speed may be present.

4.3.2 Particle Number Emissions

As shown in Figure 4.2b and 4.3a, particle number emission factors do not follow a log-normal distribution as closely as BC. Deviation from log-normal behavior is most pronounced at the low end of the reported emission factor range. Plume integrations lose precision at low emission levels due to high background number concentrations at the tunnel exit. Emission factors are not shown in Figure 4.3a below the 13th percentile for PN due to calculated negative values for the cleanest trucks. A listing of emission factors for each truck can be found in Appendix B.

The arithmetic mean of the PN emission factors was 4.7×10^{15} # kg^{-1} with a standard deviation of 6.6×10^{15} # kg^{-1}. PN emissions depend on the lower size cutoff of the particle counting instrument, and thus comparisons to other studies should be made carefully. Previous on-road chase measurements of HD truck emissions using a TSI 3025A CPC (diameter > 3 nm) reported PN emission factors between 7.2×10^{15} and 2.0×10^{16} # kg^{-1} for a range of cruise and acceleration conditions (Kittelson et al., 2006). The average PN emission factor from the Caldecott tunnel was lower, but the highest-emitting truck observed in our study had an emission factor of ~4×10^{16} # kg^{-1}.

The distribution for PN emissions was skewed with the highest-emitting 10% of HD trucks responsible for 41% of total particle number emissions, as shown in Figure 4.3b. Similar to results for BC discussed in the preceding section, no correlation was found between truck load and PN emission factor. PN emissions from diesel buses measured in Australia (Jayaratne et al., 2007) were less skewed, with the highest-emitting 25% of buses responsible for 50% of total particle emissions. Note that only high-emitting buses were analyzed in the Australian study, so a different emission distribution is expected.

4.3.3 BC vs. PN relationships

Though >40% of both BC and PN emissions came from the highest 10% of trucks, there was minimal overlap between high PN and high BC-emitting trucks. Figure 4.5 plots PN against BC emission factors for each individual truck. The boxes in the figure show the highest-emitting 10% (23 trucks) separately for BC and PN. Only one truck fell simultaneously in the highest-emitting 10% for both BC and PN. The highest emitters of BC tend to have low PN emission factors, and vice versa. This can be observed by the lack of points plotted in the upper right quadrant of Figure 4.5. The lack of overlap in the high-emitter population is consistent with a hypothesis proposed by Kittelson et al. (2006), that high BC emissions are likely to inhibit ultrafine particle formation. This is because volatile precursors of ultrafine PM condense onto BC particle surfaces instead of nucleating to form new particles when BC is abundant in the exhaust.

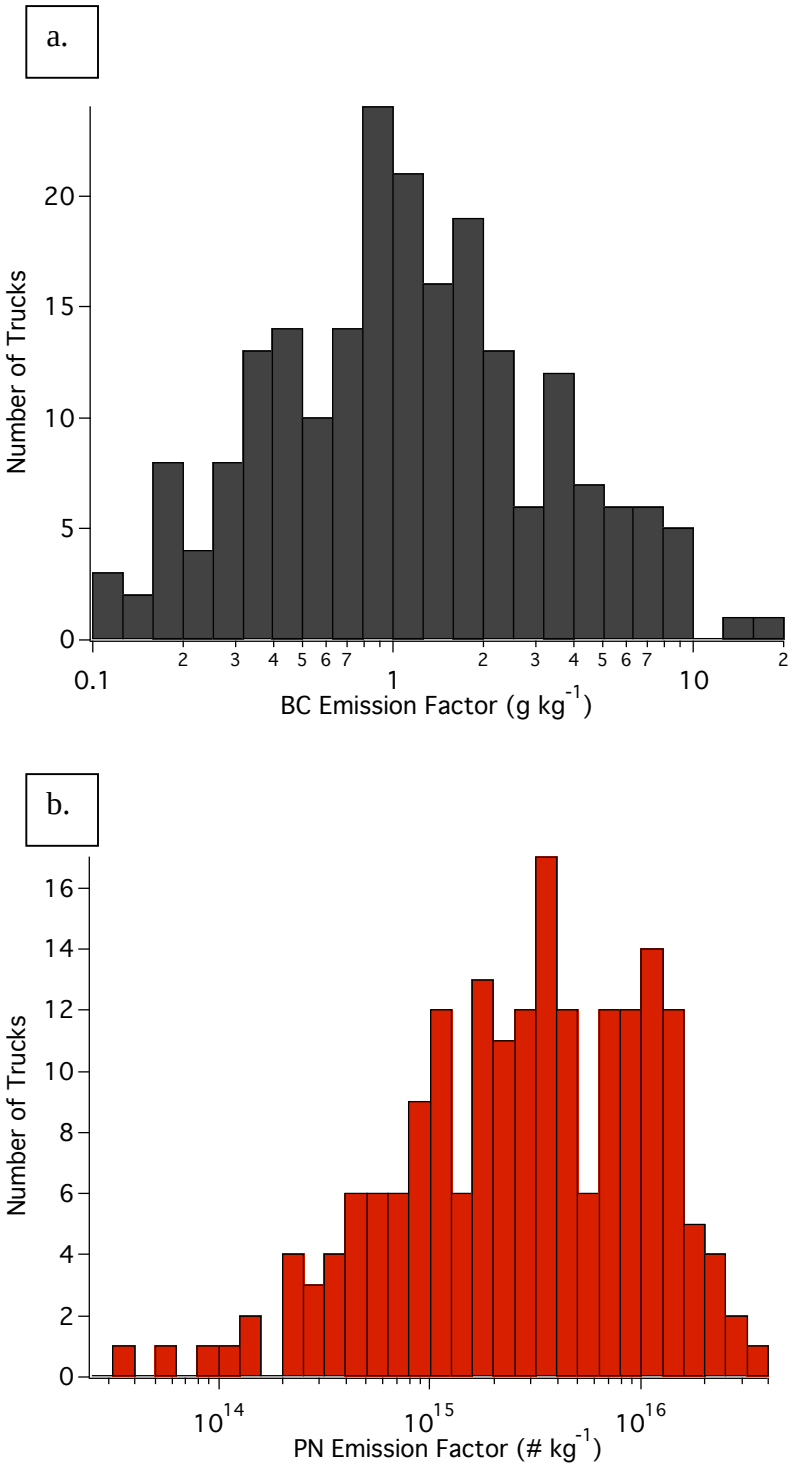

Figure 4.2. Histogram of BC (a) and PN (b) emission factors from trucks driving through the Caldecott tunnel during summer 2006. Note the log-normal scale on the horizontal axis.

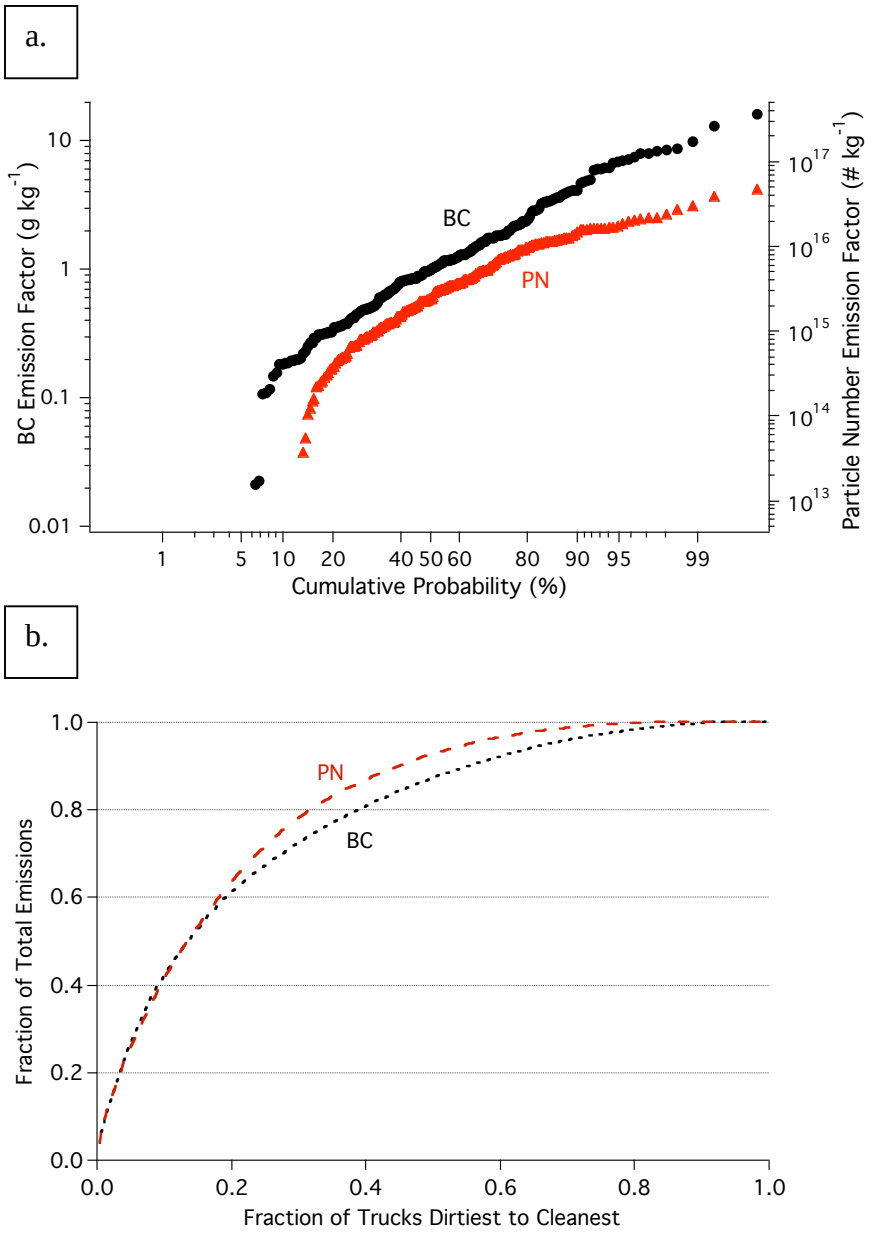

Figure 4.3. Probability plot (a) of the emission factors for BC and PN from the 226 individual HD trucks. The horizontal axis shows the probability that a truck has an emission factor less than the indicated value. Log-normal distributions plot as straight lines on these axes. The cumulative distributions (b) indicate that the highest-emitting 10% of truck are responsible for ~40% of total BC and PN. If all vehicles had identical emission rates, this would plot as a 1:1 diagonal line in (b).

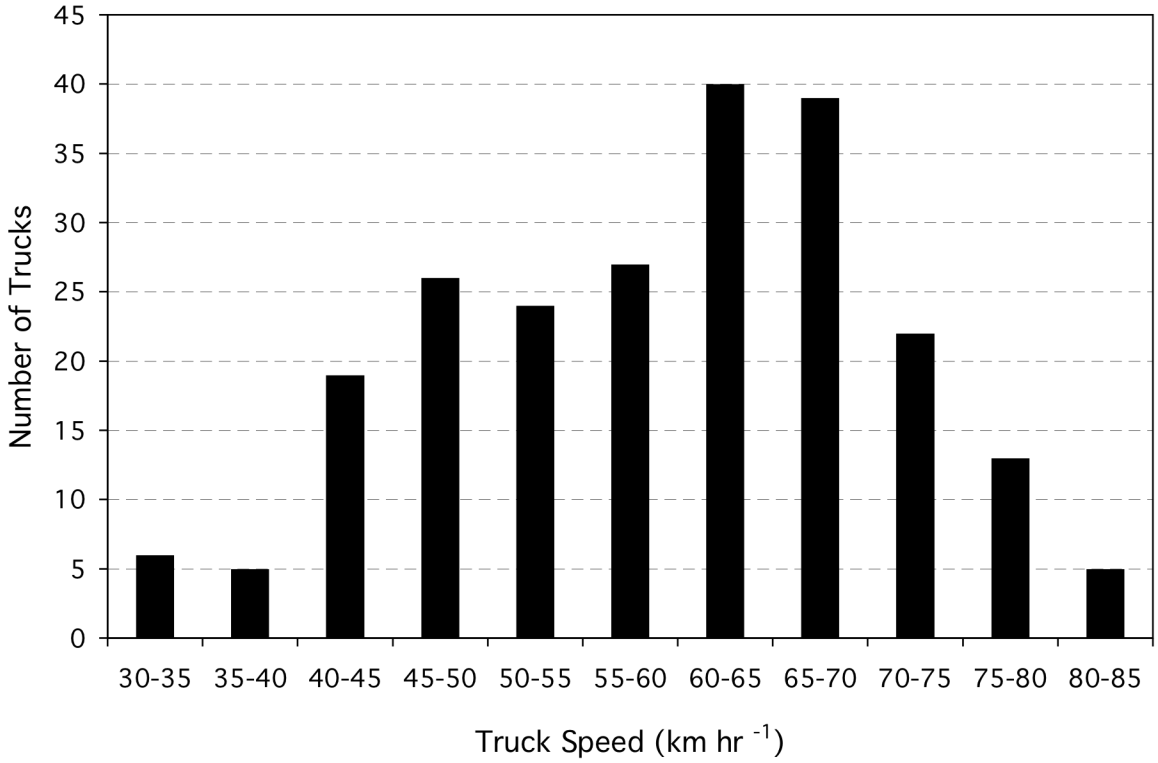

Figure 4.4. Truck speed distribution for the 226 HD trucks analyzed in this study, based on average values per truck through the tunnel.

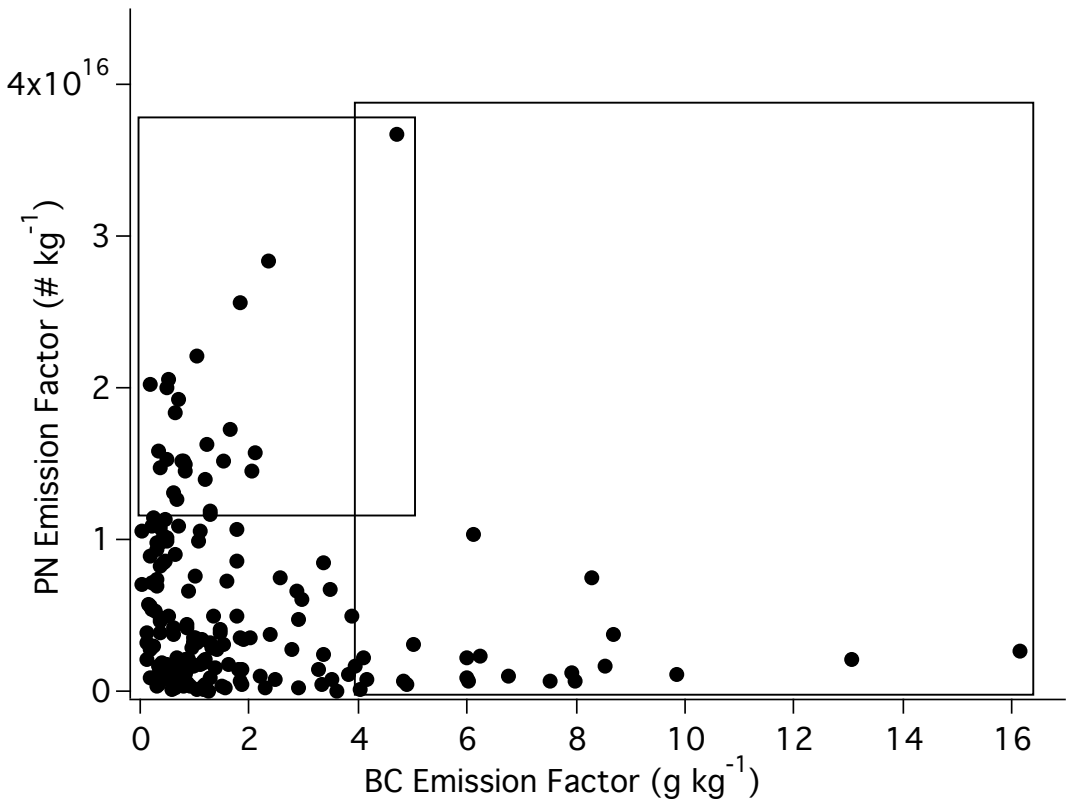

Figure 4.5. Emission factors for particle number (PN) plotted against matched BC emission factors for individual HD trucks. Boxes highlight the highest 10% of emitters for each pollutant; note minimal overlap of high-emitters.

4.3.4 Influence of Vehicle Sample Size on Uncertainty in Fleet-Average Emissions

Motor vehicle emission inventories (e.g. Bond et al., 2004) often rely on results from laboratory/dynamometer test results for individual vehicles obtained under carefully controlled conditions. Laboratory results must be extrapolated to represent the entire in-use vehicle population, with adjustments to account for differences in vehicle operating conditions, fuel properties, etc. Using the results of the current study, we address how sample size in a study of HD truck emissions could affect the uncertainty of estimated fleet-average emissions. We should note that our emission factor distribution reflects differences in basic emission rates among engines, as well as real-world effects such as engine load differences due to having a mix of loaded and unloaded trucks, as discussed previously.

Sampling with replacement from the BC emission factor distribution developed in this study, Monte Carlo simulations were performed as follows: random samples of *n* trucks were drawn from the population of measured BC emission factors shown in Figure 4.2a. The distributions of calculated means for 50 000 such experiments are shown in Figure 4.6 for each of n=10, 30, 100, and 300. Figure 4.6 also shows relative standard deviations of the means for each value of *n*. Consistent with the central limit theorem, the distributions of means shown in Figure 4.6 are normal as *n* becomes sufficiently large, even though the parent distribution of BC emission factors shown in Figure 4.2a is log-normal. For n=10, there is a mode in the distribution below the true population mean, and a tail of higher mean values that occur when a high-emitting vehicle is included in this small sample of vehicles. As expected, the probability that a reported sample mean will differ significantly from the population mean decreases as sample size increases. The results shown in Figure 4.6 are specific to BC emissions from HD trucks; the results from this analysis do not hold for other pollutants and vehicle categories. The distribution of BC emissions from HD trucks measured here is less skewed than BC emissions from LD gasoline vehicles measured in Las Vegas by Mazzoleni et al. (2004). As vehicles become cleaner on average, skewness of the emissions distributions increases (Bishop and Stedman, 2008), and thus sample sizes needed to extrapolate reliably from a subset of vehicles to the entire in-use vehicle fleet are expected to become more of a challenge in the future.

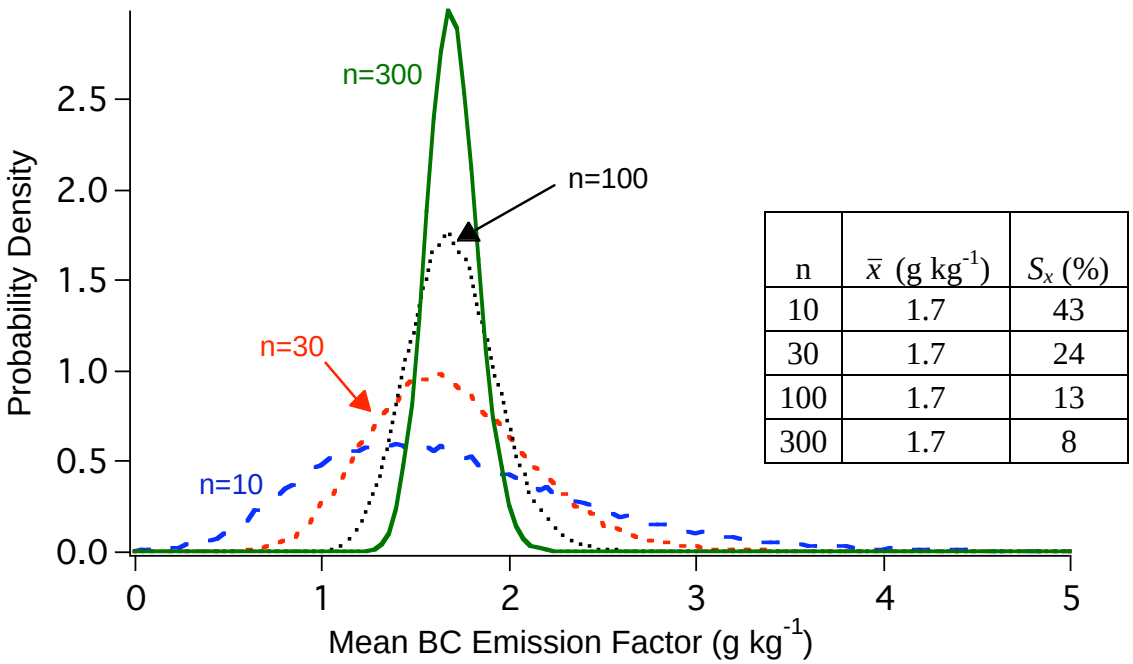

n	$\bar{x}$ (g kg^{-1})	S_x (%)
10	1.7	43
30	1.7	24
100	1.7	13
300	1.7	8

Figure 4.6. Probability density function of mean BC emission factors for n = 10, 30, 100, and 300 HD trucks. Tabulated values are number of vehicles sampled (n) in each iteration, grand mean ($\bar{x}$) of sample means, and relative standard deviation (S_x) of the sample means over 50 000 simulated samples (with replacement) from the distribution of BC emission factors shown in Figure 4.2.

5. Speciated Hydrocarbon Emission Trends

5.1 Introduction

Hydrocarbons emitted from motor vehicles include unburned gasoline and products of incomplete combustion such as ethane, ethene, acetylene, and propene among others. These compounds react in the atmosphere and promote the formation of tropospheric ozone and other photochemical air pollutants. Some individual hydrocarbons such as benzene and 1,3-butadiene also can be of concern as toxic air contaminants. Both the total mass and the detailed chemical composition of hydrocarbon emissions from motor vehicles are relevant factors to consider in air pollution assessments.

There are important effects that act to modify the mass and chemical composition of hydrocarbon emissions from motor vehicles over time. Gradual changes in emissions results from fleet turnover and improved emission control technologies installed on the newest vehicles compared to old vehicles that drop out of the in-use fleet. Fleet turnover is expected to lower hydrocarbon mass emissions over time, but also exerts gradual effects on exhaust emission speciation such as reductions in acetylene mass fraction (Lonneman et al., 1986). Changes in fuel properties can also affect the mass and chemical composition of vehicle emissions. Past examples of such changes include wintertime addition of oxygenated compounds to gasoline (Kirchstetter et al., 1996), and more wide-ranging changes to fuel properties that were made as a result of California's Phase 2 reformulated gasoline (RFG) program that took effect in the mid-1990s (Kirchstetter et al., 1999bc; Harley et al., 2006). More recently, California required further changes to eliminate methyl tert-butyl ether (MTBE) and other ethers as gasoline additives, with increased use of ethanol since the MTBE phase-out in 2003 as a result.

5.2 Methods

As discussed in previous chapters, motor vehicle emissions were measured at the Caldecott tunnel. Speciated hydrocarbon measurements were made in the center bore of the tunnel only, where heavy-duty trucks are not allowed. Integrated air samples were collected in evacuated stainless steel canisters during the afternoon peak traffic period on

8 summer weekdays (4-6 PM on 31 July-3 August and 7-10 August 2006). Samples were delivered to the Bay Area Air Quality Management District's laboratory in San Francisco for analysis using gas chromatography and flame ionization detectors (GC/FID). Dual capillary columns (PLOT and DB-1) and dual FIDs were used in the analysis procedure, which is described in detail elsewhere (ARB, 2002). To complete the carbon balance needed to calculate emission factors, CO and CO_2 concentrations were also measured as described in Chapter 2. Total non-methane organic compound (NMOC) and benzene emission factors were calculated using eq 2.1, with [NMOC] calculated as the total reported non-methane organic compound mass in each sample less the sum of reported acetone, methyl ethyl ketone, and ethanol peaks. Aldehyde and ketone emissions are considered separately using different measurement methods in the next chapter.

A chemical composition profile for tunnel NMOC emissions was developed for each day by normalizing individual hydrocarbon concentrations to total NMOC mass (all calculations were done using background-subtracted values). Separate profiles were developed for each day, and the weight fractions were then averaged over all 8 sampling days to develop a final NMOC speciation profile for tunnel emissions. Compounds for which the standard deviation in weight fraction was comparable to or larger than the mean value were not reported.

5.3 Results and Discussion

Average ratios of individual hydrocarbon concentrations at the tunnel exit relative to tunnel entrance values are shown in Figure 5.1. Note the use of a logarithmic scale on the y-axis of this plot. Methane concentrations at both ends of the tunnel were similar – around 2 ppm. While an increase in methane concentrations above background values was apparent at the tunnel in the past, the decline in hydrocarbon emissions from motor vehicles in general has made methane emissions more difficult to detect in this setting, especially given the high global background level of methane (~1.7 ppm and increasing). Most of the other hydrocarbons shown in Figure 5.1 had significant enhancements inside the tunnel, with exit/entrance concentration ratios ranging from 4-7. Propane was an exception to this rule as it is not a major constituent of gasoline-powered motor vehicle

emissions. As shown in Figure 5.1, measured concentrations of ethanol at the tunnel exit were lower than at the entrance, possibly due to contamination of the air samplers and/or ethanol losses inside the stainless steel canister surfaces.

NMOC and benzene emission factors from summer 2006 are shown in Figure 5.2 together with corresponding values from previous years that have been reported previously (Harley et al., 2006). Note benzene emissions have been scaled up by a factor of 10 for plotting purposes. Whereas benzene emissions continue to decline linearly, the observed rate of decrease in total NMOC is slowing in recent years – this is emphasized by the use of a decaying exponential rather than linear fit to the data in Figure 5.2. The NMOC data points shown in Figure 5.2 for 2004 and 2006 are biased low due to the exclusion of ethanol emissions. MTBE was measured and included in tunnel NMOC results shown for 1996-2001.

In Figure 5.2, only data from 1996 and later years were used to develop fits to the emission trends over time. These fits were extrapolated back to 1994-95 prior to the introduction of California Phase 2 RFG. Harley et al. (2006) reported reductions of 16±6% in NMOC and 50±5% in benzene emissions due to the introduction of Phase 2 RFG, apparent in Figure 5.2 as the difference between observed emission factors from summers 1994 and 1995 and the backward extrapolation of fits to the data from 1996 onward.

The chemical composition of NMHC emissions is summarized in Table 5.1. The most abundant species in vehicle emissions include isopentane, toluene, m/p-xylene, ethene, 2,2,4-trimethylpentane, and 2-methylpentane. Ethanol is also expected to be present in vehicle emissions given the significant and increasing use as a gasoline oxygenate, however measurement problems prevented it’s inclusion in the present analysis. Selected carbonyls from Chapter 6 have been included at the end of Table 5.1 for the reader’s convenience.

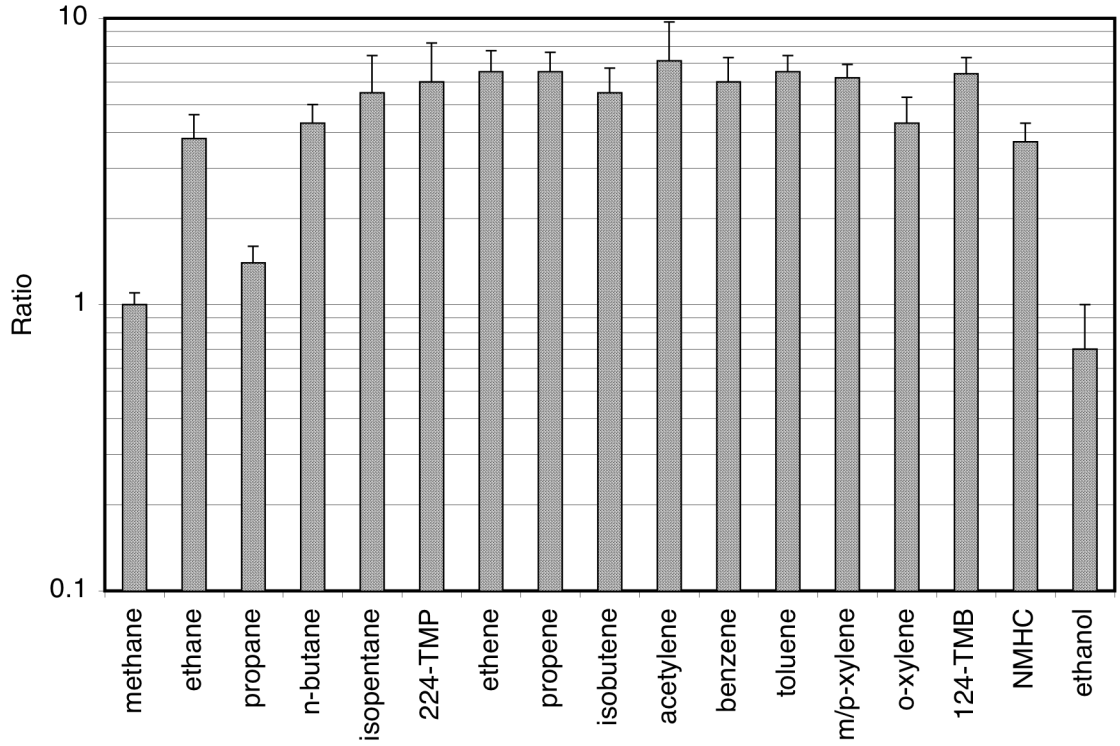

Figure 5.1. Ratios of pollutant concentrations at tunnel exit relative to entrance values.

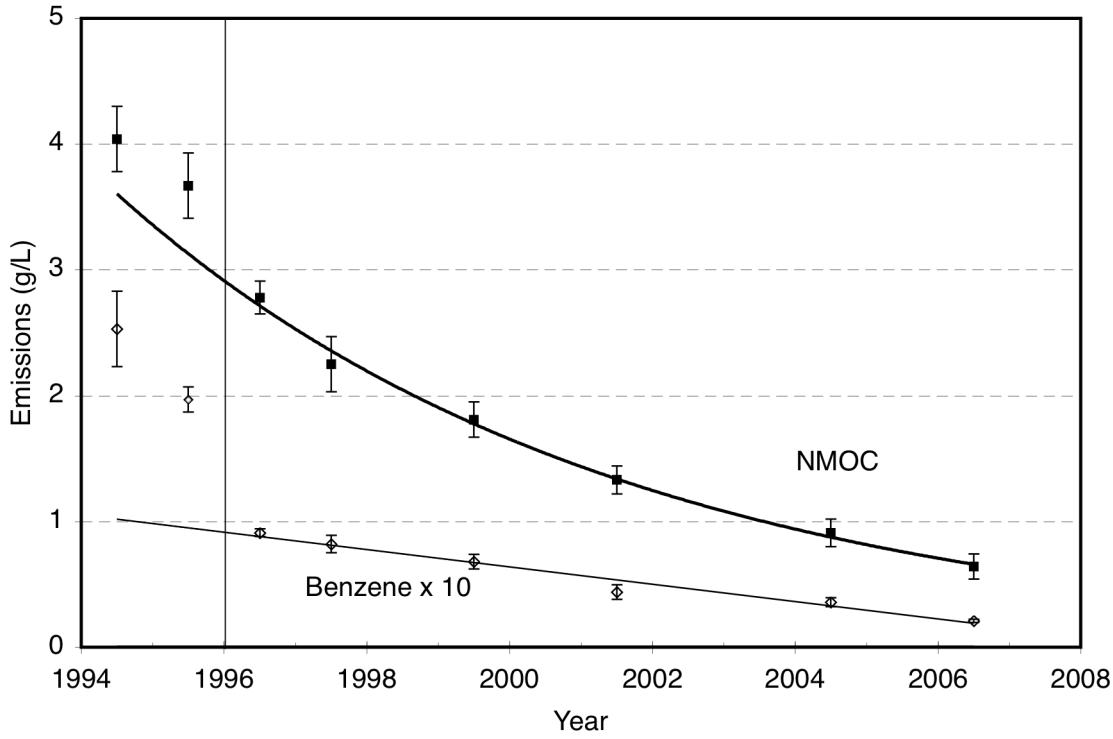

Figure 5.2. Trends in light-duty vehicle emission factors of non-methane organic compounds and benzene (emissions expressed per unit volume of gasoline burned).

Table 5.1. Volatile organic compound weight fractions in light-duty vehicle emissions measured at the Caldecott tunnel during summer 2006.

SPECIES NAME	wt% NMOC [a]	st dev (N=8)
ethene	4.91%	0.76%
acetylene	1.55%	0.25%
ethane	1.44%	0.21%
propene	3.07%	0.49%
propane	0.10%	0.04%
isobutane	0.10%	0.02%
1-butene	0.31%	0.05%
isobutene	1.39%	0.22%
n-butane	0.55%	0.12%
isopentane	11.98%	3.01%
n-pentane	3.05%	1.24%
2,2-dimethylbutane	1.58%	0.20%
cyclopentane & 2,3-dimethylbutane	1.61%	0.15%
2-methylpentane	4.01%	0.48%
3-methylpentane	2.01%	0.15%
n-hexane	1.37%	0.31%
methylcyclopentane	1.84%	0.45%
benzene	3.44%	0.49%
cyclohexane	0.55%	0.12%
2-methylhexane	1.20%	0.14%
2,3-dimethylpentane	0.90%	0.06%
3-methylhexane	1.28%	0.18%
2,4-dimethylpentane	0.71%	0.15%
2,2,4-trimethylpentane	4.50%	0.65%
n-heptane	0.84%	0.06%
methylcyclohexane	0.78%	0.14%
2,5-dimethylhexane	0.51%	0.10%
2,4-dimethylhexane	0.52%	0.09%
2,3,4-trimethylpentane	0.90%	0.14%
toluene	9.22%	1.12%
2-methylheptane	0.39%	0.04%
3-methylheptane	0.46%	0.11%
n-octane	0.33%	0.05%
2,3,3-trimethylpentane	0.77%	0.10%

Table 5.1 (continued). Volatile organic compound weight fractions in light-duty vehicle emissions measured at the Caldecott tunnel during summer 2006.

SPECIES NAME	wt% NMOC [a]	st dev (N=8)
ethylbenzene	1.65%	0.20%
m/p-xylene	6.99%	0.79%
2-methyloctane	0.28%	0.08%
o-xylene	2.26%	0.17%
n-nonane	0.26%	0.11%
m-ethyltoluene	1.47%	0.17%
p-ethyltoluene	0.56%	0.10%
1,3,5-trimethylbenzene	0.78%	0.33%
o-ethyltoluene	0.55%	0.16%
1,2,4-trimethylbenzene	2.46%	0.28%
other NMHC [b]	9.53%	
formaldehyde	1.86%	
acetaldehyde	0.85%	
acrolein	0.19%	
benzaldehyde	0.22%	
acetone	0.41%	
other carbonyls [c]	1.48%	

[a] Non-methane organic compound mass, excluding ethanol emissions (see text).

[b] Other non-methane hydrocarbons not listed above. Important species include 1,3-butadiene, C_5^+ olefins and C_{10}^+ aromatics.

[c] See Table 6.1 for a more detailed listing of aldehydes, ketones, and dicarbonyls.

Composition profiles from summers 1999, 2001 and 2004 are compared with the most recent tunnel data from 2006 in Figures 5.3-5.5 for various individual hydrocarbons. The GC analysis methods used in 2006 differ from those used in earlier years. Differences include use of a dual-column technique instead of a single DB-1 column for separating all C_2-C_{10} hydrocarbons, as well as differences in sample trapping and sample volume injected. These methodological differences may contribute to differences in the 2006 results when compared to previous years. For example, isobutene and 1-butene coeluted in prior years, but were resolved separately in 2006. Isobutene dominates the sum for these 2 isomers, as shown in Table 5.1.

Note the use of MTBE as a gasoline oxygenate in California was phased out by the end of 2003, so the latter two bars in the Figures represent vehicle emissions without MTBE in the fuel. Ethanol use in summers 1999-2001 was limited to one Bay area gasoline brand; the oxygenate of choice at the time was MTBE though it was not used universally. Figure 5.3 shows gradual long-term declines in the weight fractions of ethene, acetylene, and propene. In contrast, n-butane and MTBE emissions underwent step changes following the switch to ethanol. Propane and isobutane are not shown in Figure 5.3 as on-road vehicle exhaust is not a major emission source for these compounds unless liquefied petroleum gas (LPG) is being used as fuel. The decrease in MTBE emissions in Figure 5.3 is obvious and expected (no MTBE was detected in the 2004 and 2006 tunnel air samples). A likely explanation for the decline in n-butane emissions is that refiners reduced this especially volatile hydrocarbon to meet gasoline vapor pressure limits during summer months. Without such fuel changes, addition of ethanol would have increased gasoline vapor pressure and evaporative emissions (see Harley et al., 2000). The day-to-day variability in isopentane and n-pentane emissions was larger in 2006 than in previous years, due to unusually high abundance of these alkanes on one sampling day (9 August 2006). This can be seen in Figure 5.3 as the larger error bars for isopentane and n-pentane in 2006 compared to earlier years.

Changes in C_6-C_8 alkanes measured in tunnel emissions are shown in Figure 5.4. There are few obvious trends here; the most likely fuel-related change is a possible increase in

the addition of 2,2,4-trimethylpentane to gasoline. While MTBE and ethanol both have high octane ratings, the addition of ethanol to gasoline has so far been at lower levels (~5 vol%) compared to past use of MTBE (~10 vol%). Therefore, an increase in 2,2,4-trimethylpentane could help to compensate for the loss of MTBE and the effects of that change on fuel anti-knock properties. A possible explanation for variability in the remaining species data is batch-to-batch differences in how refiners formulate gasoline from various available blending stocks. However, the tunnel provides significant averaging by capturing vehicle emissions using the full mix of available gasoline brands from fuel fill-ups that took place over a range of past days and weeks.

Weight fractions of various aromatic hydrocarbons present in tunnel emissions are shown in Figure 5.5. There are no obvious trends that can be related to changes in fuel properties over this time period. Other C_9 aromatics were detected in tunnel emissions, but at lower and more variable levels than those shown in Figure 5.5. These include n-propylbenzene, p-ethyltoluene, and 1,2,3-trimethylbenzene. An important contribution to NMHC mass and reactivity comes from numerous small C_{10}^{+} aromatic peaks that were not quantified in this study. Other important fuel effects on vehicle emissions, specifically fuel oxygenate effects on formaldehyde and acetaldehyde emissions, are considered in the next chapter.

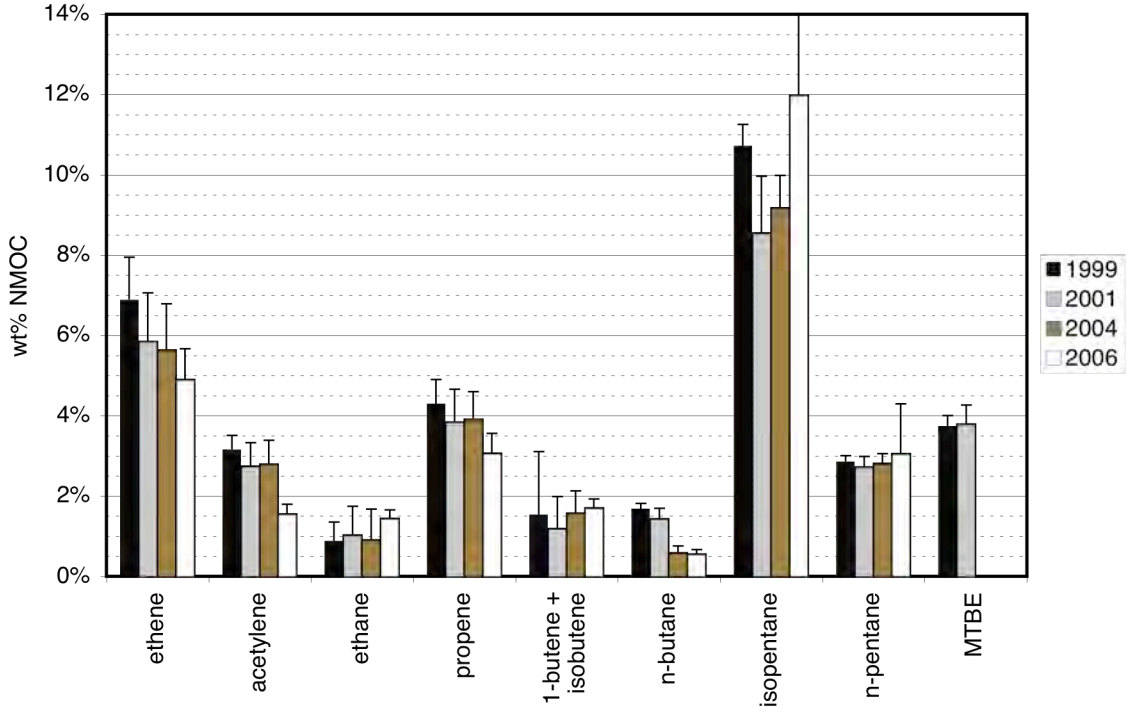

Figure 5.3. Comparison of light hydrocarbon and MTBE abundances in tunnel emissions (note that use of MTBE was phased out in California by the end of 2003).

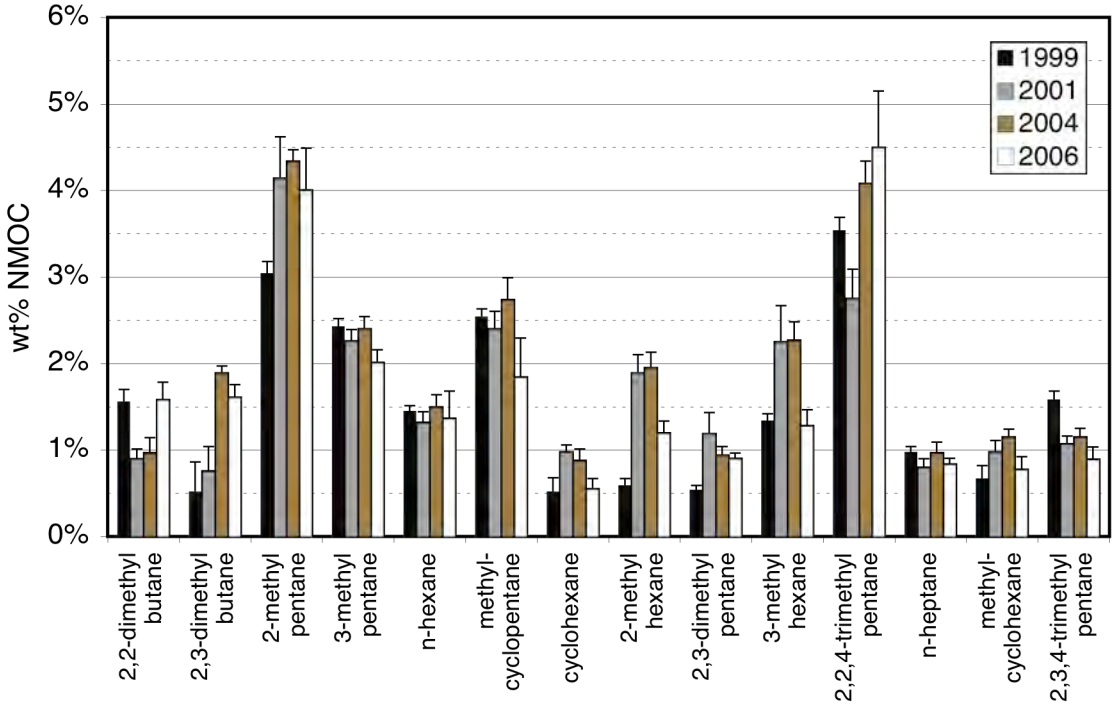

Figure 5.4. Comparison of C_6-C_8 alkane abundances in tunnel emissions.

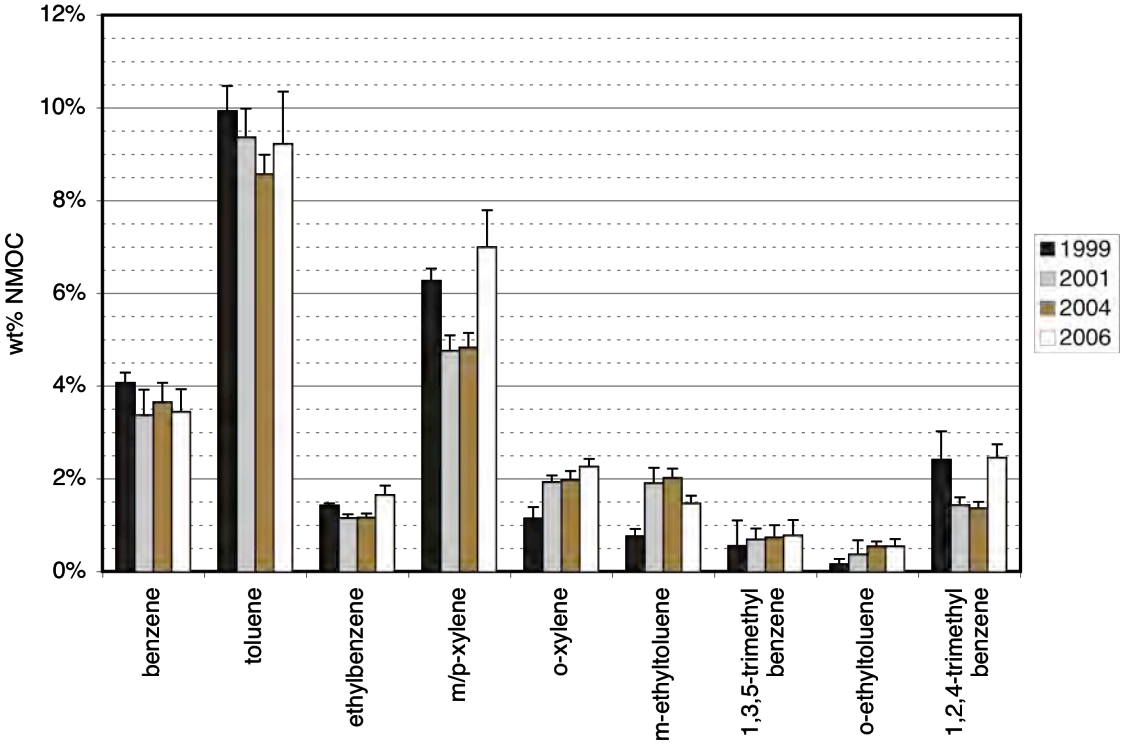

Figure 5.5. Comparison of aromatic hydrocarbon abundances in tunnel emissions.

6. Carbonyl and Nitrogen Dioxide Emissions

6.1 Introduction

Carbonyls are a subset of volatile organic compounds (VOC) that includes aldehydes, ketones, and dicarbonyls. They are emitted from sources such as motor vehicle exhaust (Grosjean et al., 2001; Kean et al., 2001), and also form as the atmospheric oxidation products of other VOC (Atkinson, 2000). Many carbonyls are highly reactive in the atmosphere contributing to formation of ozone, peroxyacyl nitrates, and other photochemical air pollutants (Atkinson, 2000). Carbonyls present in motor vehicle exhaust such as formaldehyde and acetaldehyde have been identified as toxic air contaminants, pollutants known or suspected to cause adverse health effects (EPA, 2006). Aldehydes also contribute to diesel exhaust odor (Partridge et al., 1987).

Carbonyl emissions from motor vehicles can be affected by changes in emission control technologies and fuel composition. The effects of fuel reformulation on formaldehyde and acetaldehyde have been studied extensively. In particular, a link has been found between the use of gasoline oxygenates such as methyl tert-butyl ether (MTBE) and ethanol, and increased emissions of formaldehyde and acetaldehyde, respectively (Hoekman, 1992; Reuter et al., 1992; Kirchstetter et al., 1996). Carbonyl emissions from on-road light-duty (LD) vehicles are likely to have changed as MTBE use in gasoline has declined, and ethanol use has increased in recent years. California banned ethers from gasoline outright by 2003 due in part to concerns about adverse effects on water quality. Nationally in the U.S., the Clean Air Act mandate to include 2 wt% oxygen in reformulated gasoline has been rescinded. The National Energy Policy Act of 2005 instead specifies that nation-wide use of bio-fuels (mainly ethanol) must increase to 7.5 billion gallons or about 5% of total gasoline volume by 2012 (Farrell et al., 2006). Further increases in fuel ethanol have been mandated, which may affect carbonyl emissions, air quality, and human health. Motor vehicle exhaust is a source of many other carbonyls including acetone, methyl ethyl ketone (MEK), acrolein, and acetophenone, which can also have adverse health effects.

Though diesel engines are a minor source of hydrocarbon emissions (Stone, 1999), carbonyl emission rates per distance traveled have been found to be higher from diesel vs. gasoline

engines (Grosjean et al., 2001; Schmid et al., 2001; Kristensson et al., 2004; Ho et al., 2007; Legreid et al., 2007). A 2006 emission inventory for California shows diesel engines to be the largest direct source of formaldehyde and acetaldehyde, accounting for 50 and 57% of total anthropogenic emissions, respectively (CARB, 2007).

Oxides of nitrogen (NO_x) are emitted from motor vehicles mostly in the form of nitric oxide (NO), but smaller quantities of nitrogen dioxide (NO_2) may also be present. The fraction of NO_x that is emitted as NO_2 is of interest because NO_2 is more toxic than NO, and a higher NO_2 fraction in direct NO_x emissions promotes ozone formation. Diesel exhaust is now the largest anthropogenic source of NO_x (EPA, 2007), and the NO_2/NO_x ratio is higher in diesel engines than gasoline engines (Jimenez et al., 2000). In 2007, new HD diesel trucks sold in the U.S. started using diesel particulate filters (DPF) as standard equipment to lower total particulate mass emitted. Most DPF systems include upstream catalysts that deliberately oxidize NO to NO_2 to aid in regeneration of the particle filters. Thus, the NO_2/NO_x ratio may increase in the future (Shorter et al., 2005). This study serves as a baseline for NO_2 emissions prior to the widespread deployment of DPFs in new diesel trucks.

The objective of this research is to measure carbonyl emission factors from on-road vehicles, including both gasoline powered LD passenger vehicles, and medium- (MD) and heavy-duty (HD) diesel trucks. Changes in LD vehicle emissions of carbonyls over time, and their relationship to fuel changes such as the switch from MTBE to ethanol, will be examined. The relative importance of gasoline vs. diesel exhaust as sources of direct carbonyl emissions will be evaluated. We also quantify carbonyls in unburned gasoline, and assess their importance as a source of carbonyl emissions. NO_2 emission factors are reported for LD vehicles and diesel trucks and are compared to total NO_x emission rates reported in Chapter 2.

6.2 Methods

6.2.1 Field Measurement Site.

Motor vehicle emissions were measured at the Caldecott tunnel as described in previous chapters. The middle bore of the tunnel (bore 2) carries almost entirely light-duty (LD) vehicle traffic, and consequently provides emission factors for LD vehicles directly. Bore 1 carries a mix

of LD vehicles, as well as MD and HD diesel trucks. Pollutant concentrations were measured in bore 2 during the afternoon rush hour (4-6 PM) when eastbound traffic flow was high, and midday (12-2 PM) in bore 1 when the diesel truck fraction was maximized. Vehicles were driving uphill during all measurement periods reported here. The average traffic volume in bore 1 was 1958 ± 127 LD vehicles h^{-1}, and 153 ± 9 MD/HD trucks h^{-1}. In bore 2 there were 3800 ± 131 LD vehicles h^{-1}, with a small number (23 ± 5 vehicles h^{-1}) of MD trucks. Air sampling was conducted inside the tunnel near the entrance and exit with the tunnel ventilation system turned off. Longitudinal airflow in the direction of traffic was induced by vehicles driving through the tunnel. Air samples were collected on eight weekdays in each traffic bore during summer 2006. All results reported here are for uphill (eastbound) driving on a 4% grade.

6.2.2 Pollutant Measurements.

Air samples were collected at the traffic inlet (west end) and outlet (east end) using 2,4-dinitrophenylhydrazine (DNPH)-coated silica gel cartridges. The cartridges were downstream of a KI oxidant scrubber, which was connected to the cartridges with Teflon tubing. Samples were collected for 120 minutes at a flow rate of 900 mL min^{-1}. After shipment to the laboratory, samples were extracted using acetonitrile and analyzed by liquid chromatography (LC) using diode array UV spectroscopy and negative chemical ionization mass spectrometry (Grosjean et al., 1999; Kean et al., 2001).

As a quality assurance measure, two cartridges were plumbed in series on one day of sampling to calculate cartridge collection efficiency. Collection efficiency is 100% for a particular carbonyl if the downstream cartridge contains no measurable amount of that carbonyl. Collection efficiency was found to be 100, 99.1, and 98.9% for formaldehyde, acetaldehyde, and acetone. Collection efficiency was 100% for all other carbonyls. In addition, two parallel samples were collected several times in both bores and at both ends of the tunnel; in these parallel samples, one DNPH cartridge had the usual upstream KI oxidant scrubber, and the other cartridge did not. Analysis of a pair of these cartridges showed all carbonyl concentrations to be within 2%, indicating that carbonyls were not removed by the KI scrubbers.

NO_2 concentrations were measured simultaneously using the carbonyl analysis technique described above, which can unambiguously measure NO_2 due to its reaction with DNPH to form 2,4-dinitrophenyl azide (DNPA) (Tang et al., 2004). However, analysis of the parallel samples described in the preceding paragraph (scrubbed vs. unscrubbed) showed that NO_2 was likely formed by the scrubber through NO oxidation; the scrubbed NO_2 data show a small but consistent positive bias for samples collected at the tunnel inlet (both bores), and at the outlet in bore 2. There was a higher and more variable bias in the samples from the tunnel exit in bore 1, likely due to the much higher levels of NO_x encountered there. Therefore, to calculate NO_2 emission factors we used the results from 3 unscrubbed samples at the tunnel exit of bore 1, and 5 unscrubbed samples in the exit of bore 2. Two parallel unscrubbed samples taken at the tunnel inlet were used to correct the scrubbed inlet data on the 8 days for which unscrubbed outlet samples were taken. Absolute concentrations were low at the inlet and therefore hardly affect the resulting NO_2 emission factor. In 1999 and 2001 all samples used the KI scrubbers, so we have applied correction factors to these data based on the ratio of unscrubbed/scrubbed results from 2006. There may be additional uncertainties beyond the reported NO_2 emission factor error bars for 1999 and 2001 due to these correction factors. We recommend that KI scrubbers not be used for NO_2 analysis in future studies.

CO_2 concentrations were measured at both ends of the tunnel using LICOR (Lincoln, NE) model 820 non-dispersive infrared gas analyzers. NO_x was measured using chemiluminescent analyzers (Thermo Environmental Instruments (TEI), Franklin, MA, model 42C and 42A at the exit and entrance, respectively). CO was measured using TEI model 48 gas filter correlation spectrometers. Calibration of these analyzers was verified daily.

6.2.3 Data Analysis.

Carbonyl emission factors (E_P) were calculated by carbon balance using eq 6.1.

$$E_P = \frac{\Delta[\mathrm{P}]}{\Delta[\mathrm{CO_2}] + \Delta[\mathrm{CO}]} w_c \qquad (6.1)$$

In eq. 6.1, Δ[P] is the background-subtracted (i.e., tunnel exit – entrance) concentration of pollutant P in μg m^{-3}; $\Delta[CO_2]$ and Δ[CO] are expressed in mg C m^{-3} units. Using a carbon

weight fraction $w_c = 0.85$ for gasoline (Kirchstetter et al., 1999), the resulting emission factors have units of grams of carbonyl emitted per kg of fuel burned.

Concentrations from the LD-only bore (bore 2) are used directly in eq 6.1 to obtain LD emission factors. Calculation of emission factors for diesel trucks requires apportioning CO_2, CO, and carbonyl concentrations measured in bore 1 between LD vehicles and diesel trucks. As described in more detail in Chapter 2, CO_2 is apportioned based on estimated fuel economies, fuel properties, and traffic counts for LD (2-axle, 4-tire), MD (2-axle, 6-tire) and HD (3+ axle) vehicles. Note that only the *ratio* of HD/LD fuel economy is important for CO_2 apportionment; absolute levels of CO_2 inside the tunnel are measured directly. Carbonyls and CO in bore 1 are apportioned using pollutant to CO_2 emission ratios measured in bore 2, and estimates of CO_2 emissions from gasoline engines, as shown in eq 6.2:

$$\Delta[P]_{1,D} = \Delta[P]_1 - \Delta[\mathrm{CO}_2]_{1,G}\left(\frac{\Delta[P]_2}{\Delta[\mathrm{CO}_2]_2}\right) \qquad (6.2)$$

Subscripts 1 and 2 outside the brackets in eq 6.2 indicate tunnel bore number; subscripts G and D indicate gasoline and diesel. For example, $\Delta[CO_2]_{1,G}$ is the LD vehicle contribution to CO_2 concentrations in bore 1. Diesel truck emission factors are subsequently calculated using diesel contributions to bore 1 pollutant concentrations in eq 6.1, with $w_c = 0.87$.

Previous sampling conducted in 1999 and 2001 at the Caldecott tunnel in bore 2 can be used to help define trends in LD vehicle carbonyl emissions. Carbonyl samples were collected and analyzed in the same manner as 2006. Results from the 1999 study can be found in Kean et al. (2001); results from 2001 and 2006 have not been reported previously.

6.2.4 Fuel Composition.

Regular and premium grade gasoline samples for 5 major brands were collected at Berkeley fuel stations during summer 2006. These samples were analyzed for carbonyls using liquid chromatography, as was done for the tunnel carbonyl samples. Separate analyses of liquid gasoline samples were performed using gas chromatography to quantify individual hydrocarbons, ethers, and alcohols in fuel samples collected during all three summers.

6.3 Results and Discussion

6.3.1 LD Vehicle Emissions.

Carbonyl emission factors are reported in Table 6.1. There is a general decreasing trend for total carbonyl emissions over time. Between 2001 and 2006, the total carbonyl mass emission factor decreased by 54 ± 3%. Emissions of several carbonyls decreased by more than 70% from 1999 to 2006. The five carbonyls emitted in the largest amounts in 1999, 2001, and 2006 were formaldehyde, acetaldehyde, acetone, benzaldehyde, and m-tolualdehyde, though the order of importance of mass emissions for the latter three carbonyls changed from year to year.

Formaldehyde is the most abundant carbonyl in light-duty vehicle exhaust, accounting for 38-45% of total carbonyl mass emissions depending on year. As shown in Figure 6.1, the formaldehyde emission factor did not change between 1999 and 2001, and then decreased by 61 ± 7% between 2001 and 2006. In contrast, acetaldehyde emissions decreased by the same amount (19 ± 2%) between 1999 and 2001 and between 2001 and 2006, despite the longer elapsed time between the second pair of years. Decreases in formaldehyde and acetaldehyde are due to the combined effects of vehicle fleet turnover and fuel reformulation that occurred between 2001 and 2006.

Figure 6.1 also shows formaldehyde and acetaldehyde ratios to total carbonyl mass. Analyzing carbonyls in these terms helps to remove the effect of vehicle fleet turnover, which leads mainly to decreases in total carbonyl mass emissions. The formaldehyde fraction of total carbonyl mass remained constant from 1999 to 2001, then decreased by 16 ± 2% between 2001 and 2006. The acetaldehyde fraction dropped by 19 ± 3% between 1999 and 2001, then increased by 76 ± 9% between 2001 and 2006. The acetaldehyde fraction of C_2+ carbonyls decreased from 22 ± 2 to 17 ± 1% (20 ± 3% decrease), and then increased to 27 ± 3% (57 ± 7% increase) from 1999 to 2001 to 2006, indicating that the increase in acetaldehyde mass fraction is not simply the result of decreased formaldehyde emissions. This suggests that the switch from MTBE to ethanol in gasoline between 2001 and 2006 led to decreased formaldehyde and increased acetaldehyde emissions. Note however that fleet turnover effects between 2001 and 2006 were larger than the fuel effects (phase-out of MTBE and increased ethanol use), such that acetaldehyde emissions decreased in absolute terms as shown in Table 6.1.

Table 6.1. Carbonyl and carbon monoxide emission factors for LD vehicles and MD/HD diesel trucks measured at Caldecott tunnel (mean ± 95% CI).

species name	LD Vehicle Emission Factor (mg kg^{-1}) 1999 [a]	2001	2006	MD/HD Diesel Emission Factor (mg kg^{-1}) 2006	Diesel/Gasoline Emission Ratio (no units) 2006
Saturated Aliphatic Aldehydes					
formaldehyde	43 ± 5	42 ± 3	16 ± 1.4	129 ± 18	7.9 ± 1.3
acetaldehyde	11 ± 1	9.0 ± 0.5	7.3 ± 0.7	46 ± 12	6.3 ± 1.7
propanal	1.2 ± 0.1	1.20 ± 0.09	0.46 ± 0.08	4.5 ± 2.2	9.9 ± 5.2
butanal/isobutanal	0.80 ± 0.18	0.78 ± 0.05	0.24 ± 0.06	1.7 ± 1.1	7.1 ± 5.1
pentanal	0.47 ± 0.17	0.47 ± 0.04	0.13 ± 0.02	1.9 ± 0.6	14.0 ± 4.9
isopentanal	0.46 ± 0.25	0.59 ± 0.05	0.22 ± 0.03	1.4 ± 0.6	6.7 ± 2.8
hexanal	0.30 ± 0.17	0.39 ± 0.05	0.23 ± 0.04	b	b
heptanal	0.15 ± 0.07	0.22 ± 0.03	0.33 ± 0.02	0.82 ± 0.35	2.5 ± 1.1
Unsaturated Aliphatic Aldehydes					
acrolein	1.5 ± 0.1 [c]	2.3 ± 0.2	1.6 ± 0.2	15 ± 4	9.3 ± 3.0
methacrolein	2.3 ± 0.2	1.8 ± 0.1	0.78 ± 0.14	9.2 ± 3.2	11.7 ± 4.6
crotonaldehyde	1.5 ± 0.2 [c]	1.03 ± 0.07	0.38 ± 0.04	3.8 ± 1.1	10.1 ± 3.2
2-pentenal/ISM [d]	0.21 ± 0.06 [e]	0.27 ± 0.03	0.12 ± 0.02	0.85 ± 0.34	7.1 ± 3.1
C6 UNSAT ISM #1 [d,f]	NA	0.059 ± 0.006	g	g	g
Aromatic Aldehydes					
benzaldehyde	6.7 ± 0.9	6.2 ± 0.5	1.9 ± 0.2	8.8 ± 2.5	4.6 ± 1.4
o-tolualdehyde	2.1 ± 0.2	1.9 ± 0.09	0.61 ± 0.05	1.6 ± 0.6	2.7 ± 0.9
m-tolualdehyde	4.8 ± 0.5	4.7 ± 0.3	2.4 ± 0.1	7.3 ± 2.8	3.1 ± 1.2
p-tolualdehyde	2.7 ± 0.3	2.6 ± 0.2	1.3 ± 0.2	6.1 ± 1.5	4.8 ± 1.4
2,5-dimethylbenzaldehyde	1.7 ± 0.2	1.9 ± 0.1	0.59 ± 0.05	1.5 ± 0.7	2.6 ± 1.3
2,4-dimethylbenzaldehyde/ISM [d]	1.1 ± 0.1	1.07 ± 0.09	0.39 ± 0.03	1.8 ± 0.6	4.6 ± 1.7
2,4,6-trimethylbenzaldehyde/ISM [d]	0.58 ± 0.04	0.46 ± 0.04	0.13 ± 0.02	0.66 ± 0.60	4.9 ± 4.5
o/m/p-anisaldehyde	0.52 ± 0.10	h	h	h	h
DMBZ[i] ISM #1 [d]	NA	0.62 ± 0.03	0.18 ± 0.02	0.56 ± 0.23	3.2 ± 1.3
DMBZ[i] ISM #2 [d]	NA	1.1 ± 0.1	0.41 ± 0.02	1.3 ± 0.7	3.2 ± 1.8

Table 6.1 (continued). Carbonyl and carbon monoxide emission factors for LD vehicles and diesel trucks measured at Caldecott tunnel (mean ± 95% CI).

species name	LD Vehicle Emission Factor (mg kg^{-1}) 1999 [a]	2001	2006	Diesel emfac (mg kg^{-1}) 2006	Diesel/Gasoline Emission Ratio
		Ketones			
acetone	5.6 ± 0.7	6.7 ± 0.4	3.5 ± 1.1	b	b
2-butanone (MEK)	0.77 ± 0.11	0.84 ± 0.05	0.61 ± 0.15	4.2 ± 1.4	6.9 ± 2.8
2-pentanone	0.55 ± 0.33	0.55 ± 0.09	0.22 ± 0.03	3.3 ± 1.1	15.3 ± 5.7
4-methyl-2-pentanone (MIBK)	0.68 ± 0.26	0.45 ± 0.04	0.62 ± 0.05	2.3 ± 0.5	3.7 ± 0.9
C5 ALP ISM [d,j]	0.32 ± 0.12	g	g	g	g
C6 ALP ISM #1 [d,j]	1.2 ± 0.3	0.80 ± 0.07	0.53 ± 0.07	2.6 ± 0.7	4.9 ± 1.5
C6 ALP ISM #2 [d,j]	0.76 ± 0.24	0.54 ± 0.03	0.25 ± 0.04	1.2 ± 0.3	4.6 ± 1.3
C6 ALP ISM #4 [d,j] (2-hexanone)	NA	0.13 ± 0.04	0.08 ± 0.01	0.78 ± 0.28	9.9 ± 3.8
C7 ALP ISM #3 [d,j]	NA	0.10 ± 0.02	0.077 ± 0.005	0.34 ± 0.13	4.3 ± 1.7
C7 ALP ISM #5 [d,j]	NA	0.22 ± 0.04	0.13 ± 0.02	1.0 ± 0.4	7.8 ± 3.3
2-heptanone	NA	0.15 ± 0.02	0.14 ± 0.03	0.67 ± 0.45	4.8 ± 3.3
acetophenone	0.13 ± 0.01	0.17 ± 0.02	0.07 ± 0.01	b	b
cyclohexanone	NA	0.33 ± 0.03	0.17 ± 0.03	1.3 ± 0.3	7.5 ± 2.1
indanone	NA	0.27 ± 0.04	g	g	g
methyl vinyl ketone	NA	0.67 ± 0.13	0.26 ± 0.02	3.0 ± 1.2	11.7 ± 4.8
		Aliphatic Dicarbonyls			
glyoxal	0.12 ± 0.04	0.17 ± 0.03	0.10 ± 0.02	1.0 ± 0.5	10.3 ± 5.3
methyl glyoxal	1.0 ± 0.2	0.91 ±0.10	0.29 ± 0.10	2.6 ± 1.7	9.0 ± 6.7
biacetyl	0.18 ± 0.04	0.14 ±0.03	0.14 ± 0.02	1.2 ± 0.3	8.4 ± 2.3
2-oxobutanal	0.05 ± 0.01	0.083 ± 0.017	0.06 ± 0.01	0.63 ± 0.23	11.2 ± 4.8
glutaraldehyde	NA	0.13 ±0.04	0.06 ± 0.01	0.55 ± 0.19	8.9 ± 3.7
		Other			
carbon monoxide	(52 ± 3) ×10^3 [k]	(43 ± 1) ×10^3 [k]	(24 ± 2) ×10^3	(81 ± 15) ×10^3	3.4 ± 0.7

[a]Carbonyl data from Kean et al., 2001. [b]Carbonyl emission factors are not reported for MD/HD diesel trucks when the lower bound for % diesel (lower bound = mean – uncertainty) < 20% (see text). [c]A portion of the 1999 reported crotonaldehyde is actually a second acrolein peak. [d]ISM=isomer. [e]2-pentenal/ISM was reported as 3-pentene-2-one in the 1999 samples. [f]UNSAT=unsaturated. [g]Carbonyl concentration was less than or equal to the sample blank concentration. [h]O/m/p-anisaldehyde was omitted due to interfering peaks and complex spectra. [i]Dimethylbenzaldehyde. [j]ALP=aliphatic. [k]Data from Kean et al., 2002. NA means the carbonyl was not analyzed.

Table 6.2 Oxygenate and carbonyl mass concentrations for 5 brands of regular and premium bay area gasoline in 2006.

	Regular					Premium				
	Brand A	Brand B	Brand C	Brand D	Brand E	Brand A	Brand B	Brand C	Brand D	Brand E
Oxygenates (weight %)										
ethanol [a]	5.6	5.5	5.5	0	5.7	5.5	5.5	6.0	0	5.8
MTBE [a, b]	0	0	0	0	0	0	0	0	0	0
TAME [a, c]	0	0	0	0	0	0	0	0	0	0
Carbonyls (mg kg^{-1}) [d]										
formaldehyde	0.08	0.17	0.12	0.06	0.09	0.13	0.15	0.09	0.09	0.11
acetaldehyde	6.84	15.82	4.66	0.12	8.58	8.04	15.48	9.98	0.07	11.43
acetone	e	0.50	e	1.04	1.08	0.32	0.47	0.76	e	1.74
2-furaldehyde	0.05	0.03	0.07	e	0.03	0.04	0.03	0.07	e	0.03
propanal	0.02	0.03	0.05	0.04	0.12	0.03	0.02	0.20	0.02	0.12
2-butanone (MEK)	e	0.39	1.75	1.11	8.36	1.78	1.20	3.37	e	7.48
butanal/isobutanal	0.09	0.18	0.28	0.13	0.42	0.16	0.14	0.75	0.05	0.47
benzaldehyde	0.20	0.18	0.10	0.13	0.11	0.11	0.13	0.18	0.07	0.17
2-pentanone	0.11	0.52	1.39	0.15	0.43	1.34	0.15	2.00	0.12	0.76
glyoxal	0.12	0.12	0.07	0.06	0.07	0.09	0.11	0.13	0.07	0.06
m-tolualdehyde	0.18	0.17	0.08	0.13	0.12	0.11	0.16	0.22	0.05	0.10
p-tolualdehyde	0.16	0.14	0.06	0.11	0.09	0.08	0.18	0.21	0.05	0.07
indanone	0.23	0.58	0.21	0.26	0.17	0.17	0.40	0.36	0.05	0.34
4-methyl-2-pentanone (MIBK)	e	0.13	e	e	e	0.14	e	0.14	e	e
methyl glyoxal	0.18	0.34	0.23	0.23	0.05	0.29	0.36	0.45	0.05	0.03
C6 ALP ISM #4 [f] (2-Hexanone)	0.10	0.10	0.06	0.05	0.08	0.07	0.09	0.08	e	0.12
hexanal	0.14	0.13	0.06	0.04	0.09	0.08	0.15	0.10	e	0.14
biacetyl	0.40	0.64	0.43	0.65	0.07	0.51	0.69	1.16	0.10	0.05
2,3-pentanedione	0.04	0.06	0.05	0.05	e	0.05	0.09	0.08	e	e

[a]0 values indicate below detection limit of 5 ppm. [b]Methyl tert-butyl ether. [c]Tert-amyl methyl ether. [d]Detection limits for individual carbonyls range from 20-60 pg depending on the carbonyl (Grosjean et al., 1999). [e]Carbonyl concentration was less than or equal to the sample blank concentration. [f]ALP=aliphatic, ISM=isomer

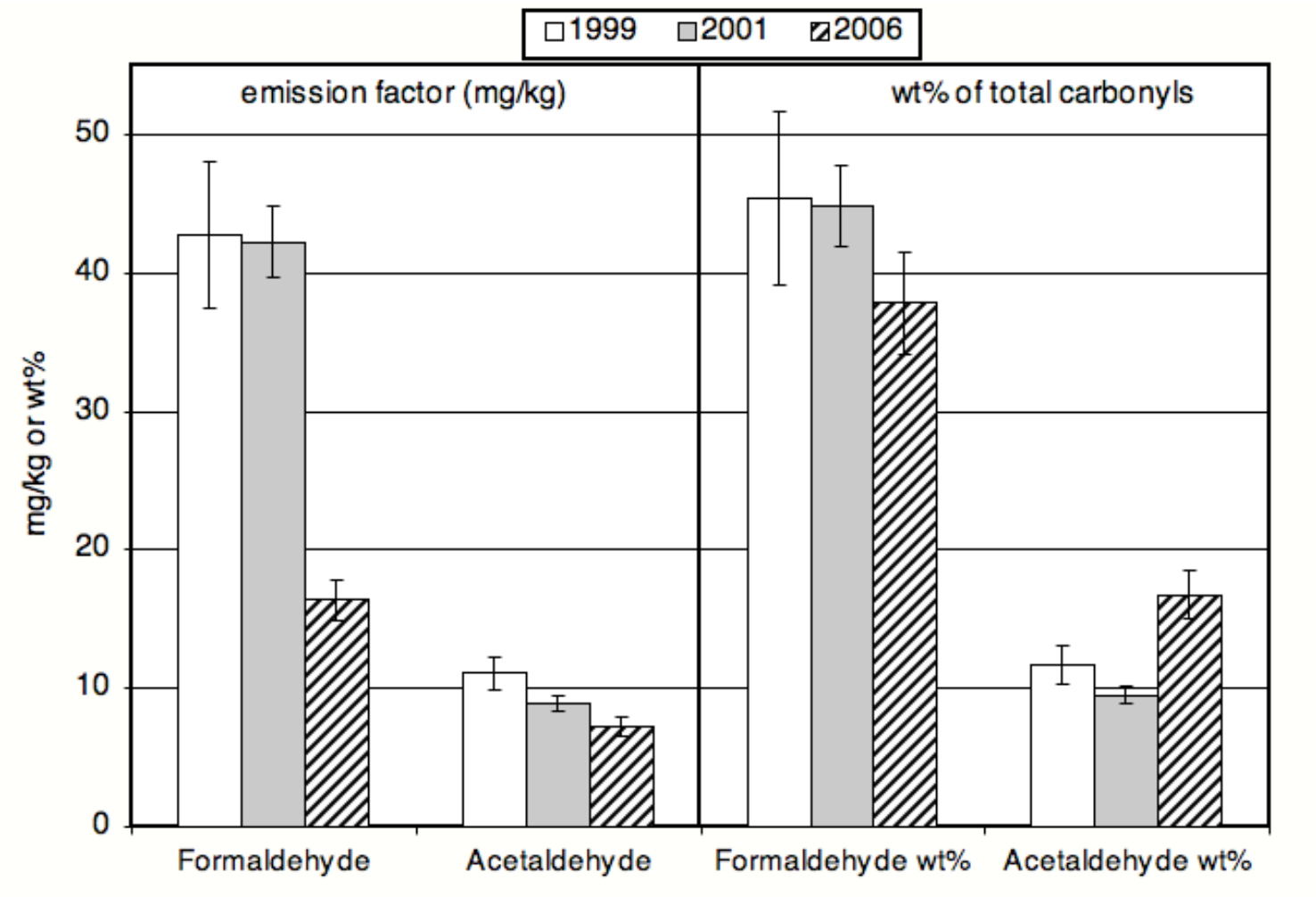

Figure 6.1: Formaldehyde and acetaldehyde emission factors for LD vehicles and weight percentages of total carbonyl emissions in 1999, 2001 and 2006. Error bars represent a 95% confidence interval for the mean. Results from 1999 are from Kean et al. 2001.

As will be discussed further in the next section, ethanol levels in gasoline increased from 0 to 4.2 vol% between 1999 and 2006. Over the same time period the acetaldehyde weight percent of C_2+ carbonyl mass emissions increased by 57 ± 7%. Various dynamometer studies report 50 to 150% increases in acetaldehyde emissions when ethanol is increased from 0 to 10 vol% (Reuter et al., 1992; Mayotte et al., 1994; Durbin et al., 2007). Tunnel results reported here lie in this range, with or without adjustment to account for the difference in fuel ethanol levels (i.e., increasing ethanol to 4.2 vs. 10%).

6.3.2 Fuel Composition.

Table 6.2 shows measured oxygenate and carbonyl concentrations in regular and premium grade gasoline samples from summer 2006. All brands except one had between 5.5 and 6.0 wt% ethanol. Brand D was formulated without ethanol or any other oxygenate. Carbonyl concentrations were low in all fuel samples (< 20 ppm). Note that more carbonyls (19 total) were identified in 2006 gasoline samples than reported previously for 1999 by Kean et al. (2001) due to a more thorough cleanup procedure that reduced interfering gasoline species.

Results from 2006 can be compared to gasoline analyses from previous years to quantify trends. Ethanol accounted for 0, 1.3, and 4.5 wt% of gasoline in 1999, 2001, and 2006, respectively, on a sales-weighted average basis including all gasoline brands and grades. MTBE decreased over the same years from 8.6 to 3.8 to 0 wt%. Determining the average concentration of MTBE in gasoline during summer 2001 is complicated because some fuel suppliers were not blending any MTBE in gasoline, while other suppliers were still adding large amounts. Other data for 30 gasoline samples (major brands) in the San Francisco Bay area indicate that MTBE accounted for 8.0 ± 4.0 and 5.9 ± 5.6 wt % (mean $\pm 1\sigma$) of gasoline in summers 1999 and 2001, respectively (Kean et al., 2002). The latter change (i.e., ~25% rather than >50% reduction) in MTBE levels in gasoline between 1999 and 2001 is more consistent with observed changes in formaldehyde emissions from LD vehicles.

Gasoline brand D, which did not contain ethanol, shows lower fuel concentrations of acetaldehyde than the other 4 brands in 2006 (i.e. 0.12 vs. 9 mg kg^{-1} for brand D vs. the average of other brands). Fuel samples collected in summer 1999 (Kean et al., 2001) when ethanol was

not observed in gasoline, also had lower concentrations of acetaldehyde compared to 2006. It appears that the origin of acetaldehyde in gasoline is therefore related to ethanol use. Carbonyls were not measured in unburned gasoline in 2001.

It is generally assumed that carbonyl emissions occur at the tailpipe, rather than in evaporative emissions of unburned fuel. Given the presence of acetaldehyde in gasoline we applied vapor/liquid equilibrium theory (Harley et al., 2000) to investigate potential acetaldehyde contributions to gasoline headspace vapors. Taking the ratio of the resulting acetaldehyde partial pressure to the vapor pressure of gasoline indicated that for the fuels reported here, the acetaldehyde contribution to gasoline headspace vapors was negligible (<<1% by mass). This analysis indicates that evaporative emissions of acetaldehyde remain at low levels, despite the increased abundance of acetaldehyde in unburned gasoline.

6.3.3 Diesel Truck Emissions.

Table 6.1 also shows carbonyl emission factors for diesel trucks measured in 2006. Inspection of Table 6.1 shows that diesel exhaust is a larger source per kg of fuel burned for all carbonyls with reported emission factors, and is especially significant as a source of saturated and unsaturated aliphatic aldehydes, as well as aliphatic dicarbonyls. Ratios of emission factors for diesel trucks vs. LD vehicles range from 2.5 to 14.0 within these carbonyl categories. The HD/LD emission factor ratios are lower for aromatic aldehydes than other carbonyl categories because absolute LD vehicle emissions of these carbonyls are relatively high; aromatic aldehydes in LD vehicle exhaust can be related to the presence of specific precursor aromatic hydrocarbons in gasoline (Kean et al., 2001). Uncertainty estimates shown in Table 6.1 for diesel trucks are larger than corresponding values for LD vehicles due to the need to apportion pollutant concentrations in the mixed traffic bore. We guard against large apportionment uncertainties by reporting diesel truck emission factors only if trucks contribute significantly to the concentrations of individual carbonyls measured in the mixed traffic bore (bore 1).

Approximately 59.0×10^{9} liters of gasoline and 11.6×10^{9} liters of diesel fuel were used on-road in California in 2005 (FHWA, 2006). Using fuel densities of 0.74 and 0.84 kg L^{-1} for gasoline and diesel fuel, respectively (Kirchstetter et al., 1999), the on-road mass ratio of gasoline/diesel fuel

use is approximately 4.5. Therefore, diesel trucks dominate LD vehicles as a direct emission source of any carbonyls listed in Table 6.1 for which the diesel/gasoline emission factor ratio exceeds 4.5.

Consideration of off-road engine emissions is likely to tip the carbonyl emission balance even more in the direction of diesel, as off-road diesel fuel accounts for ~1/3 of total diesel fuel sales nationally, whereas off-road uses of gasoline add only a few percent (Kean et al., 2000). Also diesel fuel use is growing more rapidly than gasoline (Harley et al., 2005), which may further increase the importance of diesel exhaust in future years.

Emission test methods used to certify the environmental performance of new HD diesel engines specify that only non-methane hydrocarbons should be measured, using a flame ionization detector or FID. Oxygenated VOC, such as aldehydes, are known to show reduced per carbon response on the FID versus hydrocarbons; formaldehyde especially shows very weak FID response relative to hydrocarbons (Hunter et al., 1998). Emissions of formaldehyde, the most abundant carbonyl in diesel exhaust, are therefore ignored in HD engine certification tests, and emissions of other carbonyls are likely to be undercounted due to reduced FID response.

Previous tunnel studies report carbonyl emissions from HD trucks driving through the Tuscarora mountain tunnel in Pennsylvania (Grosjean et al., 2001), Tauerntunnel in Austria (Schmid et al., 2001), Soderledstunnel in Sweden (Kristensson et al., 2004), Gubrist tunnel in Switzerland (Legreid et al., 2007), and Shing Mun tunnel in Hong Kong (Ho et al., 2007). Figure 6.2 compares Caldecott tunnel emission factors reported here with the 5 other studies. The primary emission factor results from the Caldecott tunnel are expressed per unit mass of fuel burned. However, to facilitate direct comparison of Caldecott tunnel emission factors to other studies in Figure 6.2, results from Table 6.1 are divided by estimated diesel truck fuel economy (3.4 km kg^{-1} = 6.7 mile gal^{-1}) using fuel consumption and traffic counts for MD and HD trucks reported in Chapter 2. Note that the various tunnel studies used different methods to apportion diesel vs. gasoline emissions and had different driving conditions (average speeds and road grades). Additionally, there were differences in the truck fleet due to different sampling years and national emission standards. Caldecott tunnel results are within the range of the other studies for

all but one (acrolein) of the carbonyls shown in Figure 6.2. As mentioned in a footnote to Table 6.1, acrolein was undermeasured and crotonaldehyde overmeasured in the Caldecott tunnel for 1999. In 2001, improvements were made to the LC mass spectrometry method using experiments performed in our laboratory that showed that when ambient acrolein is collected on DNPH cartridges, there are 3 major peaks, one of which co-elutes with crotonaldehyde and cannot be quantified easily without the use of mass spectrometry. Most of the studies shown in Figure 6.2 use standard LC-UV without mass spectrometry, and thus our results are expected to be higher for acrolein and lower for crotonaldehyde as Figure 6.2 indicates.

6.3.4 Carbon Monoxide Emissions.

Also shown at the bottom of Table 6.1 are CO emission factors. The LD vehicle emission factor decreased by 54 ± 5% between 1999 and 2006. Diesel engines emit CO at a rate that is 3.4 ± 0.7 times that of gasoline engines, per unit mass of fuel burned. All CO emission factors reported are for uphill traffic, however the diesel/gasoline comparison may be skewed by greater load dependence of CO emissions from diesels.

6.3.5 High Molecular Mass Carbonyls.

Table 6.3 shows a list of 20 later-eluting, high molecular mass carbonyls identified in tunnel air samples for both traffic bores in 2006. Concentrations of these carbonyls were at least 25% higher at the tunnel exit than entrance on at least 5 out of 8 sampling days in each bore. Emission factors for these carbonyls are not reported here because of coeluting peaks.

6.3.6 NO_2 Emissions.

NO_2 emissions were measured simultaneously with carbonyls using the method described by Tang et al. (2004). LD vehicle emission factors for NO_2 were found to be 64 ± 8, 57 ± 8, and 37 ± 7 mg kg^{-1} for 1999, 2001, and 2006, respectively. This suggests a rate of decrease of 6 ± 1% yr^{-1}. This is similar to the yearly rate of reduction of total NO_x for LD vehicles in the Caldecott tunnel from 1997-2006 of 7.4 ± 0.3% yr^{-1} (see Chapter 2). It should be noted that the analytical uncertainty of the 1999 NO_2 data is higher than that of 2001 and 2006. The NO_2 emission factor for diesel trucks was found to be 1470 ± 60 mg kg^{-1} in 2006.

Combining NO_2 emission factors with simultaneously measured NO_x emission factors (3.0 ± 0.2 for LD vehicles and 40 ± 3 g kg^{-1} for diesel trucks (Chapter 2)) leads to NO_2/NO_x emission ratios of 1.2 ± 0.3% for LD vehicles and 3.7 ± 0.3% for diesel trucks. The diesel truck NO_2/NO_x ratio observed in the Caldecott tunnel is smaller than reported in other studies. Average NO_2 and NO_x emission factors for HD trucks reported by Burgard et al. (2006) yield emission ratios of 5.6 ± 0.4% and 7.5 ± 0.7% in Dumont (*n*=1055 trucks) and Golden (*n*=446), respectively. Tang et al. (2004) report an NO_2/NO_x ratio of 7.7% (*n*=35, average of 2 driving cycles) for HD trucks, similar to the value of 8 ± 2% (*n*=1) reported by Jimenez et al. (2000). A possible reason for the lower NO_2/NO_x ratio observed in the Caldecott tunnel is higher engine load due to the uphill grade and faster speeds (64 km hr^{-1} for Caldecott vs. 20-40 and 5-25 km hr^{-1} for Dumont and Golden, and 32 km hr^{-1} in Jimenez et al.). There is an inverse relationship between NO_2/NO_x and engine load (Lenner, 1987). Another possible explanation is differences in analytical methods among studies used to measure NO_2, though previous comparisons indicate that chemiluminescent and DNPH-based measurement methods were in reasonable agreement (Tang et al., 2004).

It will be interesting to observe how carbonyl and NO_2 emissions are affected by oxidation catalysts associated with new DPF exhaust after-treatment systems. These systems are standard equipment on new diesel trucks starting with the 2007 model year; retrofitting of some older engines is also possible. There may be offsetting effects due to more stringent NO_x emission standards that in the U.S. are being phased in between 2007 and 2010 for new on-road HD diesel trucks.

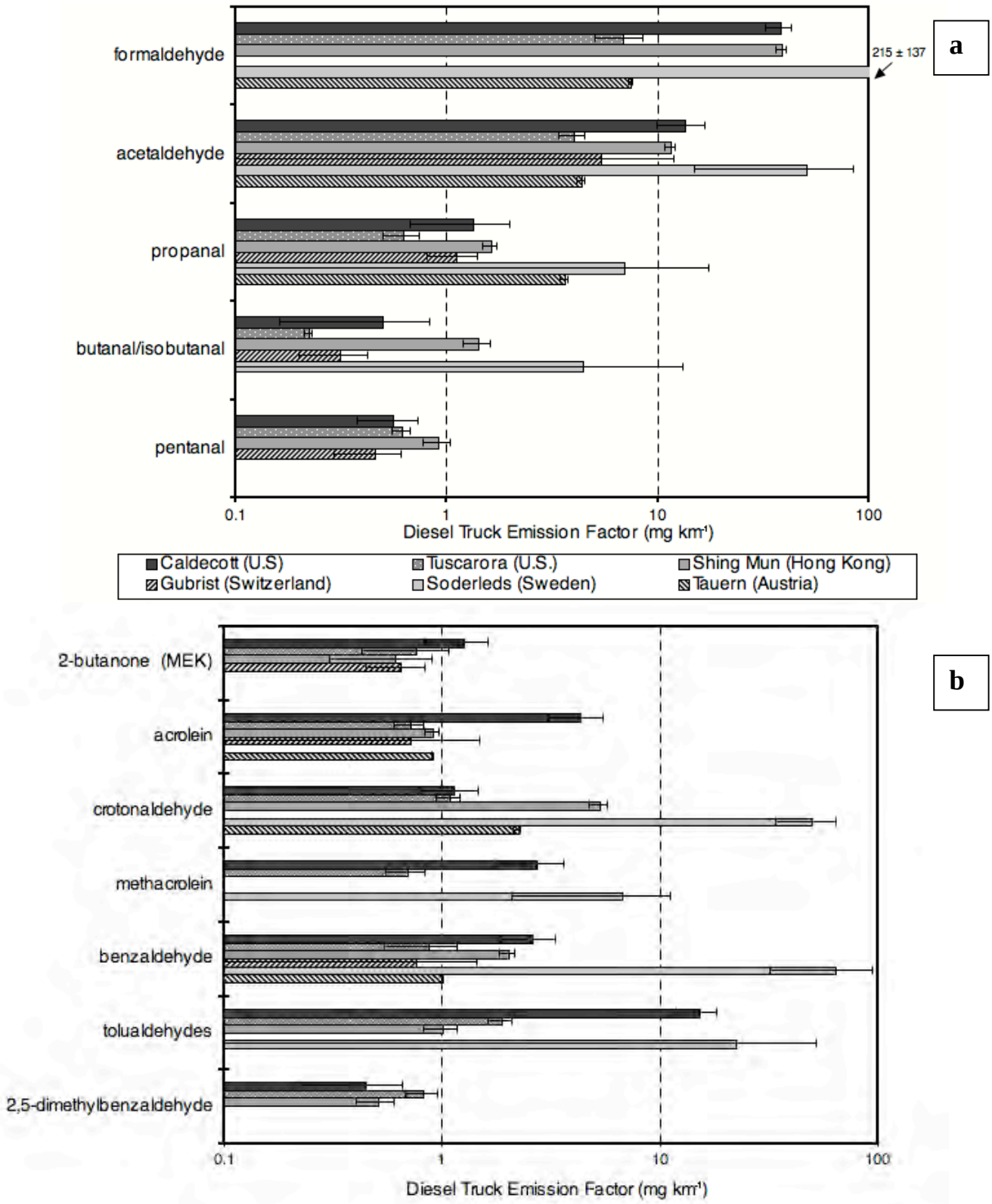

Figure 6.2 Comparison of diesel truck emission factors at the Caldecott tunnel (this study), with other recent on-road emission studies. a) saturated aliphatic aldehydes, and b) ketones, unsaturated aliphatic aldehydes, and aromatic aldehydes.

Table 6.3 Later eluting, high molecular mass carbonyls with positive emission factors (tunnel exit >25% higher than entrance for at least 5 of 8 samples in each bore).

2,3-Pentanedione
C8 ALP ISM #3 [a,b]
2-Oxohexanal
C8 ALP ISM #5 [a,b]
2,3-Hexanedione/ISM [b]
C8 ALP ISM #6 [a,b]
Octanal
Unknown #2 (ARM) [c]
C9 ALP ISM #2 [a,b]
trans-2-Nonenal/ISM [b]
C9 ALP ISM #3 [a,b]
Nonanal
trans-2-Decenal/ISM [b]
C10 ALP ISM #4 [a,b]
2-Decanone
Decanal
C9/C10 DICARB #1 [d]
C11 ALP ISM #1 [a,b]
C11 ALP ISM #2 [a,b]
Undecanal

[a]ALP=aliphatic. [b]ISM=isomer. [c]ARM=aromatic. [d]DICARB=dicarbonyl

7. Ammonia Emissions

7.1 Introduction

The use of catalytic converters has dramatically reduced most pollutant emissions from motor vehicles. Catalytic converters make use of the low activation energy of certain heterogeneous reactions on rare earth metals (e.g., palladium, platinum, and rhodium) to speed reactions in their approach to equilibrium conditions. Starting in 1975, oxidation mode (i.e, two-way) catalytic converters were introduced on automobiles in the U.S. (Heavenrich et al., 1987). These converters oxidize carbon monoxide (CO) and volatile organic compounds (VOC) to carbon dioxide (CO_2) and water. In 1981, three-way catalytic converters were introduced, with the additional capability to reduce nitrogen oxides ($NO_x = NO + NO_2$) to nitrogen gas. Having both oxidizing and reducing conditions occur simultaneously on the catalyst surface is best achieved if the air/fuel mixture is stoichiometric (Heywood, 1988). This is because hydrogen (H_2), the reducing agent for NO, and oxygen (O_2), the oxidizing agent for CO and VOC, can only be maintained in exhaust at sufficient concentrations by closely modulating air/fuel ratio around stoichiometric conditions. Feedback control of the air/fuel ratio using exhaust oxygen sensors was implemented in new vehicles starting in the 1980s to maintain near-stoichiometric operating conditions for optimum three-way catalytic converter operation.

An unwanted side effect of the use of three-way catalytic converters has been an increase in ammonia (NH_3) emissions from motor vehicles. Ammonia is the primary alkaline gas and the third most common nitrogen-containing species in the atmosphere, after nitrogen gas and nitrous oxide (Seinfeld and Pandis, 1998). Ammonia reacts with sulfuric or nitric acid in the atmosphere to generate secondary particles of ammonium sulfate and ammonium nitrate, respectively. Ammonia also is a major contributor to acidification/eutrophication processes in lakes (Pearson and Stewart, 1993; Watson et al., 1994).

Until recently, motor vehicles were not recognized to be a significant source of ammonia. However, the U.S. EPA now estimates that 5% of national ammonia emissions are due to motor vehicles, with almost all the remaining ammonia coming from agricultural processes (EPA, 2003). This figure may understate the importance of motor vehicle emissions in urban areas

where agricultural sources of ammonia are mostly absent. To date, no significant regulatory effort has been made to control NH_3 emissions from motor vehicles.

Ammonia is not created in significant quantities during typical combustion in a gasoline-powered vehicle, but is an undesirable product of NO reduction on the catalyst surface. Over-reduction of NO – beyond the formation of molecular N_2 – leads to ammonia in motor vehicle exhaust. Consequently, NH_3 emissions were low for early 1980s and older gasoline-powered vehicles (Pierson and Brachaczek, 1983) and have since increased following the widespread use of three-way catalytic converters (Cadle et al., 1979, Moeckli et al., 1996, Fraser and Cass, 1998, Kean et al., 2000).

On-road measurements of ammonia emissions from motor vehicles have been reported previously by several groups of investigators. Early studies showed that ammonia emissions from light-duty vehicles were low (Pierson and Brachaczek, 1983). These measurements were made in the Allegheny Mountain Tunnel in Pennsylvania in 1981 when less than 10% of vehicles were equipped with three-way catalytic converters. Fraser and Cass (1998) and others (see Table 7.1) showed increased ammonia emissions following the widespread use of 3-way catalytic converters. Burgard et al. (2006) used remote sensing to show that the distribution of ammonia emissions across the vehicle fleet shows an atypical pattern: the highest average ammonia emission rates were observed for ~10 year-old vehicles. It is well understood that the oldest vehicles (no catalytic converter) or those with deactivated catalysts will have negligible emissions of ammonia. In addition, Burgard et al. have shown that new vehicles also emit low quantities of ammonia. So unlike most other pollutants, ammonia emissions are dominated by "middle-aged" vehicles (Burgard et al., 2006).

Ammonia emissions from catalyst-equipped vehicles have been shown in laboratory dynamometer studies to be markedly higher than for pre-catalyst vehicles (Cadle et al., 1979; Urban and Garbe, 1979; Cadle and Mulawa, 1980; Durbin et al., 2002). The reaction that produces ammonia on the catalyst is enhanced if the engine runs fuel-rich, because that condition favors reducing processes on the catalyst surface (Cadle et al., 1979; Urban and Garbe, 1979; Cadle and Mulawa, 1980). Durbin et al. (2002) reported an average ammonia emission factor of

34 mg km^{-1} for 39 recruited gasoline-powered vehicles on the Federal Test Procedure (FTP), with increased ammonia emissions on more aggressive driving cycles. In related efforts, Huai et al. (2003 and 2005) showed that ammonia emissions are primarily generated during acceleration events for modern technology vehicles.

The primary objective of the present investigation was to determine if on-road emissions of ammonia are continuing to increase as turnover in the vehicle fleet continues to replace older vehicles whose catalysts may no longer be functional with new three-way catalyst-equipped vehicles. We have previously reported ammonia measurements from a large sample of on-road vehicles using California reformulated gasoline in 1999 (Kean et al., 2000), which are compared here to more recent measurements performed in 2006. We also present time-resolved ammonia measurements from 2001 to describe emissions as a function of vehicle operating mode.

A secondary objective of this study was to estimate ammonia emissions from heavy-duty diesel vehicles. Ammonia emissions from heavy-duty vehicles have been shown to be small relative to modern light-duty vehicles, but these measurements were made two decades ago (Pierson and Brachaczek,1983). To meet increasingly stringent nitrogen oxide emission standards, future adoption of selective catalytic reduction (SCR) by the addition of urea or ammonia to diesel exhaust is likely. If not properly controlled, use of SCR could result in elevated ammonia emissions from heavy-duty vehicles. The present study documents baseline heavy-duty diesel truck ammonia emission rates prior to SCR use.

7.2 Experimental Section

For all years of this study (1999, 2001, and 2006), NO_x, CO, and CO_2 concentrations were measured at the Caldecott tunnel inlet and outlet on summer weekdays using standard ambient air monitoring equipment (see Chapter 2 and Kean et al., 2000). Calibration of all gas-phase analyzers was checked daily prior to sampling. Ammonia measurements were made in 1999 on 8 summer weekdays between 4 and 6 PM PDT, using annular denuders coated with citric acid, with extracts later analyzed using ion chromatography with a conductivity detector (Kean et al., 2000).

In 2001, semi-continuous measurements of gas-phase ammonia were made with 15-minute time resolution at the exit of tunnel bore 2 between 2:00 and 9:30 PM on 7 days in July and August. Ammonia was stripped from the sample air stream by dissolution in a water film in cocurrent flow inside a tubular wet effluent denuder (Buhr, 1995), as shown in Figure 7.1. Sample air was drawn from the exhaust bore (located directly above the traffic bore) into a pre-cleaned 70 cm long, 0.4 cm ID etched borosilicate glass tube. The air flow rate was controlled at 1.06 L min^{-1} using a critical orifice. Deionized water was supplied to the top of the denuder by a peristaltic pump at a rate of 1.7 mL min^{-1}. The water flowed down the inner walls of the denuder tube and ammonia gas diffused towards and dissolved in the flowing film of water. Collection efficiencies were measured during instrument development and found to be close to unity. The water was collected at the bottom of the tube using a collection cup and drain attached to the bottom of the denuder tube. A second peristaltic pump conveyed the collected water to a cation concentrator column that collected sample for 13 minutes. From the concentrator column, the sample was sent to an ion chromatograph for quantification of ammonium. Calibration of the signal was accomplished with aqueous solutions of known ammonium concentration. In 2001, only the tunnel exit ammonia concentration was measured. Based on previous experience in 1999, background levels of ammonia were expected to be small and relatively constant compared to those measured at the tunnel exit.

In 2006, 2-hour average ammonia measurements were made on 8 days in bore 2 (light-duty vehicles only), and on 8 days in bore 1 (mixed traffic including both light-duty vehicles and heavy-duty diesel trucks). Measurements in bore 2 were made during the 4-6 PM peak traffic period. Measurements in bore 1 were performed from 12-2 PM, when the heavy-duty traffic contribution to emissions was highest. Samples were collected on citric acid-coated annular denuders at a nominal flow rate of 5 L min^{-1}. Flow was regulated using a critical orifice and quantified with a primary air flow standard. The ammonium collected on the denuders was analyzed after each day of sampling using an ion chromatograph with conductivity detector, similar to 1999 (Kean et al., 2000). Traffic volume and average speed through the tunnel were determined for each sampling day, as detailed in Chapter 2.

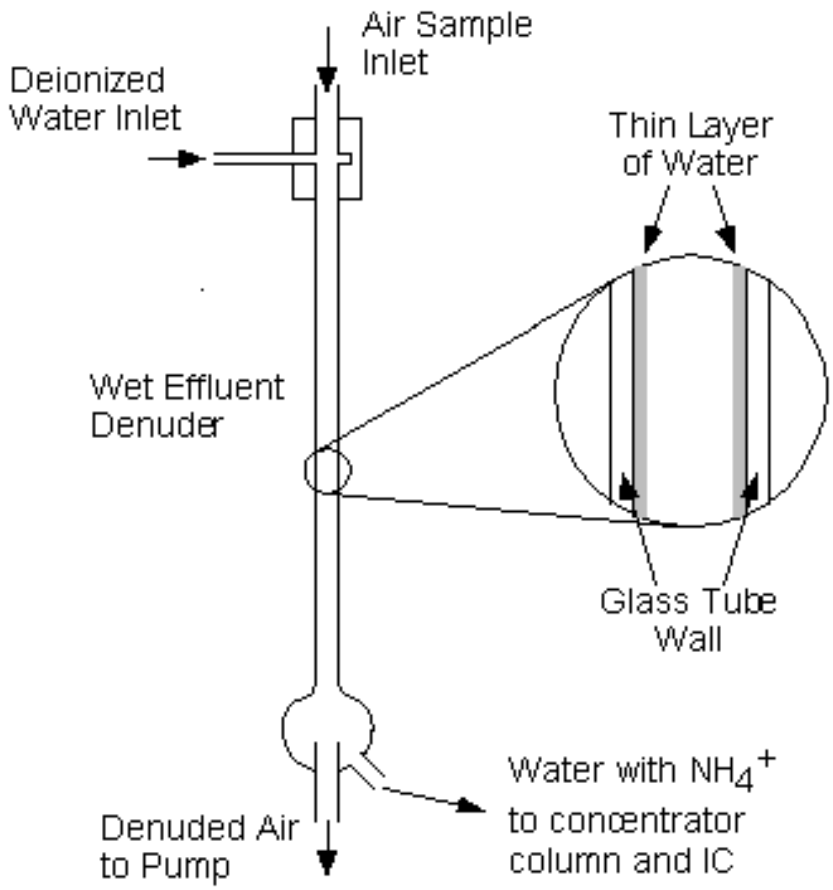

Figure 7.1 Schematic of the tubular wet effluent denuder used for ammonia sampling in 2001.

7.3 Results and Discussion

7.3.1 Light-Duty Vehicle Ammonia Emission Factor Trends

Light-duty vehicle emission factors were calculated by carbon balance using equation 7.1

$$E_{\mathrm{NH_3}} = \left(\frac{\Delta[\mathrm{NH_3}]}{\Delta[\mathrm{CO_2}] + \Delta[\mathrm{CO}]} \right) w_C \qquad (7.1)$$

where E_{NH3} is the ammonia emission factor (mg kg^{-1} of fuel burned), $\Delta[NH_3]$ is the increase in mass concentration of ammonia measured between tunnel entrance and exit (μg m^{-3}), $\Delta[CO_2]$ and $\Delta[CO]$ are similarly background-subtracted concentrations (mg C m^{-3}), and $w_C = 0.85$ is the mass fraction of carbon in oxygenated gasoline used in California. Organic compounds are not included in the denominator of eq. 7.1 because the hydrocarbon contribution to total carbon concentrations in the tunnel is known to be negligible compared to CO_2 and CO.

The ammonia emission factor for light-duty vehicles at the Caldecott tunnel in 1999 was 640 ± 40 mg kg^{-1}. The uncertainty bounds provide a 95% confidence interval for the mean based on run-to-run variability in the results over 8 days of sampling. At the time of these measurements, we estimated based on a license-plate survey that ~99% of vehicles in the center bore are gasoline-powered and >94% of the vehicles were originally outfitted with three-way catalyst systems (Kean et al., 2000). During the rush-hour period of measurement, driving conditions and the mean vehicle age (~6 years old) at the Caldecott Tunnel are consistent from year to year (Chapter 2).

The ammonia emission factor in 2006 decreased to 400 ± 20 mg kg^{-1}. This represents a 38 ± 6% reduction over the 7 years since the 1999 study (Kean et al., 2000). For comparison, over this same time period, the light-duty vehicle NO_x emission factor for NO_x decreased by 54 ± 6%. The present study clarifies that despite increasing ammonia emissions as a given vehicle ages, the Caldecott tunnel fleet as a whole is emitting less ammonia today than 7 years ago under the same driving conditions.

In 1999, the molar ratio of ammonia to total fixed nitrogen (taken to be NO_x + NH_3) in vehicle emissions was 0.21 ± 0.01 at the Caldecott tunnel. This same measurement in 2006 was 0.27 ± 0.01. While vehicle emission rates (and total emissions) of ammonia are reducing over time, the fraction of reactive nitrogen being emitted as ammonia by light-duty vehicles is increasing. This is an indication that emission controls for NO_x have had a greater effect than any efforts that have resulted in lower ammonia emissions.

A comparison of the Caldecott tunnel results to other on-road and dynamometer-based investigations is given in Table 7.1. Where possible, emission factors have been converted into the same units to facilitate comparison. An estimate of ammonia emission factors at the Caldecott tunnel on a mg km^{-1} basis can be made using vehicle fuel efficiencies measured at the Caldecott tunnel in 2001 (Kean et al., 2003). During the 4-6 PM traffic period in 2001, the measured light-duty vehicle fuel consumption for uphill traffic was 16.4 ± 0.1 L/100 km (14.4 ± 0.1 mpg). As fuel economies (EPA, 2006) and driving conditions at the tunnel have not changed significantly over the last decade (Chapter 2), it is reasonable to apply this rate of fuel consumption to both the 1999 and 2006 measurements. Focusing on the measurements made in California, it appears that early three-way catalyst fleets and modern fleets at high load emit over 600 mg kg^{-1} of ammonia. Modern fleets at lower loads emit lower rates of ammonia (350-450 mg kg^{-1}). The general similarity of the fuel-based measurements is notable given the wide range of measurement techniques used and driving conditions observed.

7.3.2 Engine Load Effects on Light-Duty Vehicle Emissions

The wet-effluent denuder used to measure ammonia at the Caldecott Tunnel in 2001 permitted measurement of ammonia concentrations at 15-minute intervals. Figure 7.2 presents the normalized ammonia emission factors (± 95% confidence interval) over the course of the afternoon with uphill driving in summer 2001. These data have been normalized by the average emission factor measured from 4-6 PM, the period emphasized elsewhere in this investigation. Absolute emission factors are not presented because the measurements in 2001 were made in the tunnel ventilation duct above the traffic and are likely biased low relative to the 1999 and 2006 measurements made inside the traffic tube. The emission factor decreases gradually from 2 to 6 PM and then increases rapidly to a maximum at 9:30 PM. Also included in the figure are vehicle

Table 7.1. Comparison of On-Road and Recent Dynamometer-Based Ammonia Emissions Measurements from Light-Duty Vehicles.

Year	Location	Authors	mg kg^{-1}	mg km^{-1}	Notes
1981	Allegheny Mountain Tunnel, PA	Pierson and Brachaczek, 1983		1.3 ± 3.5	Very few (<10%) three-way catalyst (TWC) equipped vehicles
1993	Van Nuys Tunnel, CA	Fraser and Cass, 1998	510	61	81% of vehicles were TWC equipped
1995	Gubrist Tunnel, Switzerland	Moeckli et al., 1996	230 ± 70	15 ± 4	Authors have greater confidence in mg km^{-1} than mg kg^{-1}
1999	Caldecott Tunnel, CA	Kean et al., 2000	640 ± 40	78 ± 6	Warmed-up vehicles traveling at highway speeds up 4% grade
1999	Freeway On-Ramp, CA	Baum et al., 2001	350 ± 30	37 ± 3	Remote sensing study of warmed-up vehicles
2001	Riverside, CA dynamometer	Durbin et al., 2002	420 ± 140	34 ± 11	Mixed fleet of 39 vehicles on FTP driving cycle
2002	Gubrist Tunnel, Switzerland	Emmenegger et al., 2004		31 ± 4	Investigation focused on comparing measurement techniques
2002	Riverside, CA dynamometer	Durbin et al., 2004, Huai et al., 2003	~120	9-13	Dynamometer study of twelve 2000-2001 vehicles on FTP cycle
2002	Riverside, CA dynamometer	Durbin et al., 2004, Huai et al., 2003	~680	46-56	Dynamometer study of twelve 2000-2001 vehicles on US06 cycle
2005	Denver, CO and Tulsa, OK	Burgard, et al., 2006	500 ± 10		Remote sensing study of freely flowing highway traffic
2006	Caldecott Tunnel, CA	Present investigation	400 ± 20	49 ± 4	Warmed-up vehicles traveling at highway speeds up 4% grade

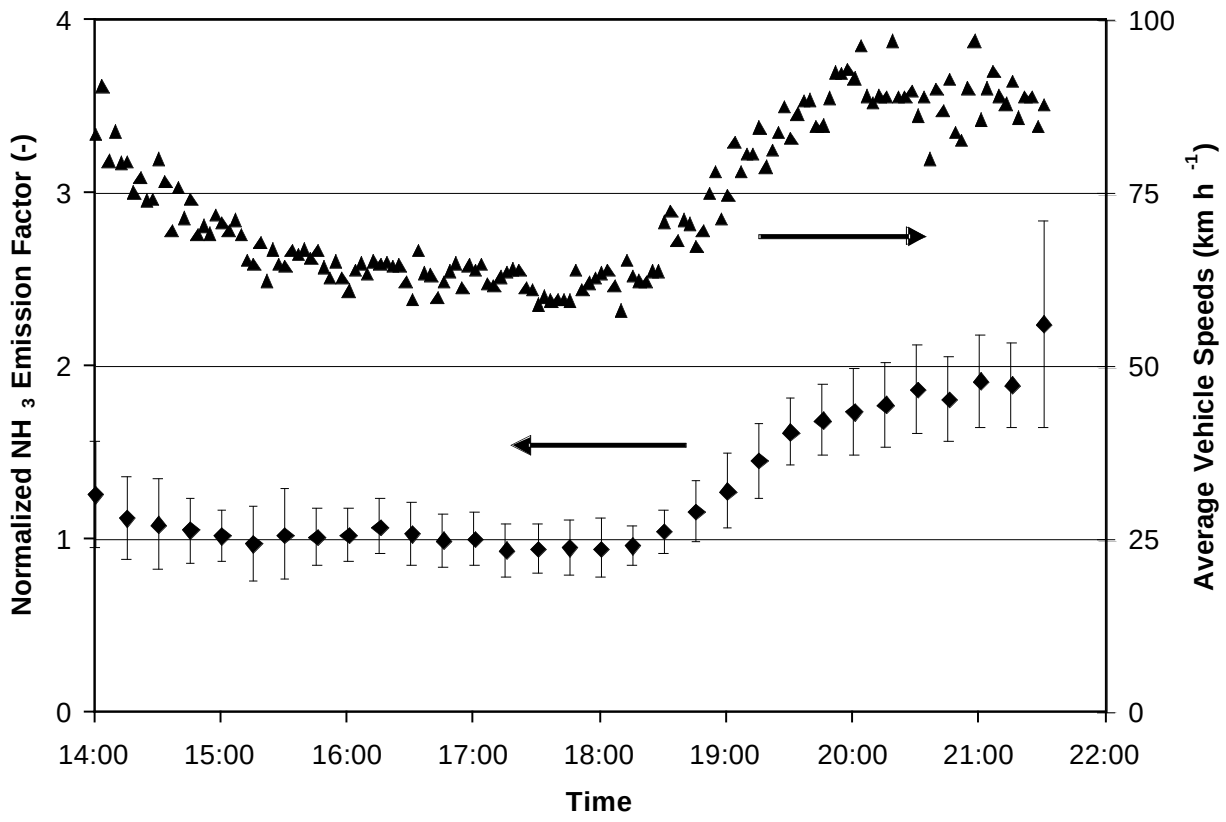

Figure 7.2 Ammonia emission factors for light-duty vehicle traffic driving uphill (plotted using diamond symbols) normalized by the average emission factor measured from 4-6 PM in 2001. Average vehicle speeds are also plotted (triangle symbols without error bars).

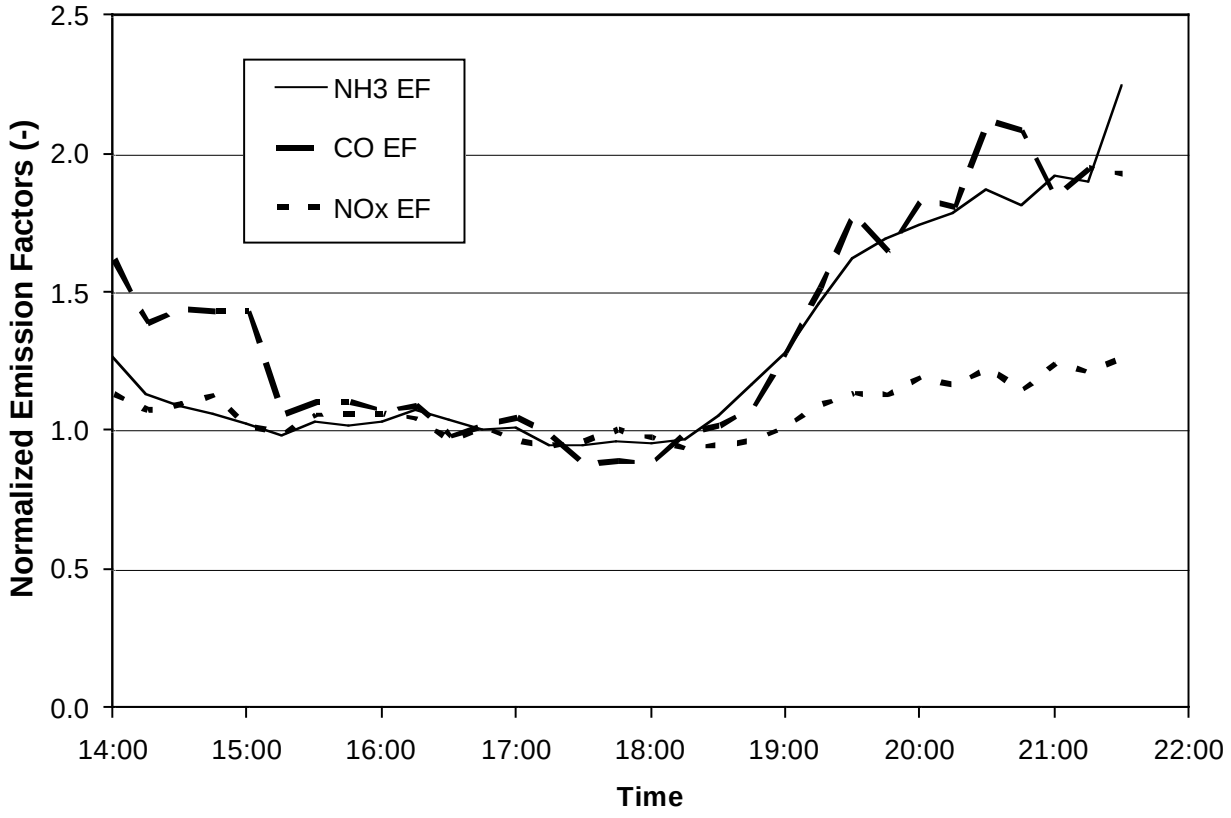

Figure 7.3 Emission factors for NH_3, CO, and NO_x normalized by 4-6 PM average emission factors measured at the tunnel; uphill light-duty vehicle traffic only.

speeds through the tunnel in 2001 (Kean et al., 2003). The increase in ammonia emissions with increasing vehicle speed and thus engine load is apparent, as we have previously reported for CO and NO_x (Kean et al., 2003).

Variations over the course of the afternoon in the ammonia emission factor during the 2001 study are compared to variations in CO and NO_x in Figure 7.3. Ammonia roughly tracks NO_x from 2-6 PM, resulting in a near constant NH_3 to fixed nitrogen ratio during this period. This suggests that the quantity of NO_x passing through the catalytic converters appears to limit ammonia emissions. After 6 PM when traffic volumes are lower and vehicle speeds are higher, NH_3 tracks CO emissions. Taking elevated CO emissions as an indication of enrichment, the more strongly reducing conditions on the catalyst appear to convert a greater fraction of NO_x to ammonia during the period after 6 PM. The ratio of ammonia emissions to total fixed nitrogen emissions therefore increases.

7.3.3 Analysis of Remote Sensing Data

The above analysis pertains to fleet-average emissions. It is unclear from the tunnel data how ammonia emission rates are distributed across individual vehicles, and how they correlate with NO_x and CO emission rates. Since most emitted NH_3 molecules likely existed as NO molecules upstream of the catalytic converter, a trade-off is likely to exist such that high ammonia emissions occur at low NO emissions. In addition, high NO emissions may indicate lean combustion, which can hinder formation of ammonia on the catalyst.

The likely correlation between ammonia and CO emissions is less obvious. High CO emissions are an indication of strongly reducing conditions on the catalyst surface, which promotes conversion of NO to NH_3. However under fuel-rich conditions, NO formation is limited, which in turn could limit formation of NH_3 by the catalytic converter. Because of these conflicting effects, it is difficult to predict in advance if high ammonia and CO emissions occur concurrently. The picture is further complicated by the fact that elevated NO and/or CO emissions may be an indication of a non-functional catalyst, in which case low ammonia emissions would be expected. Remote sensing measurements of ammonia emissions reported by Burgard et al. (2006) are used here to study relationships among pollutants. Measurements of

NH_3, NO, and CO concentrations in the exhaust plumes of 21,858 individual vehicles were made by Burgard et al. in 2005 in Tulsa and Denver.

Figure 7.4 presents average ammonia emission factors (mg kg^{-1}) as a function of NO and CO concentration in light-duty vehicle exhaust. For this, vehicles are binned based on their NO and CO exhaust concentrations, and then the average ammonia emission factor within each bin is presented. The average ammonia emission factors are: 610 ± 30 mg kg^{-1} for model year 1995 and older vehicles (Figure 7.4a), 600 ± 20 mg kg^{-1} for model year 1996-2000 (Figure 7.4b), 370 ± 20 mg kg^{-1} for model year 2001 and newer vehicles (Figure 7.4c), and 500 ± 10 mg kg^{-1} for the entire fleet. The number of vehicles in each bin varies depending on the prevalence of the corresponding emission rates and is presented in the figures.

Looking at Figure 7.4, ammonia emission factors are highest for vehicles with low exhaust NO concentrations and high exhaust CO concentrations. This trend is present for the three vehicle age groups, but is most pronounced for newer vehicles. The data suggest that there is a trade-off in the emissions of ammonia and NO; NO emissions decrease due to the formation of NH_3 on the catalyst. The data also suggest that chemically reducing conditions on the catalyst surface (as evidenced by high CO) do, in fact, enhance additional conversion of NO to NH_3.

Figure 7.4 is useful for understanding correlations between ammonia and other pollutant emissions, but does not aid in understanding which vehicles are responsible for the bulk of total ammonia emissions. Figure 7.5 estimates the contribution of each NO-CO bin to total ammonia emissions by accounting for the fact that the number of vehicles in each bin varies. For Figure 7.5, each ammonia emission factor in Figure 7.4 was weighted by the number of vehicles in that bin and then divided by the total emissions across the fleet. The results in Figure 7.5 should be considered approximate because its development effectively required assuming a constant fuel-economy value across the fleet. The model year 1995 and older vehicles were 19% of the fleet and emit ~23% of the total ammonia emissions, model year 1996-2000 vehicles were 36% of the fleet and emit ~43% of emissions, and model year 2001 and newer vehicles were 45% of the fleet and emit ~34% of ammonia emissions. Further inspection of Figure 7.5 indicates that total emissions of ammonia are dominated by the vehicles with the lowest NO emissions. For the

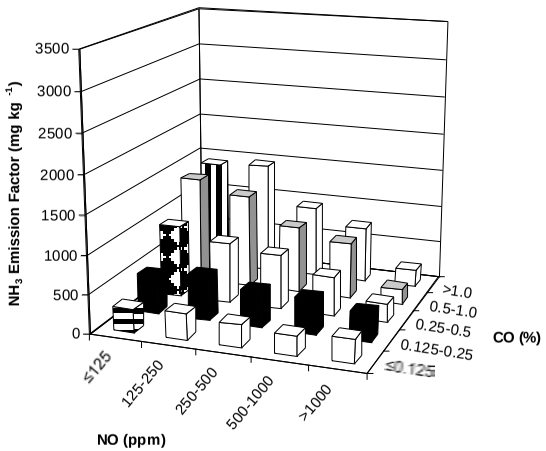

Vehicles Per Bin					
232	126	110	124	129	>1.0
148	78	97	103	147	0.5-1.0
244	107	139	123	130	0.25-0.5
287	129	129	133	143	0.125-0.25
469	162	184	207	212	≤0.125
≤125	125-250	250-500	500-1000	>1000	
NO (ppm)					

CO (%)

(a)

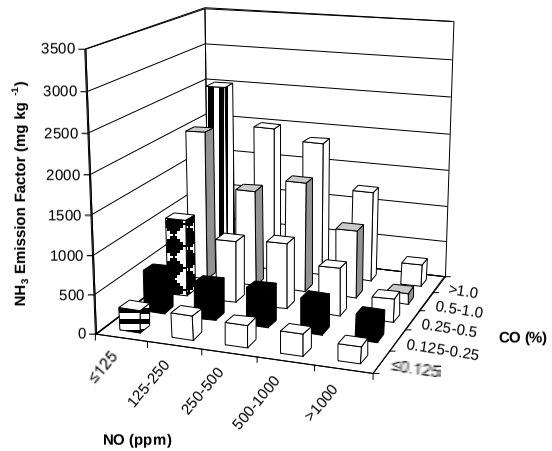

Vehicles Per Bin					
162	48	35	31	36	>1.0
302	86	46	45	59	0.5-1.0
744	174	117	79	50	0.25-0.5
1393	265	202	126	63	0.125-0.25
2703	433	326	204	115	≤0.125
≤125	125-250	250-500	500-1000	>1000	
NO (ppm)					

CO (%)

(b)

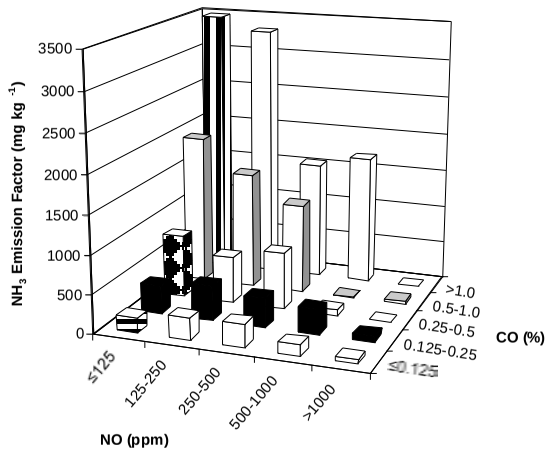

Vehicles Per Bin					
98	4	3	3	1	>1.0
180	19	6	3	10	0.5-1.0
845	44	27	6	7	0.25-0.5
2251	111	61	38	29	0.125-0.25
5634	250	127	101	64	≤0.125
≤125	125-250	250-500	500-1000	>1000	
NO (ppm)					

CO (%)

(c)

Figure 7.4 Average ammonia emission factors (mg kg^{-1}) as a function of NO and CO concentration in light-duty vehicle exhaust (calculated from Burgard et al., 2006) for **(a)** model year 1995 and older vehicles (19% of the 21,858 vehicles in their study were in this age group), **(b)** model year 1996-2000 vehicles (36% of the 21,858 vehicles in their study were in this age group), and **(c)** model year 2001 and newer vehicles (45% of the 21,858 vehicles in their study were in this age group).

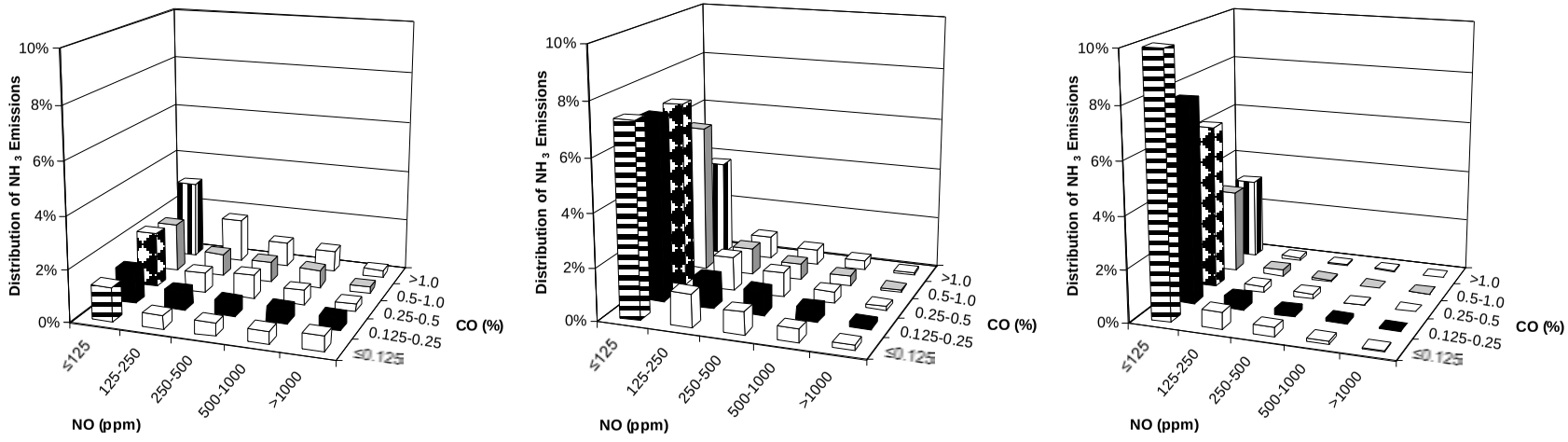

(a) **(b)** **(c)**

Figure 7.5 Estimated distribution of ammonia emissions as a function of NO and CO concentration in light-duty vehicle exhaust (calculated from Burgard et al., 2006) for **(a)** model year 1995 and older vehicles, **(b)** model year 1996-2000 vehicles, and **(c)** model year 2001 and newer vehicles. The bin heights in Figures 7.5a, 7.5b, and 7.5c sum to 100%.

oldest vehicles, the bins with high ammonia emission factors (see Figure 7.4a) also contributed significantly to total ammonia emissions. This is in contrast to the newest vehicles, where several bins with high emission factors contributed insignificantly to total emissions because of the small number of vehicles in those bins. For the newest vehicles, a low emission factor for ammonia for the cleanest vehicles (i.e., low NO and low CO) was overwhelmed by the sheer number of vehicles in this bin.

7.3.4 Ammonia Emissions from Medium- and Heavy-Duty Diesel Trucks

Contributions to ammonia concentrations in bore 1 of the Caldecott tunnel from medium- and heavy-duty (MD/HD) vehicles were estimated using CO_2 as a tracer for gasoline engine emissions, together with LD vehicle emission ratios measured in bore 2:

$$\Delta[NH_3]_{1,D} = \Delta[NH_3]_1 - \Delta[CO_2]_{1,G}\left(\frac{\Delta[NH_3]_2}{\Delta[CO_2]_2}\right) \tag{7.2}$$

where subscripts 1 and 2 outside the bracket refers to tunnel bore number and D or G refers to emissions due to diesel or gasoline vehicles, respectively. $\Delta[CO_2]_{1,G}$ is calculated as described previously in Chapter 2.

The resulting ammonia emission factor for diesel trucks in the Caldecott tunnel in 2006 is 170 ± 150 mg kg^{-1}. The 95% confidence interval is large because of the small fraction of ammonia emissions attributed to diesel engines in bore 1, only 8% on average. For comparison, the light-duty vehicle emission factor for ammonia in the same year was 400 ± 20 mg kg^{-1}. The large uncertainty for the diesel value makes a definitive comparison of these two emission factors difficult. Given other available measurements (e.g., Pierson and Brachaczek, 1983), it is likely that the true ammonia emission factor for diesel trucks lies at the low end of the range reported here. The Caldecott tunnel was not well-suited to determination of ammonia emission rates for diesel trucks, due to the large contribution to ammonia concentrations in bore 1 from light-duty vehicles. However, this implies that diesel trucks are at present a minor source of ammonia emissions compared to light-duty gasoline vehicles.

8. Conclusions

8.1 Summary of Major Findings

Light-duty vehicle emissions have declined since the 1990s for nearly every pollutant examined in this study (ethanol and carbon dioxide are noteworthy exceptions to this generalization). For CO, HC, and NO_x, the decline in LD vehicle emissions observed at the Caldecott tunnel is consistent with other long-term studies of on-road vehicle emission trends (Stedman and Bishop, 2008). LD vehicle emissions of exhaust particulate matter, carbonyls, and ammonia have also decreased. These reductions are due mainly to fleet turnover and improved emission control technologies on new vehicles, though reformulation of gasoline has played a role especially in achieving benzene emission reductions, and to a lesser extent also benefited other pollutants such as carbon monoxide and hydrocarbons. While concerns have been expressed about increased acetaldehyde emissions due to the switch from MTBE to ethanol in California gasoline, we find that fleet turnover effects have led to overall emission reductions for acetaldehyde since 2001, despite any possible increase in direct emissions due to the switch to ethanol. In addition, the removal of MTBE from gasoline led to lower direct emissions of formaldehyde.

Ammonia emissions from LD vehicles were low prior to the introduction of three-way catalytic converters, then increased starting in the 1980s. This was due to NO_x present in vehicle exhaust being over-reduced to NH_3 rather than to the desired endpoint (N_2). Recent data from the present Caldecott tunnel study suggests that the rise in ammonia emissions from LD vehicles has stopped and reversed, with improved control of CO emissions likely contributing to the recent downward trend in NH_3 emissions.

Turning to heavy-duty diesel vehicles, on-road emissions of exhaust PM mass have decreased, indicating that emission standards for exhaust PM from new HD engines have led to lower mass emissions (this trend was already apparent in results of chassis dynamometer studies of HD truck emissions conducted in the 1990s, see review by Yanowitz et al., 2000). Our assessment of trends in ultrafine particle number (PN) emissions is that there has been a significant decrease in PN emissions from HD trucks. Note that the most recent Caldecott tunnel results from 2006 include the effects of adopting ultra-low sulfur diesel fuel, which is expected to be a contributing

factor in reducing PN emissions. The distributions of black carbon (BC) mass and particle number (PN) emissions are both skewed, with the highest-emitting 10% of on-road trucks responsible for about 40% of total emissions in both cases. However, there is little overlap between high-BC and high-PN emitters, and there is reason to believe these emissions may be anti-correlated at least for high-emitting trucks.

To date progress in controlling NO_x emissions from heavy-duty diesel engines has been slow. Results in Chapter 2 are consistent with other studies that also report slow progress in diesel NO_x control (Yanowitz et al., 2000; Burgard et al., 2005). So far the rate of reduction in HD fleet-average NO_x emission factors has not been large enough to offset the effect of rapid growth in the amount of diesel fuel being consumed each year (Harley et al., 2005). Given the successes that California has seen in controlling other NO_x sources such as gasoline engines and power plants, the end result is that NO_x emissions are increasingly dominated by the contribution from diesel engines. The diesel source includes not only on-road trucks and buses, but also off-road engines used in construction, mining, and farm equipment, railroad locomotives, and ships. As control of gasoline engines has progressed, the importance of HD engines as a source of direct aldehyde emissions has also increased.

8.2 Recommendations for Future Research

1. Continue tracking mobile source emission trends through on-road/real-world studies, with emphasis on NO_x and PM emissions from heavy-duty diesel engines. Large reductions in diesel emissions are anticipated in future years due to recently adopted emission standards and other control measures, and it will be critically important for the state's air pollution programs to have greater certainty about what emission reductions have occurred by 2010, 2015, 2020, etc.

2. Further develop, combine, and apply methods that can measure NO, NO_2, formaldehyde, CO, CO_2, black carbon, particle number and size distribution, and PM mass concentrations at high time resolution in the exhaust plumes of individual diesel trucks as they drive by. Such systems could be deployed in mobile laboratories for in-use truck emission surveillance on freeway overpasses, along truck routes, at ports and freight terminals, etc.

3. Evaluate and apply in an on-road setting an electrometer-based particle spectrometer that counts the numbers of particles in multiple size ranges simultaneously. The scanning mobility particle spectrometer (SMPS) used in the present study did not permit fast enough scans over the range of relevant particle sizes to measure size-resolved PN exhaust emissions from individual vehicles as they drove by. An alternative option if no electrometer-based systems are available is to deploy multiple differential mobility analyzer/condensation particle counter (DMA/CPC) systems that operate at carefully selected fixed particle sizes of interest (i.e., hold control voltage constant and count continuously with high time resolution at one particle size only for each DMA/CPC).

4. Assess through a combination of modeling and field measurements the sources and concentrations of ethanol and acetaldehyde in the atmosphere, and their contributions to ozone production. Acetaldehyde is an especially complicated case as there are direct and poorly characterized primary emissions from multiple sources, *in situ* formation from oxidation of ethanol and other primary VOC, and rapid reaction with the hydroxyl radical leading to formation of other pollutants such as peroxyacetyl nitrate (PAN).

5. Critically evaluate the inventory of diesel engine aldehyde emissions, and assess the role that these emissions play in ozone air pollution, diesel exhaust odor, and toxic air contaminant problems.

9. References

Abu-Allaban, M., Coulomb, W., Gertler, A.W., Gillies, J., Pierson, W.R., Rogers, C.F., Sagebiel, J.C., and Tarney, L., 2002. Exhaust Particle Size Distribution Measurements at the Tuscarora Mountain Tunnel. *Aerosol Sci. Technol.* **36**, 771-789.

Atkinson, R., 2000. Atmospheric Chemistry of VOCs and NOx. *Atmos. Environ.* 34, 2063-2101.

Ayala, A., Olson, B., Cantrell, B., Drayton, M., Barsic, N., 2003. Estimation of Diffusional Losses When Sampling Diesel Aerosol: A Quality Assurance Measure. *SAE Technical Paper*, no. 2003-01-1896.

Baum, M.M., Kiyomiya, E.S., Kumar, S., Lappas, A.M., Kapinus, V.A., and Lord III, H.C., 2001. Multicomponent Remote Sensing of Vehicle Exhaust by Dispersive Absorption Spectroscopy. 2. Direct On-Road Ammonia Measurements. *Environ. Sci. Technol.* 35, 3735-3741.

Baumgard, K.J.; Johnson, J.H., 1996. The Effect of Fuel and Engine Design on Diesel Exhaust Particle Size Distributions. *SAE Technical Paper*, no. 960131.

Birch, M.E., Cary, R.A., 1996. Elemental Carbon-Based Method for Monitoring Occupational Exposures to Particulate Diesel Exhaust. *Aerosol Sci. Technol.* 25, 221-241.

Bishop, G.A., Morris, J.A., Stedman, D.H., Cohen, L.H., Countess, R.J., Countess, S.J., Maly, P., Scherer, S., 2001. The Effects of Altitude on Heavy-Duty Diesel Truck On-Road Emissions. *Environ. Sci. Technol.* 35, 1574-1578.

Bishop, G.A., Stedman, D.H., 2006. On-Road Remote Sensing of Automobile Emissions in West Los Angeles: Year 4. Department of Chemistry and Biochemistry, University of Denver, Denver, CO. Report to the Coordinating Research Council under Contract No. E-23-9.

Bishop, G.A., Stedman, D.H., 2008. A Decade of on-Road Emissions Measurements. *Environ. Sci. Technol.* 42, 1651-1656.

Bond, T.C., Streets, D.G., Yarber, K.F., Nelson, S.M., Woo, J.H., Klimont, Z., 2004. A Technology-Based Global Inventory of Black and Organic Carbon Emissions from Combustion. *J. Geophys. Res.* 109, doi:10.1029/2003JD003697.

Bond, T.C., Sun, H.L., 2005. Can Reducing Black Carbon Emissions Counteract Global Warming? *Environ. Sci. Technol.* 39, 5921-5926.

Buhr, S.M., Buhr, M.P., Fehsenfeld, F.C., Holloway, J.S., Karst, U., Norton, R.B., Parrish, D.D., and Sievers, R.E., 1995. Development of a Semi-Continuous Method for the Measurement of Nitric Acid Vapor and Particulate Nitrate and Sulfate. *Atmos. Environ.* 29, 2609-2624.

Burgard, D.A., Bishop, G.A., Stedman, D.H., Gessner, V.H., Daeschlein, C., 2006. Remote Sensing of In-Use Heavy-Duty Diesel Trucks. *Environ. Sci. Technol.* 40, 6938-6942.

Burgard, D.A., Bishop, G.A., and Stedman, D.H., 2006. Remote Sensing of Ammonia and Sulfur Dioxide from On-Road Light Duty Vehicles. *Environ. Sci. Technol.* 40, 7018-7022.

Cadle, S.H., Mulawa, P., Hunsanger, E.C., Nelson, K., Ragazzi, R.A., Barrett, R., Gallagher, G.L., Lawson, D.R., Knapp, K.T., Snow, R., 1999. Light-Duty Motor Vehicle Exhaust Particulate Matter Measurement in the Denver, Colorado, Area. *J. Air Waste Manage. Assoc.* 49, 164-174.

Cadle, S.H., Mulawa, P.A., Ball, J., Donase, C., Weibel, A., Sagebiel, J.C., Knapp, K.T., Snow, R., 1997. Particulate Emission Rates from in Use High Emitting Vehicles Recruited in Orange County, California. *Environ. Sci. Technol.* 31, 3405-3412.

Cadle, S.H., Nebel, G.J., and Williams, R.L., 1979. Measurements of Unregulated Emissions from General Motors' Light-Duty Vehicles. *SAE Technical Paper*, no. 790694.

CARB, 2002. Standard Operating Procedure for the Determination of Non-Methane Organic Compounds in Ambient Air by Gas Chromatography using Dual Capillary Columns and Flame Ionization Detection. Monitoring and Laboratory Division, California Air Resources Board, Sacramento, CA. SOP No. MLD 32.

CARB, 2006. Emission Data by Region (Statewide). California Air Resources Board. Sacramento, CA. Accessed August 2007. http://www.arb.ca.gov/ei/emissiondata.htm.

CARB, 2007a. Toxic Air Contaminant Emissions, Air Quality, and Health Risk, Ch. 5. The California Almanac of Emissions and Air Quality. Air Quality Data and Statistics Branch. California Air Resources Board. http://www.arb.ca.gov/aqd/almanac/almanac07/pdf/chap507.pdf.

CARB, 2007b. California Motor Vehicle Emission Factor/Emission Inventory Model (EMFAC V 2.3). California Air Resources Board, Sacramento, CA. Accessed March 2007. http://www.arb.ca.gov/msei/msei.htm.

CEC, 2006. Inventory of California Greenhouse Gas Emissions and Sinks: 1990 to 2004. California Energy Commission, Sacramento, CA. CEC-600-2006-013-Sf. http://www.climatechange.ca.gov/policies/greenhouse_gas_inventory/index.html.

Chow, J.C., Watson, J.G., Crow, D., Lowenthal, D.H., Merrifield, T., 2001. Comparison of IMPROVE and NIOSH Carbon Measurements. *Aerosol Sci. Technol.* 34, 23-34.

Colberg, C.A., Tona, B., Stahel, W.A., Meier, M., Staehelin, J., 2005. Comparison of a Road Traffic Emission Model (HBEFA) with Emissions Derived from Measurements in the Gubrist Road Tunnel, Switzerland. *Atmos. Environ.* 39, 4703-4714.

Dockery, D.W., Pope. A., Xu, X., Spegler, J.D., Ware, J.H., Fay, M.E., Ferris, B.G., Speizer, F.E. 1993. An Association Between Air Pollution and Mortality in Six U.S. cities. *New England Journal of Medicine* 329, 1753-1759.

Donaldson, K., Beswick, P.H., Gilmour, P.S., 1996. Free Radical Activity Associated with the Surface of Particles: A Unifying Factor in Determining Biological Activity? *Toxicology Letters* 88, 293-298.

Durbin, T. D., Miller, J. W., Pisano, J. T., Sauer, C., Younglove, T., Rhee, S. H., Huai, T., and MacKay, G.I., 2004. The Effect of Fuel Sulfur on NH_3 and Other Emissions from 2000-2001 Model Year Vehicles. *Atmos. Environ.* 38, 2699-2708.

Durbin, T.D., Miller, J.W., Younglove, T., Huai, T., Cocker, K., 2007. Effects of Fuel Ethanol Content and Volatility on Regulated and Unregulated Exhaust Emissions

for the Latest Technology Gasoline Vehicles. *Environ. Sci. Technol.* 41, 4059-4064.

Durbin, T.D.; Pisano, J.T., Younglove, T., Sauer, C.G., Rhee, S.H., Huai, T., Miller, J.W., MacKay, G.I., Hochhauser, A.M., Ingham, M.C., Gorse, R.A. Jr., Beard, L.K., DiCicco, D., Thompson, N., Stradling, R.J., Rutherford, J.A., Uihlein, J.P., 2004. The Effects of Fuel Sulfur on NH_3 and Other Emissions from 2000-2001 Model Vehicles. *Atmos. Environ.* 38, 2699-2708.

Durbin, T.D., Wilson, R.D., Norbeck, J.M., Miller, J.W., Huai, T., and Rhee, S.H., 2002. Estimates of the Emission Rates of Ammonia from Light-Duty Vehicles Using Standard Chassis Dynamometer Test Cycles. *Atmos. Environ.* 36, 1742-1482.

Emmenegger, L., Mohn, J., Sigrist, M., Marinov, D., Steinemann, U., Zumstead, F., Meier, M., 2004. Measurement of Ammonia Emissions Using Various Techniques in a Comparative Tunnel Study. *Int. J. Environment Pollution* 22, 326-340.

EPA, 2003. *National Air Quality and Emissions Trends Report, 2003*, Office of Air Quality Planning and Standards, U.S. Environmental Protection Agency, Research Triangle Park, NC.

EPA, 2006. Control of Hazardous Air Pollutants from Mobile Sources; Proposed Rule, EPA-HQ-OAR-2005-0036. Office of Transportation and Air Quality. U.S. Environmental Protection Agency, Ann Arbor, MI. http://www.epa.gov/otaq/regs/toxics/a2315a.pdf.

EPA, 2007. National Emissions Inventory (NEI) Air Pollutant Emissions Trends Data. 1970-2006 Average Annual Emissions. Office of Air Quality Planning and Standards, U.S. Environmental Protection Agency, Research Triangle Park, NC. http://www.epa.gov/ttn/chief/trends/.

Farrell, A.E., Plevin, R.J., Turner, B.T., Jones, A.D., O'Hare, M., Kammen, D.M., 2006. Ethanol Can Contribute to Energy and Environmental Goals. *Science* 311, 506-508.

FHWA, 2006. *Highway Statistics 2005*, Table MF-21. Office of Highway Policy Information, Federal Highway Administration, U.S. Department of

Transportation, Washington, D.C. http://www.fhwa.dot.gov/policy/ohim/hs05/motor_fuel.htm.

Fraser, M.P., Buzcu, B., Yue, Z.W., McGaughey, G.R., Desai, N.R., Allen, D.T., Seila, R.L., Lonneman, W.A., Harley, R.A., 2003. Separation of Fine Particulate Matter Emitted from Gasoline and Diesel Vehicles Using Chemical Mass Balancing Techniques. *Environ. Sci. Technol.* 37, 3904-3909.

Fraser, M. P., Cass, G. R., 1998. Detection of Excess Ammonia Emissions From In-Use Vehicles and the Implications for Fine Particle Control. *Environ. Sci. Technol.* 32, 1053-1057.

Gajendran, P., Clark, N.N., 2003. Effect of Truck Operating Weight on Heavy-Duty Diesel Emissions. *Environ. Sci. Technol.* 37, 4309-4317.

Geller, V.D., Sardar, S.B., Phuleria, H., Fine, P.N., Sioutas, C., 2005. Measurements of Particle Number and Mass Concentrations and Size Distributions in a Tunnel Environment. *Environ. Sci. Technol.* 39, 8653-8663.

Gertler, A.W., 2005. Diesel vs. Gasoline Emissions: Does PM from Diesel or Gasoline Vehicles Dominate in the U.S.? *Atmos. Environ.* 39, 2349-2355.

Graskow, B., Kittelson, D.B., Abdul-Khalek, I.S., Ahmadi, M.R., Morris, J.E., 1998. Characterization of Exhaust Particulate Emissions from a Spark Ignition Engine. *SAE Technical Paper*, no. 980528.

Gray, H.A., Cass, G.R., Huntzicker, J.J., Heyerdahl, E.K., Rau, J.A., 1986. Characteristics of Atmospheric Organic and Elemental Carbon Particle Concentrations in Los-Angeles. *Environ. Sci. Technol.* 20, 580-589.

Grieshop, A.P., Lipsky, E.M., Pekney, N.J., Takahama, S., Robinson, A.L., 2006. Fine Particle Emission Factors from Vehicles in a Highway Tunnel: Effects of Fleet Composition and Season. *Atmos. Environ.* 40, S287-S298.

Grosjean, D., Grosjean, E., Gertler, A.W., 2001. On-Road Emissions of Carbonyls from Light-Duty and Heavy-Duty Vehicles. *Environ. Sci. Technol.* 35, 45-53.

Grosjean, E., Green, P.G., Grosjean, D., 1999. Liquid Chromatography Analysis of Carbonyl (2,4-Dinitrophenyl)Hydrazones with Detection by Diode Array Ultraviolet Spectroscopy and by Atmospheric Pressure Negative Chemical Ionization Mass Spectrometry. *Anal. Chem.* 71, 1851-1861.

Hansen, A.D.A., Rosen, H., 1990. Individual Measurements of the Emission Factor of Aerosol Black Carbon in Automobile Plumes. *J. Air Waste Manage. Assoc.* 40, 1654-1657.

Hansen, J.E., Sato, M., 2001. Trends of Measured Climate Forcing Agents. *Proc. Natl. Acad. Sci.* 98, 14778-14783.

Harley, R.A., Coulter-Burke, S.C., Yeung, T.S., 2000. Relating Liquid Fuel and Headspace Vapor Composition for California Reformulated Gasoline Samples Containing Ethanol. *Environ. Sci. Technol.* 34, 4088-4094.

Harley, R.A., Hooper, D.S., Kean, A.J., Kirchstetter, T.W., Hesson, J.M., Balberan, N.T., Stevenson, E.D., Kendall, G.R., 2006. Effects of Reformulated Gasoline and Motor Vehicle Fleet Turnover on Emissions and Ambient Concentrations of Benzene. *Environ. Sci. Technol.* 40, 5084-5088.

Harley, R.A., Marr, L.C., Lehner, J.K., Giddings, S.N., 2005. Changes in Motor Vehicle Emissions on Diurnal to Decadal Time Scales and Effects on Atmospheric Composition. *Environ. Sci. Technol.* 39, 5356-5362.

Heavenrich, R.M., 2006. Light-Duty Automotive Technology and Fuel Economy Trends: 1975 through 2006. Office of Transportation and Air Quality, U.S. Environmental Protection Agency, Ann Arbor, MI. EPA420-R-011.

Heavenrich, R.M., Murrell, J.D., and Cheng, J.P., 1987. Light-Duty Automotive Fuel Economy and Technology Trends Through 1987. *SAE Technical Paper*, no. 871088.

Heywood, J.B., 1988. *Internal Combustion Engine Fundamentals*. McGraw-Hill, New York, NY.

Ho, K.F., Ho, S.S.H., Cheng, Y., Lee, S.C., Yu, J.Z., 2007. Real-World Emission Factors of Fifteen Carbonyl Compounds Measured in a Hong Kong Tunnel. *Atmos. Environ.* 41, 1747-1758.

Hoekman, S.K., 1992. Speciated Measurements and Calculated Reactivities of Vehicle Exhaust Emissions from Conventional and Reformulated Gasolines. *Environ. Sci. Technol.* 26, 1206-1216.

Huai, T., Durbin, T.D., Miller, J.W., Pisano, J.T., Sauer, C.G., Rhee, S.H., and Norbeck, J.M., 2003. Investigation of NH_3 Emissions from New Technology Vehicles as a Function of Operating Conditions. *Environ. Sci. Technol.* 37, 4841-4847.

Huai, T., Durbin, T.D., Younglove, T., Scora, G., Barth, M., and Norbeck, J.M., 2005. Vehicle Specific Power Approach to Estimating On-Road NH_3 Emissions from Light-Duty Vehicles. *Environ. Sci. Technol.* 39, 9595-9600.

Hunter, M.C., Bartle, K.D., Lewis, A.C., McQuaid, J.B., Myers, P., Seakins, P.W., Van Tilburg, C., 1998. The Use of the Helium Ionization Detector for Gas Chromatographic Monitoring of Trace Atmospheric Components. *J. High Resol. Chromatogr.* 21, 75-80.

Imhof, D., Weingartner, E., Prevot, A.S.H., Ordonez, C., Kurtenbach, R., Wiesen, P., Rodler, J., Sturm, P., McCrae, I., Ekstrom, M., Baltensperger, U., 2006. Aerosol and NOx Emission Factors and Submicron Particle Number Size Distributions in Two Road Tunnels with Different Traffic Regimes. *Atmos. Chem. Phys.* 6, 2215-2230.

IPCC, 2007. Climate Change 2007: The Physical Science Basis. Contribution of Working Group 1 to the Fourth Assessment Report of the Intergovernmental Panel on Climate Change [Solomon, S., D. Qin, M. Manning, Z. Chen, M. Marquis, K.B. Averyt, M. Tignor and H.L. Miller (eds.)]. Cambridge University Press. Cambridge, UK, and New York, NY, USA.

Jayaratne, E.R., Morawska, L., Ristovski, Z.D., He, C., 2007. Rapid Identification of High Particle Number Emitting on-Road Vehicles and Its Application to a Large Fleet of Diesel Buses. *Environ. Sci. Technol.* 41, 5022-5027.

Jiang, M., Marr, L.C., Dunlea, E.J., Herndon, S.C., Jayne, J.T., Kolb, C.E., Knighton, W.B., Rogers, T.M., Zavala, M., Molina, L.T., Molina, M.J., 2005. Vehicle Fleet Emissions of Black Carbon, Polycyclic Aromatic Hydrocarbons, and Other Pollutants Measured by a Mobile Laboratory in Mexico City. *Atmos. Chem. Phys.* 5, 3377-3387.

Jimenez, J.L., Mcrae, G.J., Nelson, D.D., Zahniser, M.S., Kolb, C.E., 2000. Remote Sensing of NO and NO_2 Emissions from Heavy-Duty Diesel Trucks Using Tunable Diode Lasers. *Environ. Sci. Technol.* 34, 2380-2387.

John, W., Reischl, G., 1980. A Cyclone for Size-Selective Sampling of Ambient Air. *J. Air Pollution Control Assoc.* 30, 872-876.

Johnson, J.P., Kittelson, D.B., Watts, W.F., 2005. Source Apportionment of Diesel and Spark Ignition Exhaust Aerosol Using On-Road Data from the Minneapolis Metropolitan Area. *Atmos. Environ.* 39, 2111-2121.

Johnson, T.V., 2004. Diesel Emission Control Technology - 2003 in Review. *SAE Technical Paper*, no. 2004-01-0070.

Kayes, D., Hochgreb, S., Maricq, M.M., Podsiadlik, D.H., Chase, R.E., 2000. Particulate Matter Emissions During Start-up and Transient Operation of a Spark-Ignition Engine (2): Effect of Speed, Load, and Real-World Driving Cycles. *SAE Technical Paper*, no. 2000-01-1083.

Kean, A.J., Grosjean, E., Grosjean, D., Harley, R.A., 2001. On-Road Measurement of Carbonyls in California Light-Duty Vehicle Emissions. *Environ. Sci. Technol.* 35, 4198-4204.

Kean, A.J., Harley, R.A., Kendall, G.R., 2003. Effects of Vehicle Speed and Engine Load on Motor Vehicle Emissions. *Environ. Sci. Technol.* 37, 3739-3746.

Kean, A.J., Harley, R.A., Littlejohn, D., Kendall, G.R., 2000. On-Road Measurement of Ammonia and Other Motor Vehicle Exhaust Emissions. *Environ. Sci. Technol.* 34, 3535-3539.

Kean, A.J., Sawyer, R.F., Harley, R.A., 2000. A Fuel-Based Assessment of Off-Road Diesel Engine Emissions. *J. Air Waste Manage. Assoc.* 50, 1929-1939.

Kean, A.J., Sawyer, R.F., Harley, R.A., Kendall, G.B., 2002. Trends in Exhaust Emissions from In-Use California Light-Duty Vehicles, 1994-2001. *SAE Technical Paper*, no. 2002-01-1713.

Kennedy, I.M., 2007. The Health Effects of Combustion-Generated Aerosols. *Proc. Comb. Inst.* 31, 2757-2770.

Kirchstetter, T.W., Singer, B.C., Harley, R.A., Kendall, G.B., Chan, W., 1996. Impact of Oxygenated Gasoline Use on California Light-Duty Vehicle Emissions. *Environ. Sci. Technol.* 30, 661-670.

Kirchstetter, T.W., Harley, R.A., Kreisberg, N.M., Stolzenburg, M.R., Hering, S.V., 1999a. On-Road Measurement of Fine Particle and Nitrogen Oxide Emissions from Light- and Heavy-Duty Motor Vehicles. *Atmos. Environ.* 33, 2955-2968.

Kirchstetter, T.W., Singer, B.C., Harley, R.A., Kendall, G.R., Traverse, M., 1999b. Impact of California Reformulated Gasoline on Motor Vehicle Emissions. 1. Mass Emission Rates. *Environ. Sci. Technol.* 33, 318-328.

Kirchstetter, T.W., Singer, B.C., Harley, R.A., Kendall, G.R., Hesson, J.M., 1999c. Impact of California Reformulated Gasoline on Motor Vehicle Emissions. 2. Volatile Organic Compound Speciation and Reactivity. *Environ. Sci. Technol.* 33, 329-336.

Kirchstetter, T.W., Corrigan, C.E., Novakov, T., 2001. Laboratory and Field Investigation of the Adsorption of Gaseous Organic Compounds onto Quartz Filters. *Atmos. Environ.* 35, 1663-1671.

Kirchstetter, T.W., Novakov, T., 2007. Controlled Generation of Black Carbon Particles from a Diffusion Flame and Applications in Evaluating Black Carbon Measurement Methods. *Atmos. Environ.* 41, 1874-1888.

Kittelson, D.B., 1998. Engines and Nanoparticles: A Review. *J. Aerosol Sci.* 29, 575-588.

Kittelson, D.B., Watts, W.F., Johnson, J.P., 2006a. On-Road and Laboratory Evaluation of Combustion Aerosols - Part 1: Summary of Diesel Engine Results. *J. Aerosol Sci.* 37, 913-930.

Kittelson, D.B., Watts, W.F., Johnson, J.P., Schauer, J.J., Lawson, D.R., 2006b. On-Road and Laboratory Evaluation of Combustion Aerosols - Part 2: Summary of Spark Ignition Engine Results. *J. Aerosol Sci.* 37, 931-949.

Kleeman, M.J., Schauer, J.J., Cass, G.R., 2000. Size and Composition Distribution of Fine Particulate Matter Emitted from Motor Vehicles. *Environ. Sci. Technol.* 34, 1132-1142.

Kristensson, A., Johansson, C., Westerholm, R., Swietlicki, E., Gidhagen, L., Wideqvist, U., Vesely, V., 2004. Real-World Traffic Emission Factors of Gases and Particles Measured in a Road Tunnel in Stockholm, Sweden. *Atmos. Environ.* 38, 657-673.

Kurniawan, A., Schmidt-Ott, A., 2006. Monitoring the Soot Emissions of Passing Cars. *Environ. Sci. Technol.* 40, 1911-1915.

Legreid, G., Reimann, S., Steinbacher, M., Staehelin, J., Young, D., Stemmler, K., 2007. Measurements of OVOCs and NMHCs in a Swiss Highway Tunnel for Estimation of Road Transport Emissions. *Environ. Sci. Technol.* 41, 7060-7066.

Lenner, M., 1987. Nitrogen-Dioxide in Exhaust Emissions from Motor-Vehicles. *Atmos. Environ.* 21, 37-43.

Lloyd, A.C., Cackette, T.A., 2001. Diesel Engines: Environmental Impact and Control. *J. Air Waste Manage. Assoc.* 51, 809-847.

Lonneman, W.A., Seila, R.L., Meeks, S.A., 1986. Nonmethane Organic Composition in the Lincoln Tunnel. *Environ. Sci. Technol.* 20, 790-796.

Mack, 2006. Mack to Add SCR to Meet EPA 2010 NO_x Emissions Requirements, June 28, 2006. Press Release, Mack Trucks Inc., Lehigh Valley, PA. http://www.macktrucks.com/default.aspx?pageid=1613.

Maricq, M.M., Podsiadlik, D.H., Chase, R.E., 1999a. Examination of the Size-Resolved and Transient Nature of Motor Vehicle Particle Emissions. *Environ. Sci. Technol.* 33, 1618-1626.

Maricq, M.M., Podsiadlik, D.H., Chase, R.E., 1999b. Gasoline Vehicle Particle Size Distributions: Comparison of Steady State, FTP, and US06 Measurements. *Environ. Sci. Technol.* 33, 2007-2015.

Mayotte, S.C., Lindhjem, C.E., Rao, V., Sklar, M.S., 1994. Reformulated Gasoline Effects on Exhaust Emissions: Phase 2. Continued Investigation of the Effects of Fuel Oxygenate Content, Oxygenate Type, Sulfur, Olefins, and Distillation Parameters. *SAE Technical Paper*, no. 941974.

Mazzoleni, C., Kuhns, H.D., Moosmuller, H., Keislar, R.E., Barber, P.W., Robinson, N.F., Watson, J.G., 2004. On-Road Vehicle Particulate Matter and Gaseous Emission Distributions in Las Vegas, Nevada, Compared with Other Areas. *J. Air Waste Manage. Assoc.* 54, 711-726.

Moeckli, M.A., Fierz, M., and Sigrist, M.W., 1996. Emission Factors for Ethene and Ammonia from a Tunnel Study with a Photoacoustic Trace Gas Detection System. *Environ. Sci. Technol.* 30, 2864-2867.

Mulholland, G.W., Bryner, N.P., 1994. Radiometric Model of the Transmission Cell-Reciprocal Nephelometer. *Atmos. Environ.* 28, 873-887.

Partridge, P.A., Shala, F.J., Cernansky, N.P., Suffet, I.H., 1987. Characterization and Analysis of Diesel Exhaust Odor. *Environ. Sci. Technol.* 21, 403-408.

Pearson, J., and Stewart, G.R., 1993. Tansley Review No. 56: The Deposition of Atmospheric Ammonia and Its Effects on Plants. *New Phytologist* 125, 283-305.

Pierson, W.R., and Brachaczek, W.W., 1983. Emissions of Ammonia and Amines from Vehicles on the Road. *Environ. Sci. Technol.* 17, 757-760.

Pierson, W.R., Gertler, A.W., Robinson, N.F., Sagebiel, J.C., Zielinska, B., Bishop, G.A., Stedman, D.H., Zweidinger, R.B., Ray, W.D., 1996. Real-World Automotive Emissions - Summary of Studies in the Fort McHenry and Tuscarora Mountain Tunnels. *Atmos. Environ.* 30, 2233-2256.

Pope, C.A., Dockery, D.W., 2006. Health Effects of Fine Particulate Air Pollution: Lines That Connect. *J. Air Waste Manage. Assoc.* 56, 709-742.

Pope, C.A., Thun, M.J., Namboodiri, M.M., Dockery, D.W., Evans, J.S., Speizer, F.E., Heath, C.W., 1995. Particulate Air-Pollution as a Predictor of Mortality in a Prospective-Study of US Adults. *American Journal of Respiratory and Critical Care Medicine* 151, 669-674.

Ramanathan, V., Carmichael, G., 2008. Global and Regional Climate Changes Due to Black Carbon. *Nature Geoscience* 1, 221-227.

Reuter, R.M., Benson, J.D., Burns, V.R., Gorse, R.A., Hochhauser, A.M., Koehl, W.J., Painter, L.J., Rippon, B.H., Ruterford, J.A., 1992. Effects of Oxygenated Fuels and RVP on Automotive Emissions. *SAE Technical Paper,* no. 920326.

Robinson, A.L., Donahue, N.M., Shrivastava, M.K., Weitkamp, E.A., Sage, A.M., Grieshop, A.P., Lane, T.E., Pierce, J.R., Pandis, S.N., 2007. Rethinking Organic Aerosols: Semivolatile Emissions and Photochemical Aging. *Science* 315, 1259-1262.

Sagebiel, J.C., Zielinska, B., Walsh, P.A., Chow, J.C., Cadle, S.H., Mulawa, P.A., Knapp, K.T., Zweidinger, R.B., 1997. PM-10 Exhaust Samples Collected During IM-240 Dynamometer Tests of in-Service Vehicles in Nevada. *Environ. Sci. Technol.* 31, 75-83.

Sawyer, R.F., Harley, R.A., Cadle, S.H., Norbeck, J.M., Slott, R., Bravo, H.A., 2000. Mobile Sources Critical Review: 1998 NARSTO Assessment. *Atmos. Environ.* 34, 2161-2181.

Schauer. J.J., Rogge, W.F., Hildemann, L.M., Mazurek, M.A., Cass, G.R., and Simoneit, B.R.T., 1996. Source Apportionment of Airborne Particulate Matter Using Organic Compounds as Tracers. *Atmos. Environ.* 30, 453-468.

Schmid, H., Pucher, E., Ellinger, R., Biebl, P., Puxbaum, H., 2001. Decadal Reductions of Traffic Emissions on a Transit Route in Austria - Results of the Tauerntunnel Experiment 1997. *Atmos. Environ.* 35, 3585-3593.

Seaton, A., Macnee, W., Donaldson, K., Godden, D., 1995. Particulate Air-Pollution and Acute Health-Effects. *Lancet* 345, 176-178.

Seinfeld, J.H., and Pandis, S.N., 1998. *Atmospheric Chemistry and Physics: From Air Pollution to Climate Change*. John Wiley and Sons, New York, NY, pp. 74-75, 1056-1057.

Shorter, J.H., Herndon, S., Zahniser, M.S., Nelson, D.D., Wormhoudt, J., Demerjian, K.L., Kolb, C.E., 2005. Real-Time Measurements of Nitrogen Oxide Emissions from in-Use New York City Transit Buses Using a Chase Vehicle. *Environ. Sci. Technol.* 39, 7991-8000.

Stedman, D.H., 2007. Department of Chemistry and Biochemistry, University of Denver, Denver, CO. Personal Communication, March 2007.

Stone, R., 1999. *Introduction to Internal Combustion Engines*. Society of Automotive Engineers, Warrendale, PA.

Strawa, A.W., Castaneda, R., Owano, T., Baer, D.S., Paldus, B.A., 2003. The Measurement of Aerosol Optical Properties Using Continuous Wave Cavity Ring-Down Techniques. *Journal of Atmospheric and Oceanic Technology* 20, 454-465.

Strawa, A.W., Elleman, R., Hallar, A.G., Covert, D., Ricci, K., Provencal, R., Owano, T.W., Jonsson, H.H., Schmid, B., Luu, A.P., Bokarius, K., Andrews, E., 2006. Comparison of in Situ Aerosol Extinction and Scattering Coefficient Measurements Made During the Aerosol Intensive Operating Period. *J. Geophys. Res.* 111, doi:10.1029/2005JD006056.

Sturm, P.J., Baltensperger, U., Bacher, M., Lechner, B., Hausberger, S., Heiden, B., Imhof, D., Weingartner, E., Prevot, A.S.H., Kurtenback, R., and Weisen, P., 2003. Roadside Measurements of Particulate Matter Size Distribution. *Atmos. Environ.* 37, 5273-5281.

Subramanian, R., Khlystov, A.Y., Cabada, J.C., Robinson, A.L., 2004. Positive and Negative Artifacts in Particulate Organic Carbon Measurements with Denuded and Undenuded Sampler Configurations. *Aerosol Sci. Technol.* 38, 27-48.

Tang, S.D., Graham, L., Shen, L., Zhou, X.L., Lanni, T., 2004. Simultaneous Determination of Carbonyls and NO_2 in Exhausts of Heavy-Duty Diesel Trucks and Transit Buses by HPLC Following 2,4-Dinitrophenylhydrazine Cartridge Collection. *Environ. Sci. Technol.* 38, 5968-5976.

TIUS, 1992. Truck Inventory and Use Survey. United States Bureau of Census, Washington D.C.

Turpin, B.J., Saxena, P., Andrews, E., 2000. Measuring and Simulating Particulate Organics in the Atmosphere: Problems and Prospects. *Atmos. Environ.* 34, 2983-3013.

Urban, C.M., and Garbe, R.J., 1979. Regulated and Unregulated Exhaust Emissions from Malfunctioning Vehicles. *SAE Tech. Pap. Ser.* no. 790696.

VIUS, 1997. Vehicle Inventory & Use Survey. United States Bureau of Census, Washington D.C.

VIUS, 2002. Vehicle Inventory & Use Survey. United States Bureau of Census, Washington D.C.

Volvo, 2007. Better for the Environment, Built for Your Bottom Line - 2008 Volvo Engines, April 5, 2007. Press Release, Volvo Trucks, Göteborg, Sweden, http://pnt.volvo.com/pntclient/PressRelease.aspx?pubid=3247.

Watson, J.G., Chow, J.C., Antony Chen, L.W., 2005. Summary of Organic and Elemental Carbon/Black Carbon Analysis Methods and Intercomparisons. *Aerosol and Air Quality Research* 5, 65-102.

Watson, J.G., Chow, J.C., Lu, Z., Fujita, E.M., Lowenthal, D.H., Lawson, D.R., and Ashbaugh, L.L., 1994. Chemical Mass Balance Source Apportionment of PM_{10} during the Southern California Air Quality Study. *Aerosol Sci. Technol.* 21, 1-36.

Yanowitz, J., McCormick, R.L., Graboski, M.S., 2000. In-Use Emissions from Heavy-Duty Diesel Vehicles. *Environ. Sci. Technol.* 34, 729-740.

Zhu, Y., Hinds, W.C., Shen, S., and Sioutas, C., 2004. Seasonal Trends of Concentration and Size Distribution of Ultrafine Particles Near Major Highways in Los Angeles. *Aerosol Sci. Technol.* 38(S1), 5-13.

Appendix A: Size-Resolved Particle Emission Factors

Table A1. Particle number emission factors as a function of particle size (with associated uncertainties, 95% CI). These are $dE_N/dlogD_p$ (# kg^{-1}) as plotted in Figure 3.2.

	LD Vehicles		Diesel Trucks	
D_p (nm)	Mean	Uncertainty	Mean	Uncertainty
10.2	2.63E+14	1.01E+14	2.05E+15	1.70E+15
10.6	2.75E+14	1.07E+14	2.48E+15	1.68E+15
10.9	2.87E+14	1.04E+14	2.84E+15	1.59E+15
11.3	2.96E+14	1.01E+14	3.33E+15	1.64E+15
11.8	3.09E+14	1.02E+14	3.63E+15	1.60E+15
12.2	3.16E+14	9.98E+13	4.03E+15	1.57E+15
12.6	3.26E+14	9.86E+13	4.36E+15	1.51E+15
13.1	3.34E+14	9.79E+13	4.57E+15	1.38E+15
13.6	3.46E+14	9.30E+13	4.82E+15	1.38E+15
14.1	3.54E+14	9.28E+13	5.24E+15	1.43E+15
14.6	3.62E+14	9.23E+13	5.69E+15	1.41E+15
15.1	3.67E+14	8.81E+13	6.01E+15	1.34E+15
15.7	3.77E+14	8.68E+13	6.11E+15	1.17E+15
16.3	3.80E+14	8.31E+13	6.03E+15	1.03E+15
16.8	3.84E+14	7.86E+13	5.89E+15	9.05E+14
17.5	3.86E+14	7.89E+13	5.83E+15	9.57E+14
18.1	3.87E+14	7.52E+13	5.78E+15	8.37E+14
18.8	3.92E+14	7.36E+13	5.62E+15	8.42E+14
19.5	3.94E+14	7.07E+13	5.46E+15	7.47E+14
20.2	3.88E+14	6.77E+13	5.31E+15	7.05E+14
20.9	3.92E+14	6.81E+13	5.08E+15	6.94E+14
21.7	3.94E+14	6.30E+13	4.94E+15	7.07E+14
22.5	3.90E+14	6.41E+13	4.80E+15	7.65E+14
23.3	3.85E+14	6.37E+13	4.71E+15	8.48E+14
24.1	3.80E+14	5.83E+13	4.43E+15	8.12E+14
25	3.77E+14	6.24E+13	4.27E+15	8.69E+14
25.9	3.68E+14	5.88E+13	4.12E+15	8.69E+14
26.9	3.62E+14	5.64E+13	4.02E+15	8.68E+14
27.9	3.55E+14	5.45E+13	3.89E+15	8.65E+14
28.9	3.43E+14	5.65E+13	3.75E+15	8.33E+14
30	3.29E+14	5.59E+13	3.58E+15	8.67E+14
31.1	3.18E+14	5.66E+13	3.47E+15	8.50E+14
32.2	3.13E+14	5.45E+13	3.37E+15	8.85E+14
33.4	2.98E+14	5.01E+13	3.28E+15	9.03E+14
34.6	2.90E+14	5.06E+13	3.18E+15	9.16E+14

	LD Vehicles		Diesel Trucks	
D_p (nm)	Mean	Uncertainty	Mean	Uncertainty
35.9	2.76E+14	4.71E+13	3.11E+15	9.75E+14
37.2	2.68E+14	4.21E+13	2.99E+15	1.01E+15
38.5	2.60E+14	4.13E+13	2.90E+15	9.57E+14
40	2.52E+14	3.94E+13	2.85E+15	9.92E+14
41.4	2.45E+14	3.88E+13	2.83E+15	1.02E+15
42.9	2.36E+14	3.77E+13	2.77E+15	1.02E+15
44.5	2.31E+14	3.41E+13	2.77E+15	9.98E+14
46.1	2.26E+14	3.17E+13	2.69E+15	9.90E+14
47.8	2.15E+14	2.89E+13	2.69E+15	1.01E+15
49.6	2.10E+14	2.97E+13	2.66E+15	9.65E+14
51.4	2.05E+14	2.91E+13	2.64E+15	9.68E+14
53.3	1.96E+14	2.98E+13	2.62E+15	9.60E+14
55.2	1.89E+14	2.77E+13	2.58E+15	9.48E+14
57.3	1.81E+14	2.85E+13	2.56E+15	9.11E+14
59.4	1.72E+14	2.62E+13	2.55E+15	9.08E+14
61.5	1.65E+14	2.54E+13	2.48E+15	8.83E+14
63.8	1.58E+14	2.45E+13	2.47E+15	8.78E+14
66.1	1.49E+14	2.21E+13	2.41E+15	8.60E+14
68.5	1.43E+14	2.25E+13	2.34E+15	8.13E+14
71	1.36E+14	2.18E+13	2.30E+15	7.80E+14
73.7	1.29E+14	2.14E+13	2.28E+15	7.68E+14
76.4	1.21E+14	1.86E+13	2.23E+15	7.46E+14
79.1	1.14E+14	1.84E+13	2.12E+15	6.89E+14
82	1.08E+14	1.71E+13	2.08E+15	6.63E+14
85.1	1.02E+14	1.52E+13	1.99E+15	6.53E+14
88.2	9.61E+13	1.41E+13	1.91E+15	6.39E+14
91.4	8.95E+13	1.33E+13	1.86E+15	6.42E+14
94.7	8.44E+13	1.31E+13	1.83E+15	6.57E+14
98.2	7.73E+13	1.33E+13	1.72E+15	6.23E+14
101.8	7.17E+13	1.20E+13	1.66E+15	6.03E+14
105.5	6.57E+13	1.07E+13	1.58E+15	5.48E+14
109.4	6.03E+13	1.02E+13	1.51E+15	5.23E+14
113.4	5.67E+13	9.63E+12	1.43E+15	5.10E+14
117.6	5.10E+13	8.62E+12	1.36E+15	4.75E+14
121.9	4.68E+13	8.28E+12	1.27E+15	4.41E+14
126.3	4.31E+13	8.48E+12	1.20E+15	3.81E+14
131	4.03E+13	7.51E+12	1.13E+15	3.65E+14
135.8	3.69E+13	6.82E+12	1.03E+15	3.34E+14
140.7	3.19E+13	6.86E+12	9.74E+14	3.11E+14
145.9	3.01E+13	5.87E+12	9.03E+14	2.93E+14

	LD Vehicles		Diesel Trucks	
D_p (nm)	Mean	Uncertainty	Mean	Uncertainty
151.2	2.74E+13	4.54E+12	8.26E+14	2.69E+14
156.8	2.41E+13	5.06E+12	7.70E+14	2.51E+14
162.5	2.20E+13	4.57E+12	6.98E+14	2.38E+14
168.5	1.91E+13	4.23E+12	6.48E+14	2.14E+14
174.7	1.70E+13	4.22E+12	5.68E+14	2.02E+14
181.1	1.46E+13	4.05E+12	5.30E+14	1.75E+14
187.7	1.25E+13	3.25E+12	4.75E+14	1.46E+14
194.6	1.12E+13	2.41E+12	4.31E+14	1.27E+14
201.7	9.43E+12	2.59E+12	3.94E+14	1.08E+14
209.1	8.02E+12	1.92E+12	3.55E+14	1.04E+14
216.7	6.69E+12	1.98E+12	3.18E+14	9.24E+13
224.7	5.99E+12	1.73E+12	2.73E+14	7.65E+13
232.9	5.16E+12	1.45E+12	2.45E+14	7.06E+13
241.4	4.33E+12	1.16E+12	2.20E+14	6.38E+13
250.3	3.81E+12	1.04E+12	1.98E+14	5.83E+13
259.5	3.18E+12	9.41E+11	1.84E+14	5.69E+13
269	2.73E+12	9.76E+11	1.66E+14	5.22E+13
278.8	2.35E+12	8.94E+11	1.46E+14	4.61E+13
289	2.11E+12	7.22E+11	1.32E+14	4.36E+13

Table A2. Particle volume emission factors as a function of particle size (with associated uncertainties, 95% CI). These are $dE_V/dlogD_p$ (μm^3 kg^{-1}), as plotted in Figure 3.2.

	LD Vehicles		Diesel Trucks	
D_p (nm)	Mean	Uncertainty	Mean	Uncertainty
10.2	1.46E+08	5.63E+07	1.14E+09	9.43E+08
10.6	1.72E+08	6.69E+07	1.55E+09	1.05E+09
10.9	1.95E+08	7.07E+07	1.93E+09	1.08E+09
11.3	2.24E+08	7.60E+07	2.51E+09	1.24E+09
11.8	2.66E+08	8.77E+07	3.12E+09	1.37E+09
12.2	3.01E+08	9.49E+07	3.83E+09	1.50E+09
12.6	3.42E+08	1.03E+08	4.56E+09	1.58E+09
13.1	3.94E+08	1.15E+08	5.38E+09	1.62E+09
13.6	4.56E+08	1.23E+08	6.35E+09	1.82E+09
14.1	5.20E+08	1.36E+08	7.69E+09	2.10E+09
14.6	5.90E+08	1.50E+08	9.27E+09	2.30E+09
15.1	6.62E+08	1.59E+08	1.08E+10	2.42E+09
15.7	7.64E+08	1.76E+08	1.24E+10	2.38E+09
16.3	8.61E+08	1.88E+08	1.37E+10	2.33E+09
16.8	9.54E+08	1.95E+08	1.46E+10	2.25E+09
17.5	1.08E+09	2.21E+08	1.64E+10	2.69E+09
18.1	1.20E+09	2.33E+08	1.80E+10	2.60E+09
18.8	1.36E+09	2.56E+08	1.96E+10	2.93E+09
19.5	1.53E+09	2.75E+08	2.12E+10	2.90E+09
20.2	1.67E+09	2.92E+08	2.29E+10	3.04E+09
20.9	1.87E+09	3.25E+08	2.43E+10	3.32E+09
21.7	2.11E+09	3.37E+08	2.64E+10	3.78E+09
22.5	2.33E+09	3.83E+08	2.86E+10	4.56E+09
23.3	2.55E+09	4.22E+08	3.12E+10	5.61E+09
24.1	2.79E+09	4.28E+08	3.25E+10	5.95E+09
25	3.09E+09	5.10E+08	3.50E+10	7.11E+09
25.9	3.35E+09	5.35E+08	3.75E+10	7.90E+09
26.9	3.69E+09	5.75E+08	4.10E+10	8.85E+09
27.9	4.04E+09	6.20E+08	4.42E+10	9.84E+09
28.9	4.34E+09	7.14E+08	4.75E+10	1.05E+10
30	4.66E+09	7.90E+08	5.06E+10	1.23E+10
31.1	5.00E+09	8.92E+08	5.47E+10	1.34E+10
32.2	5.48E+09	9.52E+08	5.90E+10	1.55E+10
33.4	5.81E+09	9.78E+08	6.40E+10	1.76E+10
34.6	6.29E+09	1.10E+09	6.89E+10	1.99E+10
35.9	6.67E+09	1.14E+09	7.54E+10	2.36E+10
37.2	7.23E+09	1.13E+09	8.07E+10	2.71E+10
38.5	7.77E+09	1.23E+09	8.66E+10	2.86E+10

	LD Vehicles		Diesel Trucks	
D_p (nm)	Mean	Uncertainty	Mean	Uncertainty
40	8.45E+09	1.32E+09	9.55E+10	3.32E+10
41.4	9.09E+09	1.44E+09	1.05E+11	3.78E+10
42.9	9.75E+09	1.56E+09	1.15E+11	4.21E+10
44.5	1.07E+10	1.57E+09	1.28E+11	4.61E+10
46.1	1.16E+10	1.63E+09	1.38E+11	5.08E+10
47.8	1.23E+10	1.66E+09	1.54E+11	5.78E+10
49.6	1.34E+10	1.90E+09	1.70E+11	6.17E+10
51.4	1.46E+10	2.07E+09	1.88E+11	6.88E+10
53.3	1.56E+10	2.36E+09	2.08E+11	7.61E+10
55.2	1.66E+10	2.44E+09	2.27E+11	8.35E+10
57.3	1.78E+10	2.81E+09	2.52E+11	8.97E+10
59.4	1.89E+10	2.88E+09	2.79E+11	9.97E+10
61.5	2.01E+10	3.09E+09	3.02E+11	1.08E+11
63.8	2.15E+10	3.33E+09	3.35E+11	1.19E+11
66.1	2.25E+10	3.34E+09	3.64E+11	1.30E+11
68.5	2.41E+10	3.78E+09	3.93E+11	1.37E+11
71	2.54E+10	4.09E+09	4.32E+11	1.46E+11
73.7	2.71E+10	4.49E+09	4.78E+11	1.61E+11
76.4	2.83E+10	4.33E+09	5.21E+11	1.74E+11
79.1	2.95E+10	4.76E+09	5.50E+11	1.78E+11
82	3.11E+10	4.94E+09	6.00E+11	1.91E+11
85.1	3.30E+10	4.91E+09	6.42E+11	2.11E+11
88.2	3.45E+10	5.05E+09	6.87E+11	2.30E+11
91.4	3.58E+10	5.31E+09	7.45E+11	2.57E+11
94.7	3.75E+10	5.82E+09	8.12E+11	2.92E+11
98.2	3.83E+10	6.60E+09	8.55E+11	3.09E+11
101.8	3.96E+10	6.63E+09	9.15E+11	3.33E+11
105.5	4.04E+10	6.60E+09	9.73E+11	3.37E+11
109.4	4.14E+10	7.02E+09	1.04E+12	3.58E+11
113.4	4.33E+10	7.35E+09	1.09E+12	3.89E+11
117.6	4.35E+10	7.34E+09	1.16E+12	4.05E+11
121.9	4.44E+10	7.86E+09	1.21E+12	4.19E+11
126.3	4.55E+10	8.94E+09	1.26E+12	4.02E+11
131	4.74E+10	8.84E+09	1.33E+12	4.30E+11
135.8	4.84E+10	8.94E+09	1.35E+12	4.38E+11
140.7	4.65E+10	1.00E+10	1.42E+12	4.54E+11
145.9	4.90E+10	9.55E+09	1.47E+12	4.77E+11
151.2	4.97E+10	8.22E+09	1.50E+12	4.86E+11
156.8	4.86E+10	1.02E+10	1.55E+12	5.06E+11
162.5	4.95E+10	1.03E+10	1.57E+12	5.36E+11

	LD Vehicles		Diesel Trucks	
D_p (nm)	Mean	Uncertainty	Mean	Uncertainty
168.5	4.78E+10	1.06E+10	1.62E+12	5.37E+11
174.7	4.74E+10	1.18E+10	1.59E+12	5.63E+11
181.1	4.54E+10	1.26E+10	1.65E+12	5.44E+11
187.7	4.33E+10	1.13E+10	1.64E+12	5.06E+11
194.6	4.33E+10	9.30E+09	1.66E+12	4.92E+11
201.7	4.05E+10	1.11E+10	1.69E+12	4.62E+11
209.1	3.84E+10	9.18E+09	1.70E+12	4.96E+11
216.7	3.56E+10	1.05E+10	1.70E+12	4.92E+11
224.7	3.56E+10	1.02E+10	1.62E+12	4.55E+11
232.9	3.41E+10	9.62E+09	1.62E+12	4.67E+11
241.4	3.19E+10	8.57E+09	1.62E+12	4.70E+11
250.3	3.13E+10	8.55E+09	1.63E+12	4.78E+11
259.5	2.91E+10	8.61E+09	1.69E+12	5.20E+11
269	2.78E+10	9.94E+09	1.69E+12	5.32E+11
278.8	2.67E+10	1.01E+10	1.66E+12	5.23E+11
289	2.67E+10	9.13E+09	1.67E+12	5.51E+11

Appendix B: Emission Factors for Individual HD Trucks

This table shows BC and particle number (PN) emission factors, average speed, and drive-by dates and times for all 226 HD diesel trucks analyzed in Chapter 4.

Truck #	BC (g kg^{-1})	PN (# kg^{-1})	Truck Speed (km h^{-1})	Date/Time
1	0.47	1.17E+15	62	7/19/06 12:03:07
2	1.09	1.05E+16	73	7/19/06 12:04:01
3	3.28	1.40E+15	70	7/19/06 12:04:24
4	1.26	-3.39E+15	65	7/19/06 12:06:54
5	2.56	7.45E+15	66	7/19/06 12:08:14
6	3.62	3.53E+13	67	7/19/06 12:11:35
7	2.38	3.73E+15	62	7/19/06 12:12:05
8	1.83	7.15E+14	76	7/19/06 12:17:58
9	1.59	7.26E+15	55	7/19/06 12:20:30
10	0.84	4.22E+15	78	7/19/06 12:21:41
11	0.81	8.41E+14	35	7/19/06 12:22:44
12	0.22	7.14E+15	65	7/19/06 12:32:21
13	8.69	3.73E+15	74	7/19/06 12:34:07
14	0.85	5.11E+14	53	7/19/06 12:36:35
15	1.29	9.03E+14	62	7/19/06 12:37:52
16	0.19	5.56E+15	67	7/19/06 12:43:27
17	0.48	1.80E+15	63	7/19/06 12:43:37
18	0.41	8.44E+15	65	7/19/06 12:51:34
19	1.89	3.43E+15	43	7/19/06 12:52:51
20	0.75	1.29E+15	63	7/19/06 13:00:09
21	0.49	2.00E+16	66	7/19/06 13:00:46
22	0.70	1.09E+16	46	7/19/06 13:08:30
23	2.22	-9.14E+13	50	7/19/06 13:08:39
24	0.32	3.60E+14	32	7/19/06 13:12:00
25	1.17	-4.29E+13	59	7/19/06 13:13:27
26	0.20	1.09E+16	44	7/19/06 13:14:02
27	0.85	5.94E+14	55	7/19/06 13:15:43
28	2.96	6.02E+15	59	7/19/06 13:16:30
29	2.22	-1.48E+15	68	7/19/06 13:17:27
30	0.49	9.90E+15	61	7/19/06 13:18:32
31	0.52	4.97E+15	63	7/19/06 13:19:30
32	6.24	2.26E+15	51	7/19/06 13:20:49
33	1.29	3.17E+15	49	7/19/06 13:22:03
34	2.35	-1.21E+15	66	7/19/06 13:27:31
35	0.64	1.84E+16	66	7/19/06 13:30:32
36	0.88	6.57E+15	56	7/19/06 13:31:42
37	1.37	1.59E+15	38	7/19/06 13:31:52
38	1.18	1.47E+14	46	7/19/06 13:32:08
39	0.02	7.02E+15	62	7/19/06 13:35:54
40	0.95	2.88E+15	79	7/19/06 13:36:31
41	0.67	1.27E+16	44	7/19/06 13:39:10

Truck #	BC (g kg^{-1})	PN (# kg^{-1})	Truck Speed (km h^{-1})	Date/Time
42	0.64	2.09E+14	49	7/19/06 13:39:24
43	7.19	-1.90E+15	51	7/19/06 13:39:32
44	0.35	1.07E+16	52	7/19/06 13:40:24
45	1.17	-6.09E+14	57	7/19/06 13:41:00
46	1.34	4.96E+15	61	7/19/06 13:42:54
47	4.11	2.20E+15	76	7/19/06 13:45:35
48	0.38	1.48E+16	79	7/19/06 13:47:38
49	0.91	3.33E+14	30	7/19/06 13:52:45
50	0.38	9.77E+15	51	7/19/06 13:58:04
51	2.01	-6.30E+14	43	7/19/06 13:59:11
52	1.21	1.63E+16	54	7/19/06 13:59:47
53	9.85	1.06E+15	67	7/19/06 14:00:02
54	-0.12	4.74E+14	71	7/20/06 12:02:09
55	0.16	5.77E+15	54	7/20/06 12:02:28
56	3.89	4.96E+15	51	7/20/06 12:02:40
57	0.42	1.02E+16	51	7/20/06 12:03:13
58	4.10	-5.72E+15	48	7/20/06 12:03:24
59	6.01	9.09E+14	54	7/20/06 12:03:57
60	-1.97	8.09E+14	81	7/20/06 12:06:44
61	2.47	7.41E+14	51	7/20/06 12:07:21
62	0.60	3.77E+15	65	7/20/06 12:11:25
63	1.25	5.09E+13	46	7/20/06 12:12:34
64	0.84	1.46E+16	62	7/20/06 12:17:21
65	0.65	8.98E+15	62	7/20/06 12:22:59
66	3.38	-1.95E+15	63	7/20/06 12:24:18
67	0.29	9.78E+15	67	7/20/06 12:27:18
68	6.02	6.28E+14	66	7/20/06 12:27:41
69	1.30	-4.83E+14	63	7/20/06 12:33:14
70	0.96	3.20E+15	65	7/20/06 12:33:41
71	0.27	5.28E+15	66	7/20/06 12:36:32
72	0.20	5.40E+15	48	7/20/06 12:37:39
73	1.64	-1.37E+14	76	7/20/06 12:40:12
74	0.36	9.29E+14	54	7/20/06 12:42:16
75	0.42	1.60E+15	55	7/20/06 12:42:29
76	1.77	8.57E+15	44	7/20/06 12:43:12
77	1.46	4.06E+15	73	7/20/06 12:49:15
78	1.49	3.04E+14	42	7/20/06 12:55:23
79	0.50	1.40E+15	67	7/20/06 12:57:35
80	0.79	1.52E+16	73	7/20/06 12:57:44
81	3.81	1.12E+15	71	7/20/06 13:00:24
82	1.18	1.97E+15	32	7/20/06 13:07:50
83	1.62	1.76E+15	73	7/20/06 13:09:40
84	1.03	3.19E+15	59	7/20/06 13:10:53
85	5.03	3.08E+15	67	7/20/06 13:11:19
86	4.15	7.45E+14	52	7/20/06 13:16:55
87	0.18	2.79E+15	66	7/20/06 13:19:33
88	0.69	2.17E+15	71	7/20/06 13:20:12
89	0.96	-1.06E+15	52	7/20/06 13:22:47

Truck #	BC (g kg^{-1})	PN (# kg^{-1})	Truck Speed (km h^{-1})	Date/Time
90	0.33	1.59E+16	66	7/20/06 13:24:38
91	1.04	2.22E+16	59	7/20/06 13:27:48
92	0.51	2.05E+16	56	7/20/06 13:29:57
93	3.33	3.88E+14	70	7/20/06 13:31:40
94	1.86	4.15E+14	70	7/20/06 13:34:25
95	0.02	1.05E+16	48	7/20/06 13:40:05
96	0.36	4.65E+15	50	7/20/06 13:42:28
97	0.31	7.46E+14	71	7/20/06 13:43:12
98	5.99	2.25E+15	65	7/20/06 13:44:52
99	1.46	3.90E+15	62	7/20/06 13:45:03
100	0.18	2.97E+15	76	7/20/06 13:48:06
101	0.29	7.39E+15	74	7/20/06 13:48:45
102	1.18	1.40E+16	59	7/20/06 13:49:18
103	0.73	1.76E+15	56	7/20/06 13:53:54
104	2.28	2.35E+14	36	7/20/06 13:55:05
105	1.56	2.44E+14	47	7/20/06 13:55:19
106	1.29	1.19E+16	62	7/20/06 13:56:12
107	0.48	1.52E+16	65	7/21/06 12:02:56
108	0.66	1.16E+15	66	7/21/06 12:03:30
109	6.74	9.52E+14	41	7/21/06 12:06:15
110	0.52	7.71E+14	32	7/21/06 12:06:24
111	0.88	1.49E+15	56	7/21/06 12:07:13
112	0.57	9.79E+13	42	7/21/06 12:08:29
113	1.74	-1.37E+14	50	7/21/06 12:08:37
114	-0.34	4.41E+16	76	7/21/06 12:09:03
115	1.11	1.78E+15	60	7/21/06 12:09:14
116	0.62	1.31E+16	71	7/21/06 12:09:48
117	4.88	4.32E+14	43	7/21/06 12:11:09
118	6.91	-3.57E+15	63	7/21/06 12:11:30
119	7.93	1.18E+15	60	7/21/06 12:12:11
120	0.38	3.83E+15	43	7/21/06 12:20:39
121	7.01	-1.53E+15	78	7/21/06 12:21:15
122	1.07	9.90E+15	60	7/21/06 12:23:06
123	0.61	4.66E+14	65	7/21/06 12:26:42
124	7.99	6.10E+14	61	7/21/06 12:29:05
125	4.03	1.42E+14	65	7/21/06 12:29:25
126	1.19	2.11E+15	48	7/21/06 12:33:38
127	1.06	-3.69E+13	41	7/21/06 12:35:37
128	0.96	3.16E+15	50	7/21/06 12:36:08
129	1.20	4.64E+14	51	7/21/06 12:36:37
130	0.81	1.16E+15	48	7/21/06 12:41:25
131	0.12	2.09E+15	67	7/21/06 12:41:55
132	3.64	-5.28E+14	68	7/21/06 12:42:42
133	0.18	2.02E+16	57	7/21/06 12:44:37
134	0.19	8.27E+14	78	7/21/06 12:50:20
135	0.99	7.64E+15	74	7/21/06 12:51:49
136	0.20	-1.02E+15	78	7/21/06 12:52:00
137	-0.26	6.82E+15	70	7/21/06 12:55:16

Truck #	BC (g kg^{-1})	PN (# kg^{-1})	Truck Speed (km h^{-1})	Date/Time
138	0.35	4.80E+15	65	7/21/06 12:58:35
139	0.71	1.93E+16	67	7/21/06 13:02:14
140	0.31	6.92E+15	39	7/21/06 13:04:48
141	1.65	1.73E+16	67	7/21/06 13:09:25
142	0.81	1.19E+15	47	7/21/06 13:10:39
143	-0.03	3.32E+15	49	7/21/06 13:10:46
144	0.32	4.41E+14	78	7/21/06 13:11:08
145	2.19	1.02E+15	41	7/21/06 13:12:54
146	0.84	1.13E+15	57	7/21/06 13:17:48
147	1.13	3.46E+15	58	7/21/06 13:20:33
148	1.87	1.39E+15	52	7/21/06 13:21:19
149	2.79	2.70E+15	68	7/21/06 13:22:33
150	0.45	1.14E+16	52	7/21/06 13:23:25
151	3.48	6.72E+15	68	7/21/06 13:28:20
152	2.05	1.46E+16	67	7/21/06 13:28:45
153	1.52	1.52E+16	57	7/21/06 13:32:52
154	3.35	2.38E+15	66	7/21/06 13:33:27
155	1.17	1.84E+15	67	7/21/06 13:34:47
156	0.85	4.42E+15	66	7/21/06 13:39:51
157	3.51	7.95E+14	71	7/21/06 13:40:56
158	0.88	2.09E+15	85	7/21/06 13:41:15
159	0.97	3.48E+15	85	7/21/06 13:41:21
160	0.20	8.95E+15	71	7/21/06 13:42:55
161	0.46	8.55E+15	56	7/21/06 13:45:17
162	1.73	-9.52E+14	55	7/21/06 13:46:07
163	-0.13	1.19E+16	73	7/21/06 13:47:14
164	1.76	-2.59E+14	71	7/21/06 13:48:07
165	0.51	-1.86E+14	61	7/21/06 13:50:10
166	1.38	2.89E+15	51	7/21/06 13:54:06
167	2.89	2.71E+14	51	7/21/06 13:56:40
168	1.30	2.82E+15	57	7/21/06 13:57:14
169	0.31	9.36E+15	66	7/21/06 13:59:03
170	0.37	8.27E+15	65	7/21/06 13:59:18
171	0.23	3.00E+15	85	7/21/06 13:59:44
172	3.93	1.63E+15	31	7/24/06 12:09:03
173	0.44	-2.52E+14	43	7/24/06 12:09:22
174	1.05	1.15E+14	47	7/24/06 12:09:31
175	-0.35	1.24E+15	48	7/24/06 12:10:43
176	0.32	1.69E+15	42	7/24/06 12:11:18
177	0.27	-7.17E+13	70	7/24/06 12:12:06
178	0.15	-3.57E+13	70	7/24/06 12:12:15
179	-0.24	4.73E+15	47	7/24/06 12:13:58
180	0.98	1.68E+15	79	7/24/06 12:15:04
181	0.11	3.22E+15	71	7/24/06 12:15:33
182	0.35	6.15E+14	70	7/24/06 12:15:56
183	0.31	1.04E+15	51	7/24/06 12:19:07
184	0.11	3.86E+15	47	7/24/06 12:19:50
185	1.40	2.76E+15	55	7/24/06 12:20:13

Truck #	BC (g kg^{-1})	PN (# kg^{-1})	Truck Speed (km h^{-1})	Date/Time
186	-0.10	8.49E+14	61	7/24/06 12:23:42
187	1.76	1.07E+16	41	7/24/06 12:25:40
188	0.76	1.52E+16	45	7/24/06 12:31:52
189	1.81	1.41E+15	71	7/24/06 12:33:59
190	2.36	2.84E+16	33	7/24/06 12:42:39
191	2.87	6.64E+15	67	7/24/06 12:44:24
192	2.92	4.69E+15	81	7/24/06 12:46:41
193	0.25	1.14E+16	58	7/24/06 12:49:14
194	16.15	2.62E+15	47	7/24/06 12:52:05
195	-4.02	2.24E+15	52	7/24/06 12:52:13
196	4.83	6.31E+14	41	7/24/06 12:52:32
197	-2.01	1.04E+15	43	7/24/06 12:52:40
198	1.01	3.55E+15	47	7/24/06 12:53:16
199	1.85	2.57E+16	58	7/24/06 12:55:36
200	0.84	2.14E+15	49	7/24/06 12:56:31
201	-0.08	-9.09E+14	52	7/24/06 12:56:52
202	0.83	1.50E+16	52	7/24/06 12:57:03
203	2.11	1.58E+16	38	7/24/06 12:58:58
204	8.52	1.61E+15	60	7/24/06 13:03:43
205	2.01	3.52E+15	71	7/24/06 13:06:30
206	7.52	6.34E+14	65	7/24/06 13:08:08
207	3.37	8.46E+15	67	7/24/06 13:08:23
208	1.17	2.84E+14	71	7/24/06 13:08:31
209	0.50	1.01E+16	50	7/24/06 13:09:40
210	0.54	-2.81E+14	66	7/24/06 13:12:33
211	4.70	3.67E+16	45	7/24/06 13:22:01
212	1.77	4.96E+15	60	7/24/06 13:23:56
213	1.29	1.17E+16	42	7/24/06 13:24:36
214	8.28	7.50E+15	54	7/24/06 13:31:29
215	0.40	1.88E+15	55	7/24/06 13:31:37
216	6.12	1.03E+16	56	7/24/06 13:39:17
217	2.16	-7.84E+14	57	7/24/06 13:39:42
218	13.07	2.12E+15	65	7/24/06 13:44:00
219	1.80	-3.46E+14	71	7/24/06 13:44:27
220	0.61	4.20E+15	60	7/24/06 13:50:45
221	0.79	3.38E+14	73	7/24/06 13:51:10
222	1.85	3.47E+15	67	7/24/06 13:52:38
223	1.53	3.04E+15	62	7/24/06 13:52:45
224	-0.05	2.12E+14	63	7/24/06 13:53:43
225	0.85	-1.88E+14	58	7/24/06 13:57:02
226	-0.35	6.20E+15	70	7/24/06 13:57:22